Alma Mater Studiorum - Università di Bologna

DOTTORATO DI RICERCA IN

INGEGNERIA ELETTRONICA, TELECOMUNICAZIONI E
TECNOLOGIE DELL'INFORMAZIONE

Ciclo XXXI

Settore Concorsuale: 09/F2

Settore Scientifico Disciplinare: ING-INF/03

COST-EFFECTIVE PROVISIONING OF 5G TRANSPORT NETWORKS: ARCHITECTURES AND MODELLING

Presentata da: Federico Tonini

Coordinatore Dottorato

Prof.ssa Ing. Alessandra Costanzo

Supervisore

Prof.ssa Ing. Carla Raffaelli

Esame finale anno 2019

Abstract

The next generation of mobile network (5G) has to face a completely new set of requirements coming from novel services. Applications like intelligent transportation systems, smart manufacturing, virtual and augmented reality, eHealth services require massive machine type communications, enhanced mobile broadband, ultra reliable low latency communication to be supported by single infrastructure. Mobile network operators are in need of a flexible network capable of supporting services with a wide set of different requirements over the same physical resources, possibly at the same or at a lower cost than today.

Centralized radio access network (C-RAN) architecture is a promising solution to improve both network flexibility and scalability. In C-RAN, baseband processing units (BBUs) are decoupled from remote radio units (RRUs) at the antenna sites and are placed in one of few selected locations, called BBU hotels. Thanks to the centralization, more efficient hardware can be employed, advanced radio interference management techniques can be implemented, cooling and power supply units can be shared, and network maintenance is simplified. In addition to this, the paradigms of software-defined networking (SDN) and network function virtualization (NFV) allow to virtualize baseband functions on general purpose hardware and instantiate/move virtual functions whenever and wherever needed, enhancing the network flexibility while lowering costs. However, the centralization of BBUs requires high capacity and low latency links to transport data. Given the strict requirements of these links, commonly referred to as fronthaul links, dedicated fiber connections are usually required. This may be expensive and calls for novel deployment strategies to contain the costs. The deployment of a C-RAN should also consider survivability against failures. In fact, the failure of a BBU hotel can affect a large number of RRUs, causing severe outages in the radio segment.

This Ph.D. thesis investigates the cost-efficient and resilient design of C-RAN. Minimization of network equipment as well as reuse of already deployed infrastructure, either based on fiber or copper cables, is investigated and shown to be effective to reduce the overall cost. Moreover, the introduction of wireless devices (e.g., based on free space optic) in fronthaul links is included in the proposed deployment strategies and shown to significantly lower capital expenditure. The adoption of Ethernet-based fronthaul and the introduction of hybrid switches is pursued to further decrease network cost by increasing optical resources usage. Finally, the problem of single BBU hotel failure is addressed and included in the optimal deployment of BBU resources.

Contents

List of Tables

x

List of Figures

Abbreviations

3GPP   Third Generation Partnership Project

BBU   Baseband Unit

BS   Base Station

CAPEX   Capital Expenditures

CO   Central Office

CoMP   Coordinated Multipoint

CPRI   Common Public Radio Interface

CPRIoE   Common Public Radio Interface over Ethernet

CRA   Centralized Radio Architecture

C-RAN   Centralized Radio Access Network

D-RoF   Digital Radio over Fiber

DU   Digital Unit

eICIC   Enhanced Inter-cell Interference Coordination

FLS   Farthest Location Selection

FSO   Free Space Optics

GCA   Greatest Cardinality Approach

GST   Guaranteed Service Traffic

HARQ   Hybrid Automatic Repeat Request

IEEE   Institute of Electrical and Electronics Engineers

IGCA   Improved Greatest Cardinality Approach

IHN   Integrated Hybrid Node

ILP   Integer Linear Programming

IP   Internet Protocol

ITU   International Telecommunication Union

LoS   Line of Sight

LP   Linear Programming

LTE   Long Term Evolution

MAC   Medium Access Control

MIMO   Multiple-Input and Multiple-Output

MIP   Mixed Integer Programming

MLS   Minimum Location Search

NFV   Network Function Virtualization

OBSAI   Open Base Station Architecture Initiative

OPEX   Operational Expenditures

PDV   Packet Delay Variation

PON   Passive Optical Network

PSTN   Public Switched Telephone Network

RAN   Radio Access Network

RRH   Radio Remote Head

RTB   Radio over Fiber to the Building

RU   Radio Unit

RRU   Remote Radio Unit

RRUP   RRU Placement

RUM   Radio Unit Minimization

SCP   Set Cover Problem

SDN   Software Defined Network

SFP+   Small form Factor Pluggable

SGSN   Serving GPRS Support Node

SINR   Signal to Interference plus Noise Ratio

SM   Statistically Multiplexed

UE   User Equipment

UMTS   Universal Mobile Telecommunications System

Chapter 1

Introduction

The fifth generation of mobile networks (5G) is now becoming a reality. In the coming years, the first 5G deployments will take place and will go on for many years after. 5G is expected to be a key component of a connected society, enabling unlimited access and sharing of information regardless of the place and time to either humans or machines. 5G will therefore not only be about mobile connectivity for people but will also provide ubiquitous connectivity for any kind of devices and users that may benefit from being connected [6].

So far, several use cases have been proposed in order to face challenges and explore the potential of 5G [7],[8]. Autonomous vehicles and intelligent transportation systems are emerging services posing strict latency and reliability issues. Emergency communications and eHealth applications will also contribute to push the network towards a system with extremely high reliability. Communications onboard of different high speed means of transport must be guaranteed, like in the case of high speed trains. Moreover, the deployment of massive low-cost, low-range, and low-power devices, such as sensors and wearable devices, requires support for an unprecedented number of devices at the same time. High speed coverage of special events, like matches, concerts and festivals, as well as indoor ultra-high broadband access will be required, since around 80% of the mobile data traffic is generated indoor [9].

From a radio perspective, novel technologies have been introduced to face the new challenges for 5G. A massive number of antennas can be deployed to provide higher capacity to more

users simultaneously, thanks to a higher level of spectral efficiency. In addition, beamforming techniques can be employed to further decrease interference in the network. Moreover, increasing the number of base stations (BSs), the so-called BS densification, allows to increase the frequency reuse, but advanced radio coordination schemes must be implemented to operate in dense scenarios, where users suffer from severe co-channel interference [10].

In order to provide efficient coordination mechanisms, the concept of centralized radio access network (C-RAN) has been proposed [11]. As opposed to the distributed case, where all the processing functions are performed at the BS site, connected to the core network through the packet based backhaul, in C-RAN baseband processing functions are decoupled from BS sites and placed in centralized locations, called hotels. By doing this, ultra low latency connections among BSs are provided, enabling tight coordination algorithms to be executed. In addition to this, C-RAN allows also cost and energy savings, thanks to multiplexing gains and sharing of cooling and power supply units [11]. However, C-RAN requires high capacity and low latency connections to transport data from BS sites to baseband processing units, the so-called fronthaul links. Due to its strict requirements, each fronthaul link usually requires a dedicated fiber (or wavelength), resulting in high network resource inefficiency and cost. In addition to this, centralizing the processing functions in one hotel makes the network vulnerable to failures. In fact, the failure of a single hotel may cause severe service outages, calling for efficient and reliable C-RAN design. On the one hand, several advantages can be achieved with centralized architectures. On the other hand, the cost for providing fronthaul links may be very high if not carefully planned, especially when a large number of BSs has to be deployed [12][13].

This thesis investigates cost-efficient strategies capable of reducing the amount of equipment to deploy in both indoor and outdoor scenarios. The proposed strategies, based on both heuristic and integer linear programming, aim at introducing the cost of fronthaul in the mobile radio deployment of C-RAN. Differently from conventional deployments, where the antenna placement is performed without considering transport network costs, the proposed strategies include the fronthaul constraints and cost in the mobile network design. The re-use of already deployed resources (e.g., fiber and copper cables) is investigated. Wireless devices that provide large bandwidth, like the one based on free space optics or millimeter waves, are included in

fronthaul link design along with fibers, limiting expensive fiber trenching. To further reduce the transport network cost, the use of off-the-shelf equipment (e.g., Ethernet switches) is here investigated as an alternative to dedicated links. In fact, by encapsulating fronthaul traffic into Ethernet frames, different fronthaul streams can be multiplexed together or with best effort streams (e.g., traditional packet based backhaul), increasing the transport resource usage. However, multiplexing traffic with different requirements needs the introduction of priority mechanisms in conventional Ethernet switches and must be carefully examined. Techniques for network survivability design in C-RAN are also proposed, investigating the impact of fronthaul constraints on transport and radio resources, and with the objective of minimizing the network equipment while providing resiliency against single hotel failures.

The outline of the thesis is as follows. Chapter 2 presents an overview of mobile network evolution towards C-RAN. C-RAN advantages, challenges, and future baseband splitting techniques are also discussed. Chapter 3 proposes cost-efficient deployment strategies to design and upgrade a C-RAN in case of special events in urban areas. Motivated by the fact that most of the traffic is generated by indoor users, chapter 4 tackles the problem of indoor capacity provisioning in residential areas by means of centralized networks. In Chapter 5, an architecture capable of multiplexing fronthaul and backhaul traffic together on the same optical resources is provided, with the aim of increasing transport resources usage. Chapter 6 analyzes the problem of single baseband hotel failure in C-RAN and proposes strategies for a reliable deployment. Finally, Chapter 7 summarizes the main achievements of this thesis and provides directions for future work.

Chapter 2

Distributed and Centralized Radio Access Networks

This Chapter introduces the reference network architecture for this thesis. In particular, the evolution of mobile access network architectures over the years is illustrated firstly. Then, the advantages and challenges of the next generation mobile networks are discussed, with a particular focus on centralized radio access networks.

2.1   Traditional Base Station

In general terms, a mobile network is composed of radio, transport and core segments. The radio access network (RAN) is in charge of exchanging data with the end users, by means of BSs. Each BS performs radio access functions, i.e., it manages the transfer of user and control data towards (downlink) and from (uplink) several users simultaneously, by means of physical layer and multiple access protocols, according to the so-called radio, or air, interface [14]. The processing equipment of a BS is made up of two parts: a baseband unit (BBU), sometimes referred to as a digital unit (DU), and a remote radio unit (RRU), also referred to as remore radio head (RRH) or simply radio unit (RU). An example of a traditional BS is depicted in Figure 2.1.
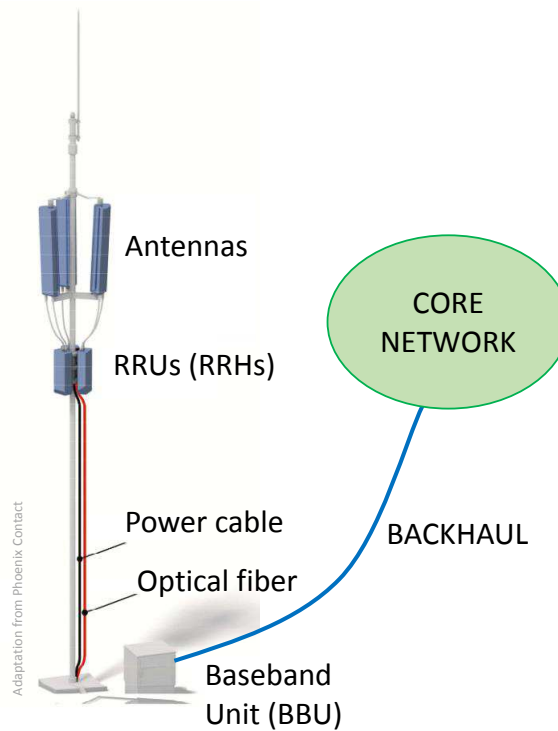
Figure 2.1: Example of a traditional BS.

The RRU is responsible for the analog-to-digital (A/D) conversion of radio signals coming from the antenna into digital baseband signals for the BBU and for the digital-to-analog (D/A) conversion of the baseband signals coming from the BBU and directed to the antenna. Moreover, the RRU contains components for the frequency up/down conversion, power amplification and filtering of the radio signals. Each RRU is connected to one or more antennas via coaxial cables and to a BBU through a digital link. There are different standards for the digitization of the radio signal between RRU and BBU. Among all, the common public radio interface (CPRI) [15] and open base station architecture initiative (OBSAI) are the most common [16]. CPRI is currently the most adopted solution, although it still has some vendor-specific implemented features, which prevent a full multi-vendor interoperability. BBU performs digital processing of the baseband version of the radio signals received (uplink direction) and transmitted (downlink direction) by the antennas. The BBU is also in charge of performing the functions of physical and upper layers, defined by different standards (e.g., LTE, UMTS), and interfaces with the transport segment of the mobile network [11].

The transport segment of the network is in charge of transporting the data from BSs to the

core network and viceversa. This segment is usually referred to as mobile backhaul. The infrastructure adopted by mobile operators uses a mixture of various backhaul technologies and architectures to provide transport connectivity to BSs in an effective way. In general, to backhaul the traffic coming from the users, wired and wireless based links are employed. The most common wired technologies are based on optical links, such as passive optical networks (PONs) and Ethernet links. Wireless technologies like microwave and millimeter waves (mmwave) links can also be employed to backhaul data in the access part of the transport network [17]. Wireless technologies allow to reduce the network deployment cost and time. Mobile backhaul can also include interconnections between different BSs. This is the case of fourth generation of mobile network (4G), where connections among BSs make use of X2 interfaces to exchange information about handovers, load management and interference level.

Finally, the core network is in charge of all remaining non radio-access related functions and acts as a gateway towards all other mobile and fixed networks, e.g., towards the Internet and public switched telephone network (PSTN). In the core, mobile operators also performs authentication and registration the user's location.

2.2 Centralized Radio Access Networks

Traditionally, the baseband processing functions are distributed over the area to serve. In high density scenarios, like urban areas, where large traffic requirements are imposed, interference may limit the performance of the system. To overcome this problem, coordination techniques (e.g., coordinated multipoint, joint transmission and reception) can be performed among BSs deployed in a certain area. However, some coordination mechanisms require latency lower than one millisecond to properly work [18], and the traditional X2 logical interface that connects BSs together is not able to provide such low latency. In fact, the interconnection of the X2 links is traditionally done via the core network access router, making impossible to satisfy strict latency requirements [19].

Centralized radio access network (C-RAN) is an architectural solution that can solve this prob-
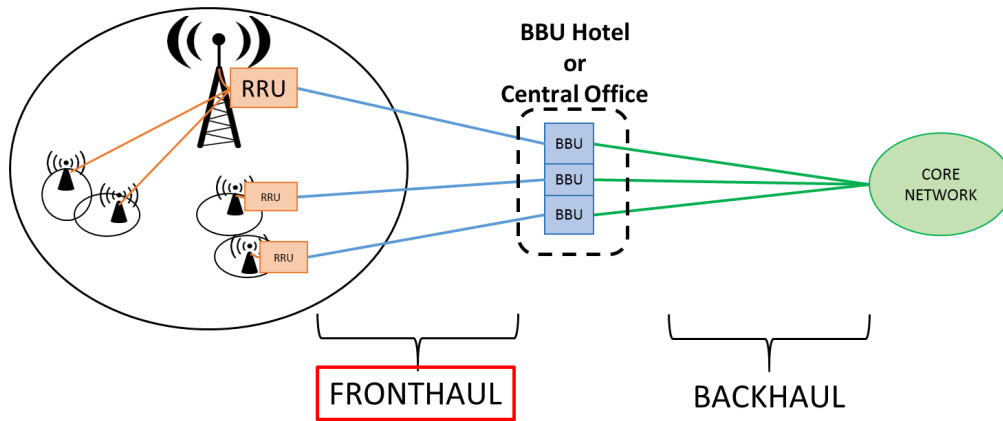
Figure 2.2: Example of a C-RAN.

lem [20]. In fact, C-RAN relies on centralization of BS baseband processing functions in few selected locations, usually referred to as BBU hotels. An example of this architecture is depicted in Figure 2.2. The BBUs installed within an hotel can be easily connected together to provide low latency communication among them in order to support efficient coordination schemes. In addition to this, C-RAN offers many other advantages, from both energy and cost perspective. Since many BBUs are co-located in the same location, cooling and power supply units can be shared, and network devices maintenance as well as deployment of new hardware is simplified [11]. Moreover, centralizing BBUs paves the way to massive virtualization of BBU functions over more convenient general purpose hardware by exploiting the so called network function virtualization (NFV) paradigm [21]. Virtual functions can be suitably managed by a software defined network (SDN) orchestrator with a global view of the underlying network resources and connectivity, placing virtual BBU functions on the fly [22], further enhancing network flexibility.

Despite its advantages, C-RAN is not becoming as popular as one would have expected, due to the extremely large capacity required to transport data from antenna sites to BBU hotels (also known as fronthaul links). In fact, C-RAN usually requires digital radio over fiber links to transport data from antenna sites to BBU hotels (also known as fronthaul links). When a large

Table 2.1: CPRI bit rate requirements for different antenna configurations.

CPRI Option	Bit rate [Mbps]
1	614.4
2	1228.8
3	2457.6
4	3072.0
5	4915.2
6	6144.0
7	9830.4
8	10137.6
9	12165.12
10	24330.24

number of antennas are employed, bitrate over fronthaul links dramatically increase, requiring high capacity connections (e.g., fiber cables), limiting the dissemination of this architectural solution.

The requirements of C-RAN can be extremely high, requiring dedicated high speed and low latency connections. Nowadays, the most common protocol used to transport data over fronthaul links is CPRI [15], which sets fixed bitrates, depending on the antenna configuration. The CPRI bitrate can be calculate as follows [15]:

$$R_{CPRI} = N_s \cdot N_{ant} \cdot R_s \cdot 2 \cdot N_{res} \cdot O_{cw} \cdot O_{lc}, \qquad (2.1)$$

where N_s and N_{ant} are the number of sectors and the number of MIMO elements per sector, R_s and N_{res} are the sampling rate and number of bits per sample, O_{cw} and O_{lc} represent the overhead introduced by CPRI control words and line coding overhead. As an example, let's consider an antenna with 3 sectors, 4 MIMO elements, a single 20 $[MHz]$ channel with a sampling rate of 30.72 $[MHz]$, 15 $[bits]$ per sample, $O_{cw} = 16/15$ and $O_{lc} = 66/64$ $[byte]$ [15, 18]. The resulting CPRI rate is $R_{CPRI} = 12165.12$ $[Mbps]$, which corresponds to CPRI option 9, as reported in Table 2.1. CPRI also imposes extremely low jitter requirements (+/- 0.002 [ppm]) to retrieve correctly the clock in the BBU. In addition to this, the hybrid automatic repeat request (HARQ) mechanism of LTE must be performed by the BBU within a computational time of 3 $[ms]$, leaving around 200 $[\mu s]$ to transport the data to/from BS site [23]. This translates into
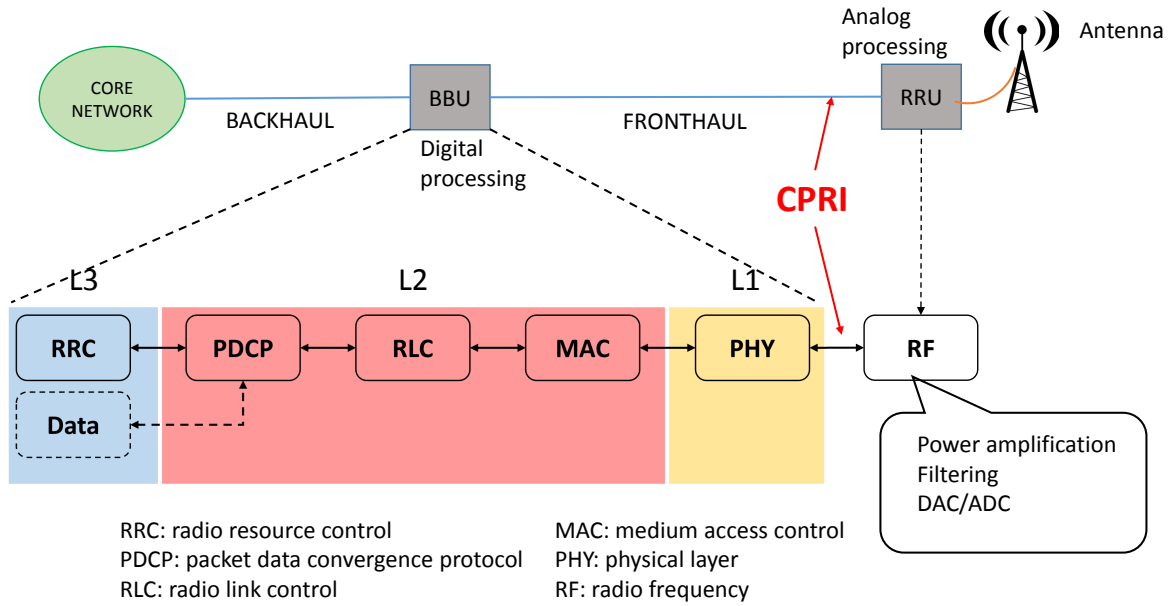
Figure 2.3: Layers of the mobile network protocol stack.

Table 2.2: eCPRI bitrate requirements for different splits and a sample antenna configuration. UL = uplink, DL = downlink.

	Split D	Split I	Split II	Split E
User Data DL	3 Gbps	<4 Gbps	20 Gbps	236 Gbps
User Data UL	1.5 Gbps	not standardized	20 Gbps	236 Gbps

a maximum one-way distance between BS sites and BBUs of around 20 $[km]$.

To relax these requirements, new baseband splits have been investigated recently, like the new eCPRI protocol [15] and different options proposed by 3GPP [5]. With the new splits, some of the functions are left at the BS site, in the RRU, while others are centralized in the BBU, depending on the selected split. Figure 2.3 depicts the protocol stack highlighting the different baseband functions. eCPRI standard proposes 4 different splits within the physical layer and an example of the related requirements is reported in Table 2.2 for a BS with 64 antennas, 100 $[MHz]$ channel, modulation format 256 QAM, coding rate 0.8, 30 $[bits]$ per sample, a sampling frequency of 122.88 $[Msps]$. Here the user throughput is assumed to be 3 $[Gbps]$ in dowlink and 1.5 $[Gbps]$ in uplink [15]. Split D is the CPRI split, while split E is in between physical and MAC layers. It is possible to notice that the requirements decrease with higher layer splits. This is because more functions are performed at the BS sites and the transported traffic becomes more user-dependent. Figure 2.4 depicts the functional splits proposed by
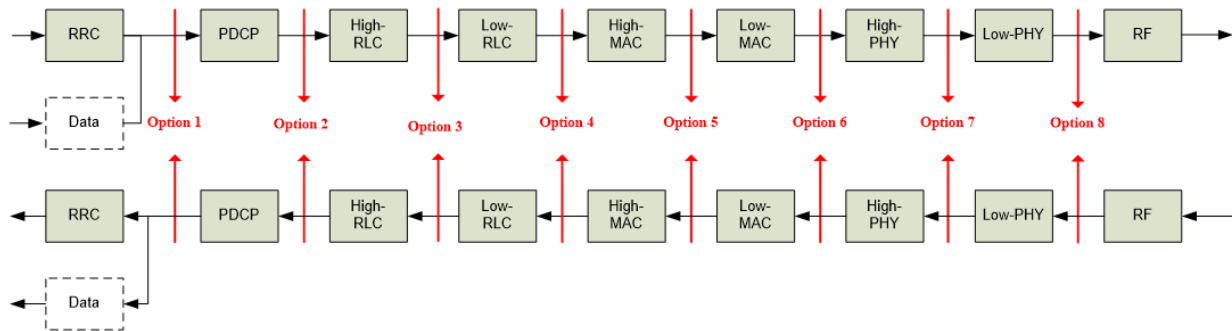
Figure 2.4: Function splits proposed by 3GPP [5].

Table 2.3: 3GPP splits bitrate requirements in Gbps for a sample antenna configuration. UL = uplink, DL = downlink.

Option	1	2	3	4	5	6	7a	7b	7c	8
DL bandwidth	4	4	<Opt.2	4	4	4.1	10.1-22.2	37.8-86.1	10.1-22.2	157.3
UL bandwidth	3	3	<Opt.2	3	3	5.6	13.6-21.6	53.8-86.1	53.8-86.1	157.3

3GPP, that spans over the whole protocol stack. The related requirements are reported in Table 2.3 for a BS site with similar characteristics to the previous one, with the exception of a variable number of bits per sample (from 14 to 32), 32 antennas, and a user throughput of 4 [*Gbps*] in dowlink and 3 [*Gbps*] in uplink [5].

Similarly to the eCPRI case, the requirements decreases with higher splits, as more and more functions are performed at the BS site. On the one hand, using a higher layer split relaxes the requirements, on the other hand, efficient coordination mechanisms cannot be performed and limited gains can be achieved. The question of which the best split option is remains open [24] [25]. In order to take advantage of both, a two level fronthaul network architecture can be deployed [26]. A low layer split (e.g., one of the proposed eCPRI splits) can be performed close to BS sites, performing a first elaboration of the signals, avoiding to carry deep in the transport network highly demanding traffic. Then, an higher layer split can be performed in more remote locations, in order to benefit also from high layer split centralization.

Chapter 3

Outdoor Capacity Provisioning for Special Events

Among the use cases envisioned for 5G [7], provisioning of high capacity in dense urban scenarios (e.g., shopping malls, crowded areas, etc.) is challenging [27]. In some cases, like festivals or concerts, the additional capacity is required only for a limited amount of time (i.e., for the duration of the event). Therefore, ad-hoc strategies for C-RAN can be developed to provision the extra capacity "on demand" in a cost efficient way.

In C-RAN, wired or wireless solutions can be employed to connect antennas and RRUs with BBUs [28]. Wired solutions have to reach the antenna sites along or below ground, requiring the installation of costly and time consuming wired infrastructure, due to labor costs and legal arrangements with landowners en route. Therefore, the possibility of re-using existing infrastructure must be taken into account whenever possible. Wireless solutions can also be employed, as they not require to deploy cables, thus reducing network deployment cost and time, as shown in [29] and [30]. However, high data rates carried by fronthaul links limits the choice of wireless technologies to the ones that are able to guarantee tens of Gbps rates, such as free space optics (FSO) devices [31]. FSO is a technology which relies on optical signals generated by light emitting diodes or lasers and uses air as propagation medium. FSO systems typically operates in the unlicensed wavelength range of $800 - 1700 \, [nm]$, allowing to reach tens

of Gbps over short distances under line of sight conditions [32]. In [33] and [34], the results of outdoor field trials are presented and show high reliability against weather and misalignment conditions and limited data rate degradation for relatively low distances ($< 100 \, [m]$). BSs can be equipped with FSO devices to replace expensive fiber cables in fronthaul links, simplifying the BS deployment. Moreover, FSO can be considered as possible solution for the "on-demand" capacity deployments, where BSs can be temporarily deployed to upgrade existing networks when a planned special event requires additional capacity in a certain area.

In the past, many works have been published on deployment of radio resources based on traffic and capacity requirements. In [35], different ILP models for coverage and capacity planning of third and fourth generation of cellular systems are proposed. Considerations related on cost minimization, interference problems as well as radio resource assignment are also discussed. In [36], the authors propose an extensive study of existing techniques for BS positioning and investigate cell planning objectives for future cellular networks. Over the last few years, the BS densification, a technique widely used to increase network capacity, has drown the attention of industry and academia due to the high cost for backhauling such large number of BSs [37], [38]. Cost efficient strategies for backhaul have been developed. Example of cost-efficient passive optical network (PON) design algorithms are proposed in [39] and [40]. In [29] and [30], strategies for cost-efficient backhaul networks based on FSO devices are reported.

The works introduced so far are for minimizing cost of either radio or transport segment. So far, very few works on joint planning have been conducted. In [41], the authors propose an ILP to deploy small cells and fiber transport resources under certain capacity requirements. This strategy is suitable for greenfield scenarios, where there is no existing infrastructure (e.g., existing ducts). However, trenching fiber cables is very expensive, and the reuse of already deployed fiber ducts may lead to significant cost savings, as well as using wireless devices. In [42], the authors propose to use a series of heuristic techniques to find the optimal placement of RRHs and routes for fiber based fronthaul jointly. Even though the work shows a great scalability of their deployment strategy, which can in turn be used to plan network deployment in city-wide scenarios, with their strategy there is no possibility of using wireless devices and there is no mention of minimum requirements for users.
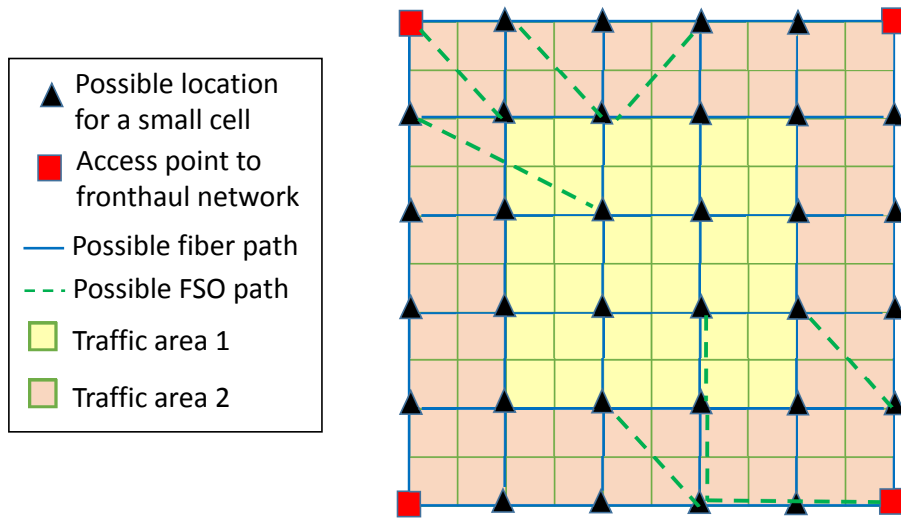
Figure 3.1: Schematic view from the top of a possible scenario.

Differently from the existing works, the model presented in this Chapter is capable of (*i*) deploying radio and transport networks jointly, (*ii*) using fiber and FSO devices for fronthaul links, (*iii*) re-use and upgrade existing infrastructure, (*iv*) satisfy given capacity requirements for broadband access in dense areas[1]. Since the focus of this work is on C-RAN, in this Chapter the term BS placement is used to indicate the selection of proper locations for antenna and RRUs, while all BBUs are placed in BBU hotels.

3.1   Network Design Framework

In the following, a flexible framework describing a general scenario in which a mobile network has to be deployed or upgraded is proposed. The framework contains the suitable antennas locations (i.e., where an antenna can be placed) and models the obstacles (e.g., walls, trees) that may attenuate signals or create multipath. Moreover, the framework provides a detailed description of transport network infrastructure, both existing and to be deployed, such as fiber paths, wireless links (i.e., it tells if two points on the map are in LoS or not and thus can be connected by means of FSO devices). Finally, the framework accounts for user requirements (e.g., minimum bit-rate to be guaranteed) and supports different user distributions.

Figure 3.1 depicts a two-dimensional schematic view from the top of a possible deployment

---

[1]The outcome of this work is included in [43], [44].

scenario. In the following, the elements that characterize the framework are described in detail. The modeling of the radio part of the network, concerning potential BS locations and coverage is explained firstly, then the transport network resources, such as fiber and wireless fronthaul links and fiber access points, are analyzed.

3.1.1 Radio Network Modeling

In general, the main actors of the radio network segment are users and BSs [45],[46]. In this study, the point of view of an user, the so called downlink (i.e., the signal path from a BS to a user), is considered. Each user, in order to communicate with the network, is equipped with a terminal referred to as user equipment. The user equipment is characterized by a receiver sensitivity, defined as the minimum signal power level that the receiver can distinguish from the thermal noise. A certain area is considered covered if the users in the area receive a signal power, from at least one BS, higher than the receiver sensitivity. The received signal power depends on many factors: mobile network devices and user equipment characteristics (e.g., antenna gain and receiver sensitivity), transmitted signal power, and attenuation due to signal propagation and obstacles (also known as path loss). Usually, the parameters that characterize network and user equipment are set by the different producers or standards, and the transmitted signal power relies within a given range of values. Therefore, the only variable factor that determines the coverage and, implicitly, the cell radius in different scenarios is the path loss.

In literature, many different propagation path loss models can be found. They can be categorized in three different types: deterministic, empirical, and stochastic [47]. Deterministic models reproduce by simulation the laws governing electromagnetic wave propagation to determine the received signal power at a particular location. For this type of models, an exhaustive description of the propagation environment is required and they are usually extremely precise. An example for this category can be found in [48]. Empirical models are based on observations and are usually obtained by measurement campaigns. Parameters are derived from the measures and included in the models, making them very easy to use but also inaccurate when applied in specific scenarios. Examples for this type of model can be found in [49] and [50].

Stochastic models describe the environments as a series of random variables. These models do not require detailed information of the propagation scenario, but their accuracy is usually not as high as the one provided by deterministic models [51].

Once the path loss is computed using a model, the received signal power from each BS can be derived and the BS to which the end user is assigned to can be identified (e.g., based on the largest received power). The effect of the noise on the system performance can be evaluated through the signal to noise ratio (SNR), defined as the ratio of received signal power to noise power. The maximum achievable channel capacity C in the system is given by the Shannon's formula (over additive white Gaussian noise (AWGN) channel):

$$C = BW \cdot log_2(1 + SNR), \tag{3.1}$$

where BW is the channel bandwidth. If BW is set, to higher SNR corresponds higher achievable capacities. The capacity achieved in a digital mobile system depends on the format modulation in use, and parameters to tune (3.1) can be found in literature (e.g., the ones reported in [52]).

If more than one BS is active in the area, an user may receive signals coming from different BSs, depending on the path loss. When signals received by the end user share the radio resources with the useful signal, that comes from the BS to which the user is assigned, the effects of the interference are experienced, resulting in performance degradation. Under the assumption of Gaussian distribution of the interference, the effects of both noise and interference can be taken into account using the signal to interference plus noise ratio ($SINR$):

$$SINR = \frac{S}{\sum_{i \neq useful} I_i + N}, \tag{3.2}$$

where S is the received signal power (useful), I is the received signal power from BS i, and N is the noise power. The $SINR$ can be used instead of SNR in (3.1) to compute the maximum achievable channel capacity for the system:

$$C' = BW \cdot log_2(1 + SINR). \tag{3.3}$$

Given that a certain capacity requirement (C_{min}) is imposed, the minimum $SINR$ to be provided to the users can be computed by inverting (3.3):

$$SINR \geq SINR_{min} = 2^{\frac{C_{min}}{BW}} - 1. \tag{3.4}$$

Considering a BS location, a model can be applied to compute the received power in different points of the area under consideration in order to form a coverage map. In the proposed framework, the area to cover is divided in pixels forming a grid, referred to as coverage grid. For each pixel of the coverage grid, the received power from each possible BS location can be computed by means of empirical or physical models, and the choice of the model to use is left to the designer. It is worth noting that, at this stage, no BS placement is performed and data related to coverage are used by the placement algorithms presented below. Since the received signal power in each pixel is known for every possible BS location, information about signal to interference plus noise ratio (SINR) can be used by the algorithm to guarantee a minimum bitrate in each pixel. Moreover, the coverage grid allows also to account for areas with different traffic requirements. In fact, a value of traffic can be assigned to each pixel according to the requirements of the users in that pixel, and pixels can be assigned to (or covered by) a BS until its capacity is exceeded.

3.1.2 Transport Network Modeling

Providing connectivity to users requires each BS to be connected to the mobile core network. As it is possible to see in Figure 3.1, different transport links (i.e., fibers or wireless) can be used to connect BSs to access points. In this framework, an access point is considered to be a cabinet owned by the operator that is already connected to the mobile core network or to a BBU hotel, in case it hosts BBUs or not.
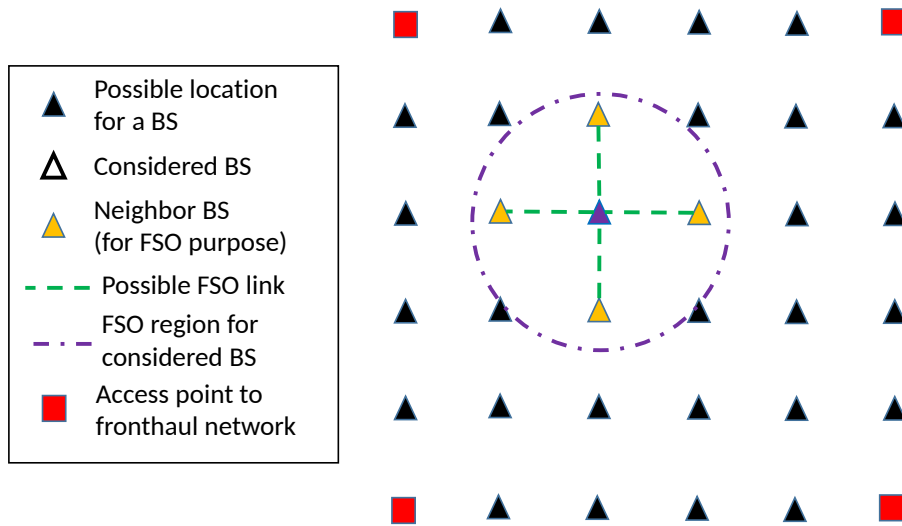
Figure 3.2: Example of FSO LoS region.

The proposed framework supports both wired and wireless transport solutions. High capacity wireless solutions like mmWave or FSO equipment may be employed and require knowledge of the LoS between points on the map. In fact, obstacles in between transmitter and receiver can block signals degrading the performance of the network. Therefore, a parameter telling whether there is LoS or not is required, and wireless connections are allowed only over those links. In the proposed framework, the LoS is modeled by means of two parameters, namely LoS *radius* and *probability*. By looking at Figure 3.2, it is possible to see a circular region, determined by a radius, that can be defined for each BS. BSs outside the LoS area are considered not to be in LoS with the considered BS. The BSs within this area are in LoS with a certain probability (i.e., the link connecting the two BSs exists with a given probability). A certain LoS probability is obtained by using a random variable following an uniform distribution between 0 and 100. Given the typical (short) distances considered for areas hosting special events, it is here assumed that when two points are in LoS they keep the condition for the whole operational time. Wired connections are also included in this framework and require knowledge of the surrounding area, to know where it is allowed to trench fibers, and already deployed infrastructure (e.g., fiber ducts) that can be reused, aiming at reducing the deployment cost. Mixed solutions are also allowed, where part of a fronthaul link is wireless and part employs fiber cables.

3.2 Deployment Problem and Optimal Solution

3.2.1 Problem Definition

Given a generic deployment scenario, the *minimum cost mobile network deployment problem* consists in finding the BSs to activate and the placement of transport network resources (i.e., wired and/or wireless links) to fronthaul the data, such that the total cost to purchase and install BSs, wireless fronthaul devices, and fiber cables is minimized. The solution must guarantee that (*i*) the average bit-rate provided by each BS does not exceed the bit-rate that the BS can carry, (*ii*) at least a certain portion of the area is covered, (*iii*) the overall traffic requirement over the area is satisfied, and (*iv*) a minimum bit-rate can be achieved in each pixel of the coverage grid.

In the following, two ILP-based strategies are proposed to solve the planning problem. The first one, called joint planning (JP), aims at finding the lowest cost solution by finding the best locations for the BSs and the fiber or FSO paths, while considering radio and transport constraints together. The second one, referred to as disjoint planning, is based on a two-step approach in which, firstly, the number of the BSs to be activated is minimized and, secondly, the cost for the fronthaul infrastructure is minimized.

3.2.2 Joint Planning (JP)

Notation:

- S: set of all possible locations for BSs.
- A: set of all possible locations for access points.
- I: set of all possible locations for intersections.
- V: set of possible points on the map. $V = S \cup A \cup I$
- M: set of traffic areas.
- Q_m: set of pixels in the m-th traffic area, $m \in M$.
- Q: set of pixels in which the map is divided. $Q = \bigcup_{m \in M} Q_m$.

Input parameters:

- $a_{i,q}$: received power in pixel q from BS i.

- $b_{i,q}$: 1 if pixel q is within reach of BS i, 0 otherwise.
- C_{bs}: cost for a single BS.
- C_f: cost of fiber cables per unit length.
- C_w: cost of a single wireless device for data fronthaul.
- C_t: cost to trench a unit length.
- γ_{wir}: max number of wireless devices that can be installed over a single pole for fronthaul.
- $d_{i,j}$: distance, in [m], between points $i \in V$ and $j \in V$, equal to 0 if they are not adjacent.
- $g_{i,j}$: 0 if the link between point $i \in V$ and $j \in V$ is given (i.e., is part of the existing infrastructure), 1 otherwise.
- $l_{i,j}^f$: 1 if exists a link that connects point $i \in V$ and $j \in V$, 0 otherwise.
- $l_{i,j}^w$: 1 if point $i \in V$ and $j \in V$ are in line of sight, 0 otherwise.
- L: a large number.
- N: noise power in the used channel expressed in [W].
- $p_{cov} \in [0,1]$: represents the percentage of the total pixels that must be covered.
- R_{cell}: average cell capacity.
- $SINR_{min}$: minimum SINR value that must be guaranteed for all the users.
- $\mathcal{T}_m$: total traffic offered in the sub-area Q_m, $m \in M$.
- $\mathcal{T}_q$: total traffic offered in pixel q. $\sum_{q \in Q_m} \mathcal{T}_q = \mathcal{T}_m, \forall m \in M$

Decision variables:

- $\alpha_i \in \{0,1\} = 1$ if location $i \in S$ is selected to host a BS, 0 otherwise.
- $x_{i,q} \in \{0,1\} = 1$ if pixel $q \in Q$ is covered by BS $i \in S$, 0 otherwise.
- $y_{i,j}^f \in \mathbb{N} =$ number of fibers to be installed between node $i \in V$ and $j \in V$.
- $y_{i,j}^w \in \mathbb{N} =$ number of wireless devices required to transmit from node $i \in V$ to $j \in V$.
- $w_{i,j} \in \mathbb{N} =$ number of wireless devices required at node $i \in V$.
- $z_{i,j} \in \{0,1\} = 1$ if path between node $i \in V$ and $j \in V$ hosts fibers, 0 otherwise.

The minimum cost mobile network placement problem is formulated as follows:

$$\underline{Minimize} \quad C_{bs} \sum_{i \in S} \alpha_i \quad + \quad C_f \sum_{i \in V} \sum_{j \in V} d_{i,j} y_{i,j}^f \quad + \quad C_t \sum_{i \in V} \sum_{j \in V} d_{i,j} z_{i,j} \quad + \quad C_w \sum_{i \in V} w_i, \quad (3.5)$$

The multi-objective function is composed of four members and aims at minimizing the total network deployment cost. In (3.5), the first term is related to the purchasing and installation cost for BSs. The second term accounts for fiber cables while the third term accounts for the fiber trenching and installation costs. Finally, the fourth term takes into account the purchasing and installation cost for wireless devices.

Radio network planning constraints:

$$\sum_{i \in S} \sum_{q \in Q_m} x_{i,q} \geq p_{cov_m} \cdot |Q_m|, \forall m \in M \tag{3.6}$$

$$x_{i,q} \leq \alpha_i \cdot b_{i,q}, \forall i \in S, q \in Q \tag{3.7}$$

$$\sum_{i \in S} x_{i,q} \leq 1, \forall q \in Q \tag{3.8}$$

$$\sum_{q \in Q} x_{i,q} \cdot \mathcal{T}_q \leq R_{cell}, \forall i \in S \tag{3.9}$$

$$\sum_{i \in S} \alpha_i \geq \sum_{m \in M} p_{cov_m} \cdot \frac{\mathcal{T}_m}{R_{cell}} \tag{3.10}$$

$$\sum_{i \in S} x_{i,q} a_{i,q} + L \cdot \left(1 - \sum_{i \in S} x_{i,q}\right) \geq SINR_{min} \cdot \left(\sum_{i \in S} \alpha_i a_{i,q} - \sum_{i \in S} x_{i,q} a_{i,q} + N\right), \forall q \in Q \tag{3.11}$$

Constraint (3.6) ensures that at least a certain percentage of the total area is covered. In order to ensure the same coverage probability in all the traffic areas, p_{cov_m} percent of the pixels composing the m-th area must be covered. Constraint (3.7) ensures that the BS-pixel assignment can be performed if and only if the pixel is within the BS reach (i.e., the received power from the BS is higher than the receiver sensitivity). Constraint (3.8) imposes that each pixel is assigned to only one BS, in order to avoid waste of radio resources. It is worth noting that if a pixel is split in two (or more) new pixels, each of them can be assigned to a different BS, realizing a different radio resource allocation. Constraint (3.9) guarantees that the total number of pixels assigned to each BS, which is related to the total traffic requirement for a BS, does not exceed the maximum number of pixels that a BS can cover, due to its finite capacity. Constraint (3.10) sets a lower bound on the minimum number of BSs that are required to cover the area, which depends on the total traffic and on the capacity provided by each BS. This constraint is not necessary to find a feasible solution, but helps the solver in finding solutions in a less time by removing a part of the solution space that is infeasible. Constraint (3.11) ensures that the $SINR$ in each pixel covered by a BS is greater than $SINR_{min}$.

Transport network planning constraints:

$$\sum_{i \in V}(y_{i,v}^f + y_{i,v}^w) - \sum_{i \in V}(y_{v,j}^f + y_{v,j}^w) =$$

$$= \begin{cases} \leq 0 & \text{if } v \in A & \text{(3.12a)} \\ 0 & \text{if } v \in I - A - S & \text{(3.12b)} \\ \alpha_v & \text{if } v \in S - A & \text{(3.12c)} \end{cases}$$

$$y_{v,v}^f + y_{v,v}^w \leq \alpha_v, \forall v \in A \cap S \tag{3.13}$$

$$\sum_{i \in S} \alpha_i = \sum_{v \in A} \sum_{j \in V}(y_{v,j}^f + y_{v,j}^w) \tag{3.14}$$

$$y_{i,j}^f \leq |S| \cdot l_{i,j}^f, \forall i, j \in V \tag{3.15}$$

$$y_{i,j}^w \leq |S| \cdot l_{i,j}^w, \forall i, j \in V \tag{3.16}$$

$$z_{i,j} \leq y_{i,j}^f \cdot g_{i,j}, \forall i, j \in V \tag{3.17}$$

$$z_{i,j} \geq \frac{y_{i,j}^f \cdot g_{i,j}}{|S|}, \forall i, j \in V \tag{3.18}$$

$$w_i \geq \sum_{j \in V} y_{i,j}^w + \sum_{j \in V} y_{j,i}^w, \forall i \in V \tag{3.19}$$

$$w_i \leq \gamma_{wir}, \forall i \in V \tag{3.20}$$

Constraint (3.12) guarantees that each BS is connected to an access point. This constraint assumes a point to point link, either wireless or wired, originating at an access point and terminating at a BS site. The left hand side of the constraint represents, for a node v, the difference between the sum of the number of incoming and outgoing links. The right hand considers three cases. If node v is an access point (constraint (3.12a)), then the difference between incoming and outgoing links should be lower or equal than 0. It is equal to 0 if v is not used, if v hosts a BS to which it is connected to, or if it is used as an intersection point. It is lower than 0 when the number of outgoing links is greater than the one of incoming links (i.e., the case in which v is connected to at least one BS). If v is an intersection point

(constraint (3.12b)), then the number of incoming links equals the number of outgoing links and their difference must be 0. If v is a possible location for a BS (constraint (3.12c)), but not an access point, a link may be required for that node, depending on whether v hosts a BS or not (i.e., a situation described by α_v). If BS v is active, one link is required to connect that node to the fronthaul network. Therefore, the difference between the number of outgoing and incoming links in v must be 1. If BS v is not active, the difference must be 0, since no links are required for that site. It should be noticed that constraint (3.12) does not limit the number of links for an access point that is selected to host a BS. Therefore, constraint (3.13) is introduced to set this number to 1. Constraint (3.14) guarantees that the number of active BSs is equal to the sum of outgoing links from all the access points. Constraint (3.15) makes sure that fibers are assigned only to existing links while constraints (3.16) guarantees that wireless links are selected only if there is LoS between the nodes. Constraints (3.17) and (3.18) ensures that the trenching is performed only for the links that require it. Constraint (3.19) counts the number of wireless devices required by the solution. Constraint (3.20) limits the number of wireless devices to be installed in each node to γ_{wir}.

Finally, the following constraints are applied to ensure the feasibility of the solution.

$$y_{i,j}^f \geq 0, y_{i,j}^w \geq 0, \forall i, j \in V \tag{3.21}$$

$$w_i \geq 0, \forall i \in V \tag{3.22}$$

3.2.3 Disjoint Planning (DP)

This strategy resembles a conventional deployment approach composed of two separate phases. In the first step, only the minimization of active BSs is considered and the radio network planning constraints (from (3.6) to (3.11), and (3.22)) are imposed. The related objective function is as follows:

$$\underline{Minimize}\ C_{bs} \sum_{i \in S} \alpha_i. \tag{3.23}$$

The outcome of this step is the vector w containing the BS placement. In the second step, the objective is the minimization of the transport network cost:

$$\underline{Minimize} \qquad C_w \sum_{i \in V} w_i \qquad + \qquad C_f \sum_{i \in V} \sum_{j \in V} d_{i,j} y_{i,j}^f \qquad + \qquad C_t \sum_{i \in V} \sum_{j \in V} d_{i,j} z_{i,j}. \tag{3.24}$$

The outcome of the previous step is imposed by adding a set of constraint to set $w_i = 1$ or $w_i = 0$ if the BS location i has been selected or not, respectively. Transport network planning constraints (from (3.12) to (3.21)) are also imposed.

3.3   Strategy Evaluation in a Dense Urban Scenario

The area under consideration is depicted in Figure 3.1. The size of the scenario is 200 x 200 $[m^2]$, which is suitable to model a park or a public square. This area is divided in 10 x 10 pixels to form the coverage grid. The values of the received power in each pixel is computed applying the same formula used in the Open Air Festival case in [53], considering LoS between users and BS sites. All the parameters have been set according to the values in Table 3.1 and derived from [1] and [2]. For the simulations, a system that works at 15 $[GHz]$ with 500 $[MHz]$ aggregated bandwidth (FDD mode) is considered. The possible locations for a BS site are considered to be the intersections formed by the grid used for the received power calculation, as shown in Figure 3.1. The antennas are omnidirectional and the emitted power is 1 $[W]$, while the average capacity per cell equals 4.875 $[Gbps]$, computed using the formula reported in [1] for a small cell. The receiver sensitivity at the user side is set to 10^{-10} $[mW]$ while the thermal noise is -174 $[dBm/Hz]$. The minimum data rate to be guaranteed in each pixel is 300 $[Mbps]$ while 3 different traffic requirements over the area are considered $\{10, 20, 30\}$ $[Gbps]$. For example,

Table 3.1: Input parameters, requirements, and normalized cost of network components [1, 2].

Parameter	Value
Small cell emitted power [W]	1
Small cell average rate [Mbps]	1200
Small cell antenna height [m]	10
Carrier frequency [GHz]	15
Bandwidth [MHz]	500
User antenna height [m]	1.5
User receiver sensitivity [mW]	10^{-10}
Thermal noise [dBm/Hz]	-174
Minimum data-rate for each pixel [Mbps]	300
Offered traffic [Gbps]	{10, 20, 30}
Min. % of the area to be covered	90

Component	Cost [CU]
Fiber cable [m]	1
Fiber trenching [m]	1300
Small cell (RRU+BBU)	16000
Single FSO device	5000

$\mathcal{T} = 30$ [$Gbps$] corresponds to a traffic of 750 [$Gbps/km^2$], which is the expected traffic density for broadband access in dense areas for the next generation of mobile network [7]. Two distinct traffic areas have been considered, as reported in Figure 3.1, where the traffic is divided equally in two, to simulate a more dense area in the center of the map. The traffic over the area is then increased to simulate a possible infrastructure upgrade or an increment due to a special event in place.

Each problem formulation is solved using CPLEX [54]. The numerical results are averaged over 100 different cases where the LoS is randomly applied in each link. The obtained confidence interval is always less than 5% with a confidence level of 95%.

Figure 3.3 depicts the total cost, in cost units, of the solution obtained using the JP and DP strategies for different LoS probabilities, when the LoS radius is fixed to 50 [m]. It is possible to notice that the joint strategy always overcomes the disjoint approach. This is due to the fact that the joint approach considers the position of the existing infrastructure (the access points) in the radio deployment, thus it is always able to find a solution where the antennas are close to these points. From the figure, it is also possible to observe that the higher the LoS probability,
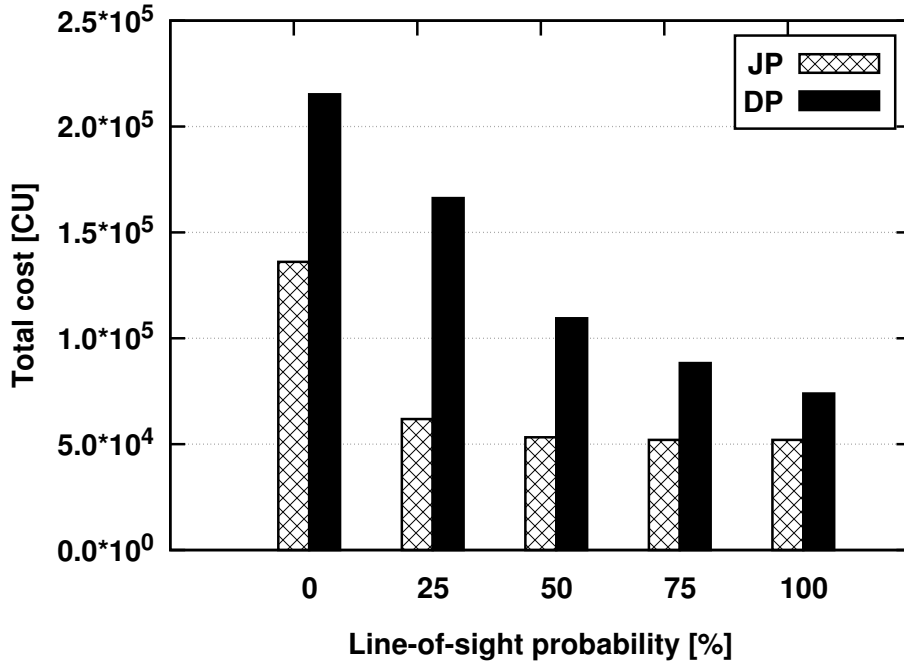
Figure 3.3: Total network deployment cost for traffic requirement 10 [*Gbps*] as a function of LoS probability among FSO devices within 50 [*m*] radius.

the lower is the difference between the two strategies. In fact, when LoS exists between couples of points on the map, FSO devices can be used instead of fiber cables, thus avoiding expensive and time consuming fiber trenching. In addition to this, it can be noticed that even a low LoS probability is sufficient to considerably reduce the costs and, in general, the higher the LoS probability, the lower is the difference between the two strategies. However, even when 100% LoS is available, the DP strategy is not aware of the location of the access points, thus requires multiple hops with FSO devices to reach them.

Similarly to Figure 3.3, Figures 3.4 and 3.5 show the total cost, for the two strategies, as a function of different LoS probabilities for 50 [*m*] LoS radius when the traffic requirement is 20 and 30 [*Gbps*], respectively. From the Figures, it is possible to notice that by increasing the traffic requirement the total cost of the two solutions increases while the difference between them slightly decreases. In the worst case (i.e., when the LoS probability is 25%), the cost of the JP strategy, with respect to the 10 [*Gbps*] traffic requirement, is 123% and 271% higher in case 20 [*Gbps*] and 30 [*Gbps*], respectively. This is due to the fact that more equipment is required with respect to the 10 [*Gbps*] case. Increasing the amount of equipment creates a more
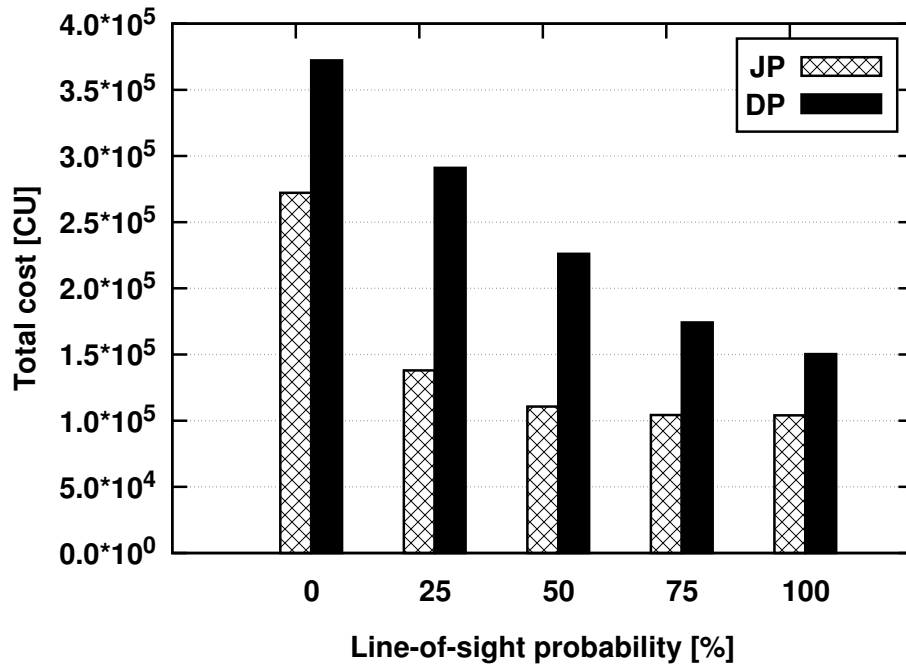
Figure 3.4: Total network deployment cost for traffic requirement 20 [*Gbps*] as a function of LoS probability among FSO devices within 50 [*m*] radius.

dense scenario, in which more BSs are deployed, slightly reducing the advantages of the JP strategy. To show this aspect, Table 3.2 reports the cost increment, defined as the percentage of the JP cost that has to be added to the JP solution to obtain the DP cost, for different values of LoS probability when LoS radius is fixed to 50 [*m*]. When only fiber cables can be used (i.e., LoS probability equal to 0%), the DP strategy requires 58%, 36% and 21% additional cost, with respect to the JP solution, in case of traffic requirements 10, 20 and 30 [*Gbps*] over the area, respectively. When LoS is available with low probability, like in the case 25% or 50%, the cost increment of the DP strategy dramatically increases, even tough the total cost is reduced with respect to the case with LoS probability 0%. The reason behind this lies in the fact that knowing in advance which BS locations can be connected to the transport network by means of FSO devices is a great advantage, because those BS locations can be selected, avoiding expensive fiber trenching and multi-hops with FSO devices. Further increasing the LoS probability reduces the cost increment in all cases because it becomes easier to fronthaul data with FSO devices, and fiber trenching is not required. In particular, under 100% LoS probability condition, the lowest experienced cost increment is 42%, showing remarkable cost
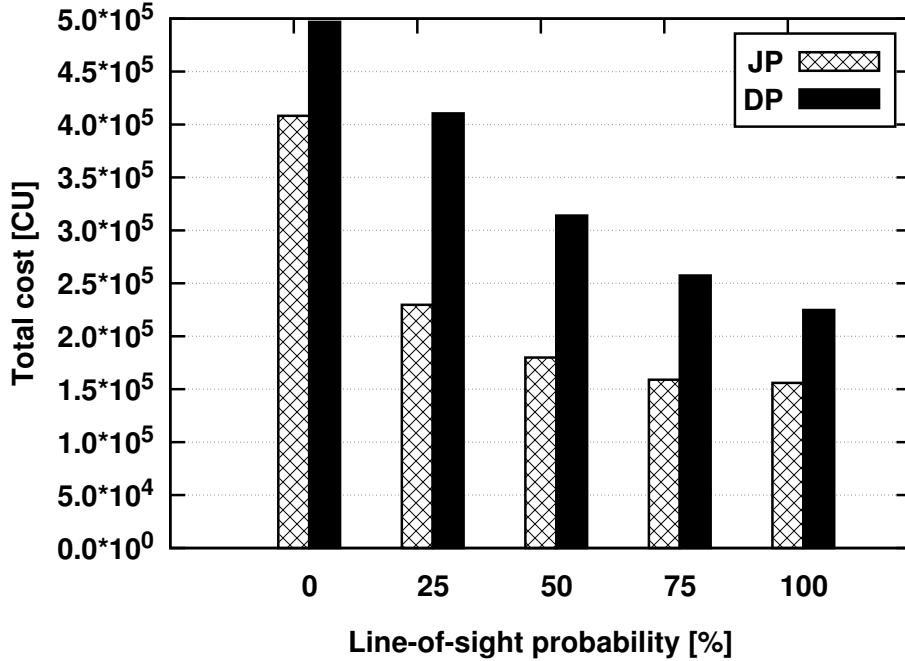
Figure 3.5: Total network deployment cost for traffic requirement 30 [*Gbps*] as a function of LoS probability among FSO devices within 50 [*m*] radius.

Table 3.2: Cost increment for different LoS probabilities under 3 traffic requirements when LoS radius is 50 [*m*].

LoS probability	Increment		
	10G	20G	30G
0%	58%	36%	21%
25%	168%	110%	78%
50%	105%	104%	74%
75%	69%	67%	61%
100%	42%	44%	44%

savings can be achieved through a JP design even in cases where no fiber is required.

In order to understand the effects of the LoS radius on the network cost, Tables 3.3, 3.4 and 3.5 report the deployment costs with the three traffic requirements for different LoS probabilities when the LoS radius is set to 75 [*m*]. The case of LoS probability equal to 0% is not reported as LoS radius has no impact and the results are the same as the ones presented before. Similarly to the case with LoS radius equal to 50 [*m*], the JP strategy overcome the DP approach and the cost decreases when the LoS probability increases. On the contrary, the cost increment shows that the DP solution is closer to the one provided by the JP when compared to the

Table 3.3: Cost, in CU, for the different deployment strategies under different LoS probabilities when the traffic requirement is 10 [*Gbps*] and LoS radius is 75 [*m*].

LoS probability in %	Strategy	Cost [CU] 10 G			
		Radio	Transport	Total	Increment
25	JP	32000	23344	55344	116%
	DP	32000	88092	120092	
50	JP	32000	20000	52000	63%
	DP	32000	52887	84887	
75	JP	32000	20000	52000	32%
	DP	32000	37141	69141	
100	JP	32000	20000	52000	21%
	DP	32000	31200	63200	

Table 3.4: Cost, in CU, for the different deployment strategies under different LoS probabilities when the traffic requirement is 20 [*Gbps*] and LoS radius is 75 [*m*].

LoS probability in %	Strategy	Cost [CU] 20 G			
		Radio	Transport	Total	Increment
25	JP	64000	58130	122130	86%
	DP	64000	163672	227672	
50	JP	64000	41100	105100	54%
	DP	64000	98163	162163	
75	JP	64000	40000	104000	33%
	DP	64000	74621	138621	
100	JP	64000	40000	104000	21%
	DP	64000	64100	128100	

cost increment of the 50 [*m*] cases. This is due to the fact that the larger the LoS radius, the easier is to reach access points with FSO devices in few hops. In the worst case, that is when LoS probability is 100%, the cost increment is between 21% and 23% for the three traffic requirements, showing remarkable cost savings can be achieved also with higher radius when the LoS conditions are favorable. On the one hand, further increasing the LoS radius would further reduce the increment. On the other hand, many studies show that FSO devices are usually limited in range, due to weather conditions and obstacles [34] [33], thus considering a LoS probability of 75% or higher for radius of hundreds of meters is not likely to be a real case for urban scenarios.

Table 3.5: Cost, in CU, for the different deployment strategies under different LoS probabilities when the traffic requirement is 30 [*Gbps*] and LoS radius is 75 [*m*].

LoS probability in %	Strategy	Cost [CU] 30 G			
		Radio	Transport	Total	Increment
25	JP	96000	100491	196491	69%
	DP	96000	236879	332879	
50	JP	96000	67575	163575	49%
	DP	96000	148850	244850	
75	JP	96000	60400	156400	31%
	DP	96000	110304	206304	
100	JP	96000	60000	156000	23%
	DP	96000	96700	192700	

Figure 3.6 reports the total cost obtained with the JP strategy, for different values of LoS probability, as a function of different capacity increments, using as initial scenario the one obtained in the case 10 [*Gbps*] with 0% LoS. This case can be considered as a brownfield scenario, that is a scenario in which antennas and fiber cables are already deployed, but not sufficient to satisfy the new requirements, and therefore the infrastructure must be upgraded. The capacity increment is the additional capacity that is required with respect to the 10 [*Gbps*] case. The case 0% LoS represents the case in which FSO devices cannot be used, and therefore is the most expensive. Moreover, the difference with the LoS cases increases with the capacity increment. From the figure, it is also possible to notice that, for a capacity increment of 50% and 100%, a LoS probability of 25% is sufficient to ensure optimality. For higher traffic demands instead, the increment of the network equipment requires higher LoS probability to provide fronthaul connections by means of FSO devices only, requiring fiber trenching in lower LoS probability cases. As a final note, the reported solution for the case 400% of capacity increment, when LoS probability is 25% and 50%, the solution gap provided by CPLEX after 24 hours is 5%, showing a complexity of the problem when the solution space is large (i.e., when many multiple options are feasible).

To see the impact of each network component on the total cost, Table 3.6 reports the cost breakdown for 0% and 25% LoS when the capacity increment is 250%. From the table, it is possible to see how the fiber and fiber trenching costs decrease when the LoS probability
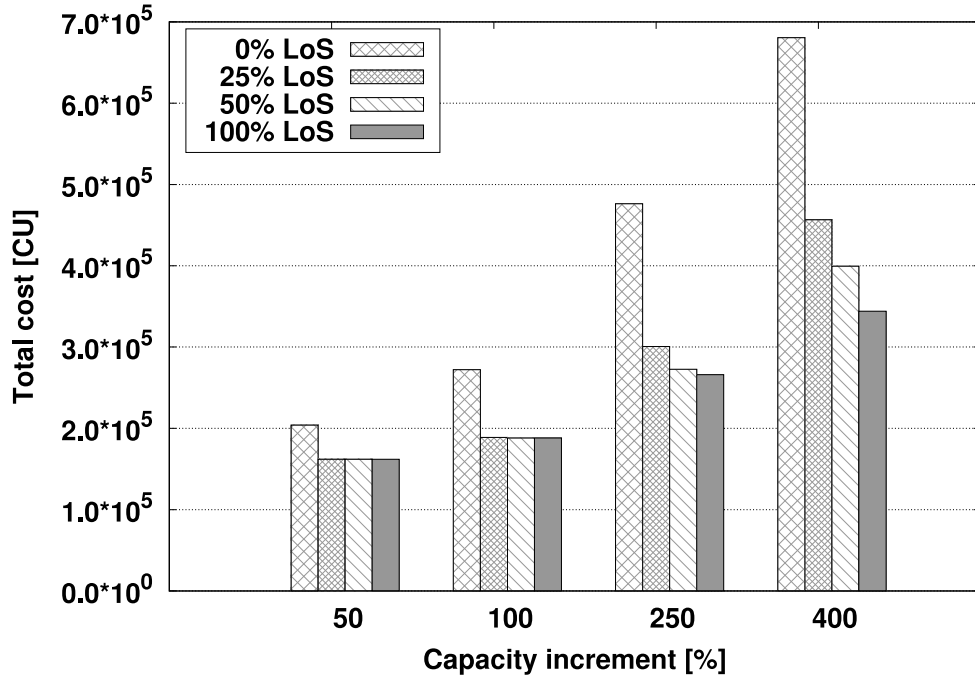
Figure 3.6: Total cost obtained by the JP strategy with different LoS probabilities and LoS radius equal to 75 [*m*], as a function of different capacity increments using as a starting deployment the JP case (0% LoS) in Figure 3.3.

Table 3.6: Equipment cost breakdown for different LoS probabilities with 250% traffic increment when LoS radius is 75 [*m*].

LoS probability	Network component cost [CU]			
	Radio equipment	Trenching	Fibers	FSO devices
0%	112000	364000	280	0
25%	113280	122720	153	64400
50%	112160	104000	99	56500
100%	112000	104000	80	50000

increases. To a higher LoS probability corresponds a lower cost for FSO devices, as more devices are in LoS and it is easier to reach the access points.

For completeness, also the impact of a different propagation environment has been evaluated. An area with vegetation has been considered with a diameter of 30 [*m*]. The empirical results included in [50] have been used as a reference values for the attenuation introduced by leaves and trees. The results of this evaluation are reported in Table 3.7 for the traffic requirements 10 [*Gbps*] and 30 [*Gbps*] considering only fiber infrastructure. From the figure, it is possible to observe that the impact of the added attenuation seems to be very limited when compared to

Table 3.7: Cost obtained by running JP and DP strategies with additional attenuation due to vegetation in the park. Results are for the cases 10 [*Gbps*] and 30 [*Gbps*] requirements using only fibers.

	Cost [CU]	
Strategy	**10G**	**30G**
JP	136080	215734
DP	408240	496973

the results in Figures 3.3 and 3.5. This is because of the limited size of the scenario, where the introduced attenuation is not sufficient to substantially change the received useful power and, consequently, the deployment.

As a final remark, the proposed model is capable of providing optimal solutions in dense urban scenarios, where several BSs must be deployed to provide high speed connectivity in limited areas. The benefits of a joint approach have been shown in comparison to a conventional two step approach. However, when dealing with large scenarios, the applicability of the proposed model may be limited by high computational resources required to solve the large problem instances, as shown also in [55]. Allowing several different options for fronthaul further enlarges the solution space, increasing the time to evaluate all different possibilities. In the case of large instances, network planning area must be decomposed in sub-areas and so that the problem can be tackled in small pieces. Alternatively, ad-hoc heuristics could be developed, allowing to reach near-optimal solutions even in large scenarios.

Chapter 4

Indoor Capacity Provisioning for Residential Areas

As already shown in the previous Chapter, network densification increases the performance of the network. However, it is well known that radio signals experience high attenuation when penetrating walls [56] [57] [58]. A cost effective solution to cover indoor areas could be to use Wi-Fi access points of end users already connected to the fixed telephony network. However, this is not a feasible solution, due to high latency [59] and lack of efficient interference management, that significantly degrades the performance when the number of Wi-Fi access points and users increases [60] [61]. In recent years, operators proposed a solution based on small size and low energy cells, called femto cells. Conventional indoor small cells are user-deployed and are connected to the operators core networks through a fixed broadband infrastructure. However, these cells have no ability to coordinate among themselves or with the macro BSs. As a result, the overall mobile network performance is degraded because of the high interference levels among neighboring cells and between small cells and other macro BSs. As inter-cell interference has become one of the limiting factors of cellular systems, to further maximize the capacity some traffic management mechanisms were introduced such as coordinated multipoint (CoMP) and enhanced inter-cell interference coordination (eICIC). The key idea of such mechanisms is to offload traffic from the macro-cell to the high capacity small cells even if the reference

signal received power from a small cell is lower [62]. These techniques require coordination mechanisms among macro and small cells.

C-RAN, with its efficient coordination mechanisms, is therefore a promising candidate to cover indoor areas. Big companies like Ericsson and Huawei have already provided 5G centralized based architectures to cover commercial areas like shopping malls, sports arenas and offices [63] [64]. However, a massive deployment of such networks in residential areas may be extremely expensive if not planned carefully, due to the large amount of network equipment. To reduce network cost, the reuse of existing in-building infrastructure (e.g., already deployed LAN cables) can be combined with efficient deployment strategies to drastically reduce the amount of necessary network equipment.

Motivated by this, in this Chapter the concept of centralized radio architecture (CRA) for indoor is introduced and used to cover buildings in residential urban scenarios. In particular, optimized and approximated solutions for the indoor mobile network deployment are proposed, focusing on their deployment cost[1].

4.1   Centralized Radio Architecture for Indoor

The CRA architecture that has been used in this thesis is based on the Centralization concept and is suitable to cover the indoor areas of buildings is depicted in Figure 4.1.

The CRA is made up of three main blocks: the indoor antennas, the RRUs, and the BBUs. Antennas are ultra compact, equipped with a small power amplifier, and they provide high-capacity wireless access to a relatively large indoor area (i.e., 500 to 800 $[m^2]$). Antennas are connected to RRUs, which perform analog signal processing of the radio signal; a single RRU can be connected to at most k antennas. RRU communicates with the antennas via analog transmission over a standard copper cable (e.g., Ethernet cable Cat 5/6/7) that allows to reuse the existing copper infrastructure inside a building. However, copper cables are subject to high attenuation imposing a limitation on the maximum length of the links between the antennas

---

[1]The outcome of this work is included in [65], [66], [67].
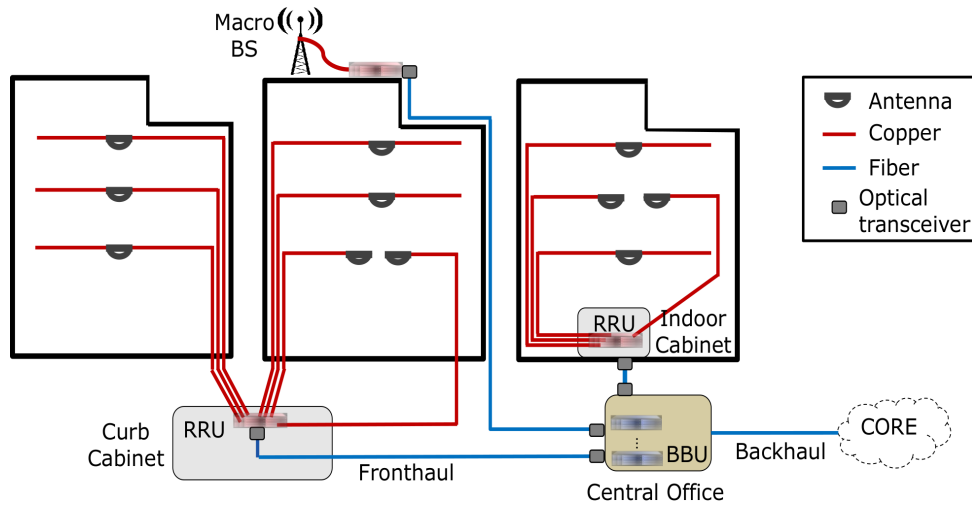
Figure 4.1: The centralized radio architecture (CRA) concept.

and the RRU (i.e., a few tens of meters depending on the category of the copper cable). RRUs are connected to BBUs in charge of performing the digital baseband processing, which includes interference management and cells coordination.

This architecture is based on C-RAN concept; the fronthaul segment that connects a RRU and a BBU uses D-RoF techniques and CPRI as a interface that limit the maximum length of the fiber link to 20 $[km]$. The centralized approach allows to place multiple BBUs in a single BBU hotel so that a single BBU hotel may cover an entire residential area. In a BBU hotel, it is possible to share BBU resources among RRUs and macro BSs in order to achieve better radio performance and to reduce the number of sites that an operator needs. In addition, having all BBUs in the same site allows to share power supply, cooling, and interconnection network equipment. For this reason the CRA concept is a feasible way to reduce both capital and operational expenditure of mobile operators. However, increasing the distance between BBUs and RRUs leads to a higher amount of fiber cables required in the fronthaul network, which may translate into higher deployment costs for the transport network. Finally, the last segment of the network that connects BBU with the core network is a packet-based traditional backhaul.

The origins of the CRA concept can be traced back to [68], where the authors proposed a new paradigm called FemtoWoC (Femto Wireless over Cable). The proposed architecture did not introduce a real separation of radio and baseband units, but proposes to leave the analog RF processing (i.e., antenna and analog-to-analog converter) at the in-home device, transporting

analog signals to a remote location. This study proves that it is possible to re-use existing copper infrastructure in indoor mobile network deployments, that can be exploited to reduce network costs.

A CRA-based system was introduced in [69], where the authors proposed to use Ethernet cables to carry intermediate frequency (IF) signals between antennas and RRUs. The experimental results presented in the article show that IF signals can be sent over Cat. 6a cables over distances longer than 100 $[m]$. LTE signal propagation over Ethernet cables (Cat-5/6/7) is analyzed in [70], where the authors investigate the maximum available bandwidth and the maximum number of antenna flows that can be transported over LAN cables of different lengths (up to 200 $[m]$). Results showed that for 75 $[m]$ almost no degradation is experienced in Ethernet cables, and at least 60 antennas using 20 $[MHz]$ LTE channels can be served by a single 100 $[m]$ Ethernet cable, with this number decreasing rapidly for larger distances. Further analysis of a mobile indoor system architecture based on the CRA concept, can be found in [71, 72] and show that twisted pairs copper lines in CRA can be used in ranges of 300 $[m]$ if crosstalk mitigation and cancellation techniques are applied.

4.1.1 CRA Planning Problem Description

While in the case of C-RAN the position of the BBUs is the only variable to consider, the position of the RRUs is an additional key parameter to consider in CRA, which increases the complexity of the network deployment problem. So far, only a few works on CRA network deployment have been proposed. BBU placement strategies based on ILP and heuristic were proposed in [73], where the authors aimed at minimizing the cost for BBUs and fibers by placing BBU sites only in selected buildings. However, in this strategy BBUs are not fully centralized in hotels, which may lead to coordination problems with macro BSs in the area. Optimal placement of RRUs was not addressed in this work.

In the following, the deployment of a CRA in a residential *greenfield* scenario with no existing network infrastructure other than the copper inside the buildings, e.g., pre-installed Ethernet
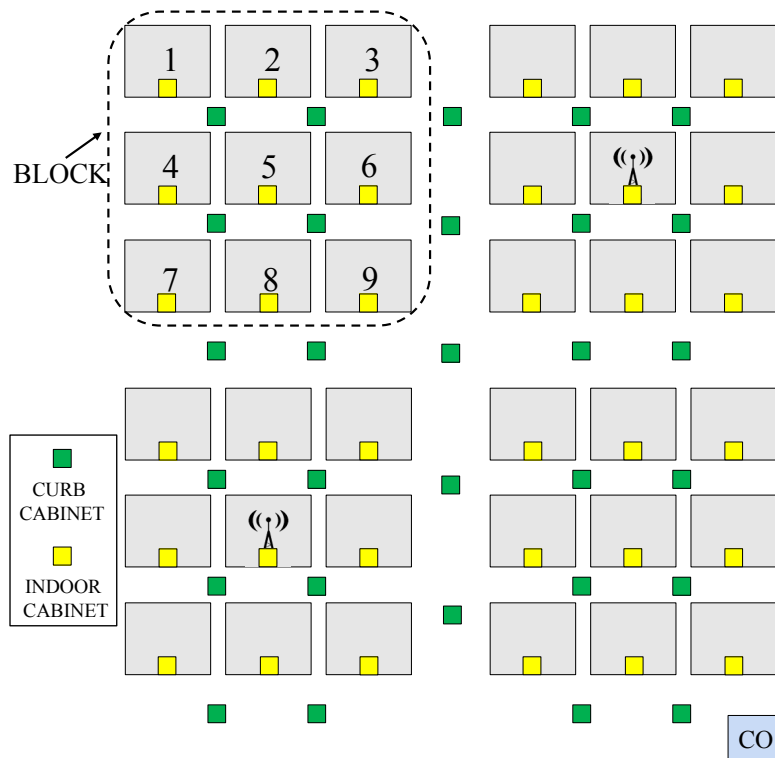
Figure 4.2: View from the top of a possible scenario considered in the study.

cables, is studied. Figure 4.2 depicts a schematic view (from the top) of the considered residential area, where the grey squares represent the buildings. It is here assumed that one or more indoor antennas are placed in each floor of every building to provide broadband wireless access to the indoor users. Depending on the distance limitations of the copper links, RRUs can be placed either in indoor cabinets or in curb cabinets located nearby (denoted with the yellow and green squares in Figure 4.2, respectively). When inside a building, RRUs are placed at the entrance, where they can be connected to the in-building copper infrastructure. In this case a RRU can be connected only to antennas located in the same building. A RRU placed in a curb cabinet can be connected to antennas in different buildings, which increases the sharing factor of the RRUs, provided that their distances from antennas are shorter than the maximum allowed length of the copper link. In this work, the cabinets that host one or more RRUs are referred to as active cabinets. To serve the outdoor users in the residential area macro BSs are placed on the top of some of the buildings. Moreover, a CO owned by the mobile operator is set up in the area. All BBUs are placed in the CO and serve the whole residential area (i.e., all RRUs and macro BSs). This is possible under the assumption that the maximum distance between RRUs, macro BSs, and the CO is lower than the maximum reach of a fronthaul link

(i.e., 20 km), which is typically the case in urban scenarios.

In order to calculate the length of fiber/copper, the Taxicab geometry formula is used, also known as l_1 norm. For example, given a 3D space and two points (x_1, y_1, z_1) and (x_2, y_2, z_2), the length of fiber/copper d needed to connect these two points is computed as:

$$d = |x_1 - x_2| + |y_1 - y_2| + |z_1 - z_2| \tag{4.1}$$

Formula (4.1) is also used to obtain the distance between an antenna and a RRU located inside a building. The distance between an antenna and a RRU located in a curb cabinet is computed as the sum of: *(i)* the distance from the antenna to the entrance of the building and *(ii)* the distance from the entrance of the building to the curb cabinet, both computed using (4.1).

The placement of RRUs directly impacts the overall network cost by affecting: *(i)* the total length of copper and fiber cables to be deployed, *(ii)* the amount of network equipment to buy/operate (i.e., the total number of RRU and BBU units in the network), and *(iii)* the number of cabinets to activate and manage (i.e., the total number of RRU sites). Therefore, the minimization of the network cost requires judicious policies for solving the cost-minimizing RRU placement problem.

4.2   Optimal Placement Problem

4.2.1   RRU Placement (RRUP) Problem Definition

Given a set of possible RRU locations R, the set of antennas A to connect, and the maximum distance D allowed between antennas and RRUs, the objective of the RRU placement problem is to select which cabinets to activate for RRU deployment and which antenna to assign to each RRU such that the total amount of radio resources (i.e., number of RRU and active cabinets) is minimized. A solution must guarantee that each antenna is connected to one RRU while making sure that the distance between any RRU and the antenna it is covering does not exceed D.

4.2.2 ILP Formulation for the RRU Placement Problem (RRUP-ILP)

Notation:

- R : set of possible RRU cabinets; each cabinet can host 1 or more RRUs.
- A : set of antenna locations.
- D : maximum allowable distance between a RRU and an antenna.
- d_{ij} : distance between a candidate RRU cabinet $i \in R$ and an antenna $j \in A$.

Input parameters:

- $C[|R| \times |A|]$: coverage matrix, where $C_{ij} = 1$ if a RRU placed in cabinet $i \in R$ can cover antenna $j \in A$, i.e., if $d_{ij} \leq D$, 0 otherwise.
- $M \in \mathbb{N}$: a large number (e.g., 10000).
- $\alpha, \beta \in \mathbb{N}$: tuning parameters.
- $k \in \mathbb{N}$: maximum number of antennas that can be connected to a RRU.

Decision variables:

- $m_{ij} \in \{0, 1\} = 1$ if a RRU placed in cabinet $i \in R$ is covering antenna $j \in A$; 0 otherwise.
- $r_i \in \mathbb{N} =$ the number of RRUs placed in cabinet $i \in R$.
- $z_i \in \{0, 1\} = 1$ if at least one RRU is placed in cabinet $i \in R$; 0 otherwise.

The RRU placement problem is formulated as follows:

$$Minimize \ \ \alpha \cdot \sum_{i \in R} r_i + \beta \cdot \sum_{i \in R} z_i \tag{4.2}$$

The objective of RRUP-ILP, modelled by the objective function (4.2), is to minimize the total number of RRU cabinets to be activated and the total number of RRUs to be deployed. Parameters α, β balance the contributions of the two components of the objective function.

Subject to the following constraints:

$$\sum_{i \in R} C_{ij} m_{ij} = 1, \forall j \in A \tag{4.3}$$

$$k \cdot r_i \geq \sum_{j \in A} C_{ij} m_{ij}, \forall i \in R \tag{4.4}$$

$$M \cdot z_i \geq r_i, \forall i \in R \tag{4.5}$$

$$r_i \geq 0, \forall i \in R \tag{4.6}$$

Constraint (4.3) guarantees that each antenna in the network is covered by a RRU within the reach. Constraint (4.4) ensures that the RRUs placed in cabinet i cover all antennas which are assigned to that cabinet. Constraint (4.5) models the deployment of RRUs in cabinet i by marking only the locations that host the selected RRUs as active. Finally, constraint (4.6) guarantees the feasibility of the solution.

4.2.3   Proof of RRUP NP-Hardness

Following the antenna-cabinet assignment modelled by matrix C, the RRU placement problem can be seen as a variation of the Set Cover Problem (SCP) [74, 75], which is NP-hard [76]. Consequentially, RRUP is also NP-hard.

In order to prove NP-hardness of the RRUP problem, let's first decompose it into two sub-problems, denoted as RRUP_{CAB} and RRUP_{RRU}. RRUP_{CAB} refers to the problem of finding a minimum number of cabinets to host the RRUs, while RRUP_{RRU} refers to the placement of a minimum number of RRUs at the locations selected by RRUP_{CAB}. In this section, the complexity of the RRUP problem is shown by proving that the RRUP_{CAB} sub-problem is NP-hard.

RRUP_{CAB} takes as input a set of antennas $A = \{a_1, a_2, ..., a_n\}$ and a collection of possible cabinet locations $\mathcal{R} = \{R_1, R_2, ..., R_m\}$, where R_i contains a subset of antennas within reach of cabinet i. Every antenna is within reach of at least one cabinet location, i.e., $\bigcup_{i \in \mathcal{R}} R_i = A$. The output of the problem is a subset $\mathcal{C} \subseteq \mathcal{R}$ with minimum cardinality that covers all antennas, i.e., $\bigcup_{i \in \mathcal{C}} R_i = A$. The NP-hardness of the RRUP_{CAB} is proved by reducing the well-known Set Cover Problem (SCP) to it. An instance of the SCP is defined by a set of elements $U = \{x_1, x_2, ..., x_p\}$ called universe, and a collection of subsets $\mathcal{S} = \{S_1, S_2, ..., S_q\}$ of the universe such that every element of U belongs to at least one subset in $\mathcal{S}$, i.e., $\bigcup_{i \in \mathcal{S}} S_i = U$. The solution of the SCP is a subset $\mathcal{D} \subseteq \mathcal{S}$ with minimum cardinality that guarantees that $\bigcup_{i \in \mathcal{D}} S_i = U$.

To show that RRUP_{CAB} is NP-hard, first it is shown that solving the SCP on the same input

data of RRUP_{CAB} would solve the RRUP_{CAB} problem as well. For this reason let us first assume the following instance of the SCP. Let us build set U as the set of antennas to be covered, i.e., each element $u \in U$ corresponds to an element $a \in A$. Let us also assume that each subset $S_i \in \mathcal{S}$ defines the subset of antennas $a \in A$ reachable from cabinet location i, i.e., by construction set $\mathcal{S}$ and set $\mathcal{R}$ are the same.

By assuming that $\mathcal{D} \in \mathcal{S}$ is a solution of the SCP of U, it is possible build a set $\mathcal{C} \in \mathcal{R}$, where each $S_i \in \mathcal{D}$ corresponds to one $R_i \in \mathcal{C}$. In order for $\mathcal{C}$ to represent a solution of RRUP_{CAB}, $\mathcal{C}$ must cover all antennas and must be of minimal cardinality. The first statement can be derived from $\mathcal{C} = \mathcal{D}$, $\bigcup_{i \in \mathcal{D}} S_i = U$, and $U = A$, which imply that $\bigcup_{i \in \mathcal{C}} R_i = A$. The second statement can be proven by contradiction as follows. Sets $\mathcal{C}$ and $\mathcal{D}$ are constructed so that $|\mathcal{C}| = |\mathcal{D}|$. Let us assume that there is a subset $\mathcal{F} \subseteq \mathcal{R}$ solving the RRUP_{CAB} problem such that $|\mathcal{F}| < |\mathcal{C}|$. If $\mathcal{F}$ is a solution of RRUP_{CAB} this means that $\bigcup_{i \in \mathcal{F}} R_i = A$, but since $A = U$ and $\mathcal{R} = \mathcal{S}$ this also means that $\mathcal{F}$ is a solution of the SCP (i.e., $\bigcup_{i \in \mathcal{F}} S_i = U$), where $|\mathcal{F}| < |\mathcal{D}|$. The last statement contradicts the hypothesis that $\mathcal{D}$ is minimum-sized set cover for U.

To complete the proof, it is shown that a solution of the RRUP_{CAB} problem is also a solution of the same instance of the SCP, which can be derived in a straightforward way. Let us assume that subset $\mathcal{C} \subseteq \mathcal{R}$ solves the RRUP_{CAB} problem. This implies $\bigcup_{i \in \mathcal{C}} R_i = A$, but since $A = U$ and $\mathcal{R} = \mathcal{S}$, it also means that $\bigcup_{i \in \mathcal{C}} S_i = U$, i.e., $\mathcal{C}$ is a solution of the SCP. The minimum cardinality of $\mathcal{C}$ can be proved by contradiction in the same way as it was done before. Let us now assume that there is a subset $\mathcal{F} \subseteq \mathcal{S}$ solving the SCP such that $|\mathcal{F}| < |\mathcal{C}|$. If $\mathcal{F}$ is a solution of SCP this means that $\bigcup_{i \in \mathcal{F}} S_i = U$, but since $U = A$ and $\mathcal{S} = \mathcal{R}$ it also means that $\mathcal{F}$ is a solution of the RRUP_{CAB} problem (i.e., $\bigcup_{i \in \mathcal{F}} R_i = A$), where $|\mathcal{F}| < |\mathcal{C}|$. The last statement contradicts the hypothesis that $\mathcal{C}$ is minimum-sized set that covers all antennas in A.

4.3 Heuristic Strategies

Given the intrinsic np-hardness of the proposed problem, solutions based on heuristic approach can be suitably developed to allow deployment of CRA in large scenarios, where optimization

algorithms are not a viable option due to their computational complexity.

4.3.1   Heuristic solution to the RRU placement problem (RRUP-H)

The proposed heuristic is denoted as RRUP-H. RRUP-H aims at minimizing the number of active cabinets and RRUs needed to cover the area in two subsequent phases. The first phase, referred to as Minimum Location Search (MLS), minimizes the set of RRU cabinets that an operator needs to activate in order to serve the area. The second phase, referred to as Radio Unit Minimization (RUM), minimizes the number of RRUs to be placed in the cabinets selected after running MLS.

The pseudocode of the MLS phase is shown in Algorithm 1. The basic idea behind the approach is to increase the chances of sharing the cabinet locations among multiple antennas by assigning blocks of consecutive antennas to the furthest possible RRU location that satisfies the reach constraint. In the initialization phase, the antennas that belong to the same building block are numbered in sequential order starting from the top left corner of the area, as shown in Figure 4.2. In addition to the notation used by RRUP-ILP, the MLS phase uses the following sets:

- V : for each cabinet i, V_i contains the index of the first unassigned antenna that cannot be connected to i due to the limit on D.

- CS : the solution of MLS, containing all the cabinets used by the algorithm (i.e., RRU placement).

Algorithm 1 RRUP-H - First phase: MLS

1: **Initialization:**
2: $CS \leftarrow \emptyset$
3: $V \leftarrow \emptyset$
4: **Algorithm:**
5: **while** $\sum_{\substack{i \in R \\ j \in A}} C_{ij} > 0$ **do**
6:     **find** min $j \in A$ such that $\sum_{i \in R} C_{ij} > 0$
7:         **compute** $V_i = $ min q such that $C_{iq} = 0$,
    $q \in [j, |A|] \ \forall \ i \in R$
8:     **find** $i \in R$ such that V_i is maximum
9:     **add** i to CS
10:     **for all** $j \in A$ such that $C_{ij} = 1$ **do**
11:         **set** $C_{pj} = 0 \ \forall \ p \in R$
12:     **end for**
13: **end while**
14: **Stop**

The MLS algorithm is executed iteratively until all antennas are covered, i.e., as long as there are non-zero elements in matrix C (line 5). It starts from the lowest-indexed unconnected antenna j, represented by the first column in C containing non-zero elements (line 6). It then searches for the RRU cabinet that covers antenna j and the maximum number of consecutive antennas q, $q > j$. For each cabinet i, the value of V_i is set as the lowest antenna index $q, q > j$ for which C_{iq} is 0 (line 7). The algorithm then selects the RRU location i with the maximum value of V_i, i.e., the cabinet which covers the largest number of consecutive antennas (line 8). As only blocks of consecutive ones are considered, selecting cabinet i guarantees that no antennas are left disconnected after making this choice. The selected cabinet is added to CS (line 9) and all antennas within its reach are removed from matrix C by changing the values of elements C_{ij} from 1 to 0 in all corresponding columns (lines 10 - 12).

The set of cabinets CS obtained by MLS is passed to the Radio Unit Minimization (RUM) phase, aimed at minimizing the number of RRUs placed at the cabinets to cover the area. The idea is to obtain the utilization of RRU ports as close to 100% as possible, in order to reduce the number of unconnected ports and, consequently, the waste of RRU resources. To model the antenna-RRU assignment, RUM uses the following additional structures:

- C' : updated coverage matrix obtained from C by considering only the cabinets included in the solution CS. Element C'_{ij} is equal to 1 if a RRU placed at a selected cabinet i can

cover antenna j, and to 0 if it is out of reach.

- AC : the final solution of RRUP-H, containing the assignment of antennas to cabinets. Each AC_i contains the set of antennas assigned to cabinet i.

Algorithm 2 RRUP-H - Second phase: RUM

1: **Initialization:**
2: $AC \leftarrow \emptyset$
3: **Algorithm:**
4: **for all** $j \in A$ such that $\sum_{i \in CS} C'_{ij} = 1$
5:      **find** $i \in CS$ such that $C'_{ij} = 1$
6:      **add** j to AC_i
7:      **set** C'_{ij} to 0
8: **end for**
9: **for all** $j \in A$
10:      **for all** $i \in CS$ such that $C'_{ij} = 1$
11:         **if** $AC_i.size()$ mod $k \neq 0$
12:            **add** j to AC_i
13:            **set** C'_{ij} to 0 $\forall i \in CS$
14:         **end if**
15:      **end for**
16: **end for**
17: **for all** $i \in CS$
18:      **while** $\sum_{j \in A} C'_{ij} \geqslant k$
19:         **for** $count = 1$ to k
20:            **find** $j \in A$ such that $C'_{ij} = 1$
21:            **add** j to AC_i
22:            **set** C'_{ij} to 0 $\forall i \in CS$
23:         **end for**
24:      **end while**
25: **end for**
26: **while** $\sum_{\substack{i \in CS \\ j \in A}} C'_{ij} > 0$
27:      **find** $i \in CS$ that maximizes $\sum_{j \in A} C'_{ij}$
28:      **for all** $j \in A$ such that $C'_{ij} = 1$
29:         **add** j to AC_i
30:         **set** C'_{ij} to 0 $\forall i \in CS$
31:      **end for**
32: **end while**
33: **Stop**

The pseudocode of the RUM phase is shown in Algorithm 2. It assigns antennas to cabinets and places RRUs at cabinet locations in four steps. The first step (lines 4 - 8) performs assignment of antennas that can be linked to only one cabinet, making sure that RRUs are placed at these indispensable locations. The algorithm identifies such antennas as those whose corresponding columns in C have only a single non-zero element (line 4), and determines their matching cabinets (line 5). The assigned antennas are added to the solution set AC (line 6) and matrix

C' is updated by deleting these antennas (line 7). The second step of RUM (lines 9 - 16) tries to maximize the utilization of the RRUs deployed in step 1 by using up as many of their ports as possible. To do so, the algorithm identifies cabinets that host RRUs with free ports (line 11), assigns to them antennas within reach (line 12), and updates matrix C' to reflect this assignment (line 13). The third step of RUM deploys additional RRUs that can be fully utilized by the unconnected antennas (lines 17 - 25). For each of the cabinets contained in CS, the algorithm checks whether they can be connected to k antennas (lines 17 and 18). Groups of k antennas are iteratively connected to selected locations (lines 19 - 22) by adding each antenna to the chosen cabinet (line 21) and updating the C' matrix (line 22). Finally, the fourth step of RUM connects the remaining antennas (lines 26 - 32). In this phase, the algorithm starts from the cabinet capable of connecting to the highest number of unconnected antennas, identified by the row of matrix C' with the greatest number of ones (line 27). Each antenna which can be connected to that cabinet (see condition in line 28) is assigned to it (line 29) and matrix C' is updated (line 30). This is the final phase of the RUM algorithm, which ends when all antennas are covered (line 26).

4.3.2 Radio over Fiber To the Building (RTB) Approach

To show the benefits of the proposed approach, it is compared with a conventional deployment approach called Radio over Fiber To the Building (RTB) [77]. This approach places RRUs only at the building entrances (denoted with yellow squares in Figure 4.2) and connects them to the BBU hotels with a dedicated fiber. Since RTB does not place RRUs in curb cabinets, each RRU covers only the antennas inside the building in which it is located.

Figure 4.3 shows a simple example illustrating the operation principles and the solutions obtained by RTB (Figure 4.3a) and RRUP-H (Figure 4.3b). From the figures it can be observed that, in the RTB case, three cabinets are activated to host RRUs (i_1, i_2, i_3). Considering that up to 8 antennas can be connected to a single RRU [69], three RRUs are required. On the other hand, RRUP-H, which maximizes the sharing of RRUs among different buildings, requires only one active cabinet (i_5) and two RRUs, decreasing the amount of components to be deployed

$$CS = \{i_1, i_2, i_3\}$$
$$AC_1 = \{j_1, j_2, j_3\}, AC_2 = \{j_4, ..., j_8\}, AC_3 = \{j_9, j_{10}, j_{11}\}$$
$$AC_4 = AC_5 = AC_6 = \emptyset$$

(a) RTB based design.

$$CS = \{i_5\}$$
$$AC_5 = \{j_1, ..., j_{11}\}$$
$$AC_1 = AC_2 = AC_3 = AC_4 = AC_6 = \emptyset$$

(b) RRUP-H based design.
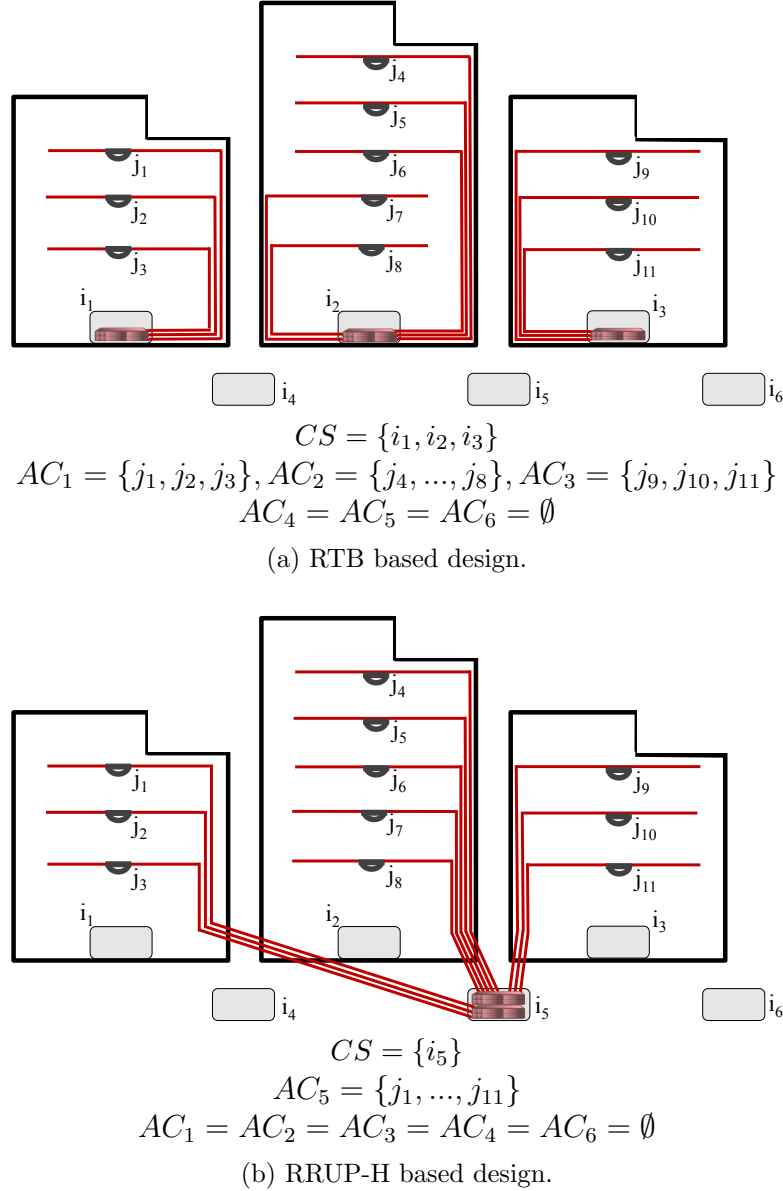
Figure 4.3: Example of network deployment using RTB and RRUP-H.

and lowering the associated costs.

4.4 Reference Scenarios and Numerical Results

The performance of the RRUP-ILP and RRUP-H approaches is evaluated via simulations in two deployment scenarios. First, it is evaluated the efficiency of RRUP-H as a good solution to the RRUP problem by comparing it to the optimal solutions obtained by RRUP-ILP in a small-sized scenario denoted as Residential District. Then, the savings attainable by RRUP-H in a
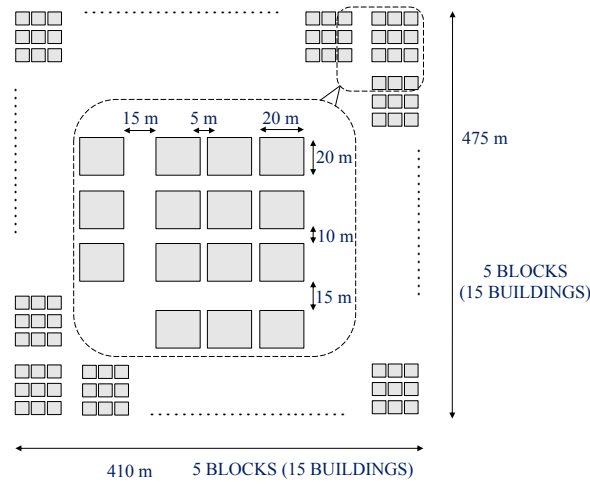
Figure 4.4: Example of a residential district simulation scenario showing the size.

full-sized realistic network scenario are evaluated, with various positions and numbers of BBU hotels, denoted as Urban. Optimal solutions are obtained by using the commercially available solver CPLEX [54], run on a HP workstation with a 2.67 $[GHz]$ processor and 16 $[GB]$ RAM.

4.4.1 Residential District

The Residential District scenario is based on a Manhattan street model with buildings arranged in blocks, as depicted in Fig. 4.4. The considered area is composed of 25 blocks organized in a 5×5 matrix. The total size of the map is $410 \times 475 \ [m^2]$. Each block is composed of 9 buildings organized in a 3×3 matrix and the blocks are divided by 15 $[m]$ wide streets. Buildings within a block are separated by 10 $[m]$ wide horizontal streets and 5 $[m]$ wide vertical streets. Each building is represented by a square with 20 $[m]$ sides, while the height of each floor is 3 $[m]$. The number of floors in each building is a random variable following a discrete uniform distribution over the interval $[1, 12]$ and the results are averaged over 10 different configurations of the scenario. In this case study, it is assumed that one omnidirectional indoor antenna is placed in the center of the ceiling on each floor and is sufficient to cover the entire floor. Each antenna is connected to a RRU through a Category 6 copper cable and each RRU is connected to a BBU port through a dedicated fiber. Each point-to-point fiber link between a RRU and a BBU requires two enhanced small form pluggable (SFP+) optical transceivers. An operator, to serve the outdoor users, has already deployed two macro BSs in the area. These BSs are connected

Table 4.1: Impact of different values of α and β on the solutions obtained by RRUP-ILP for $D = 50\ [m]$ and $D = 100\ [m]$.

D=50 [m]					
(α, β)	(10,1)	(2,1)	(1,1)	(1,2)	(1,10)
# RRU cabinets	203	203	198	186	184
# RRUs	228	228	233	245	249
D=100 [m]					
(α, β)	(10,1)	(2,1)	(1,1)	(1,2)	(1,10)
# RRU cabinets	26	26	26	26	26
# RRUs	186	186	186	186	186

to the CO hosting their assigned BBUs through dedicated optical fibers. The limited size of this scenario allows placing all BBUs in the CO that is located in the right bottom corner of the map.

To evaluate the impact of the maximum link length (D) between RRUs and antennas, in the simulations, the value of D is set to 50 $[m]$, 75 $[m]$ and 100 $[m]$, the latter corresponding to the maximum distance over a twisted pair cable in the 1000 BASE-T standard. The values for α and β were determined via a sensitivity analysis, whose results are reported in Table 4.1 for the case $D = 50\ [m]$, and $D = 100\ [m]$ The table shows that, for the case $D = 50\ [m]$, when $\alpha >> \beta$ the number of RRUs decreases, at the expense of a higher number of RRU cabinets. Conversely, when $\beta >> \alpha$ the number of RRU cabinets is reduced, but a larger number of RRUs is required. For the case $D = 100\ [m]$ no changes are experienced, therefore the choice of the values of α and β has no impact on the number of RRUs and cabinets. Since the cost of a cabinet is higher than the cost of a RRU, α and β are set to 1 and 2, respectively. In all scenarios, the value of k was set to 8 [69] while the maximum number of RRUs that can be connected to a single BBU was set to 6 [69].

Figure 4.5 shows the number of RRUs required by the RRUP-ILP, RRUP-H and RTB approaches to serve the area as a function of D. The figure also includes a theoretical lower bound (LB) on the number of RRUs that would be required to cover the area without any limitation on the length of the copper links (i.e., for $D=\infty$), allowing for full RRU centralization at a single site. It can be observed that RRUP-H and RRUP-ILP achieve a significant reduction in the number of RRUs compared to the conventional RTB approach. In general, RRUP-H
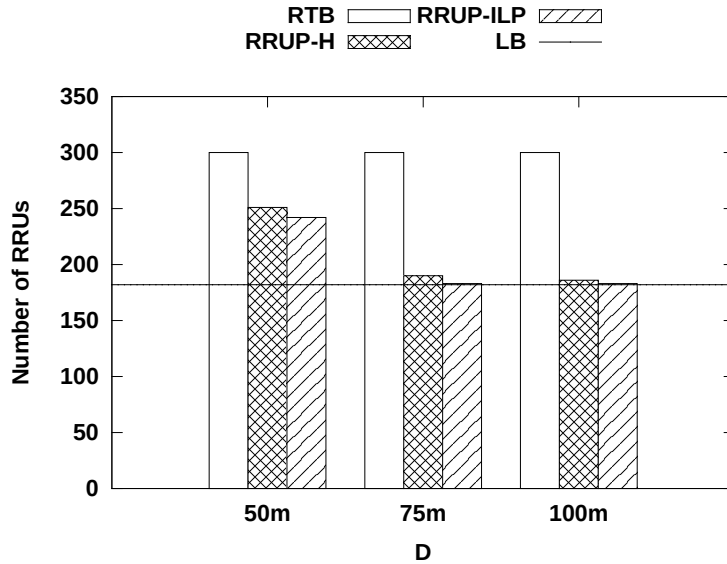
Figure 4.5: Number of RRUs as a function of D, the maximum distance between antennas and RRU, in residential district scenario.

performs very closely to RRUP-ILP, deploying only 3% more RRUs on average over all test instances. While the amount of radio equipment required by RTB and LB remains the same for different values of D, RRUP-ILP and RRUP-H reduce the equipment volume for longer reach values. In particular, RRUP-H uses 16%, 37%, and 38% less units than RTB in case of $D = 50$ $[m]$, $D = 75$ $[m]$, and $D = 100$ $[m]$, respectively. In addition, for medium and higher reach, RRUP-H performs very close to the LB and uses only 4%, and 2% more RRUs than LB for D equal to 75 and 100 $[m]$, respectively. Since all BBUs are placed in the same BBU hotel, the number of BBUs required by the different strategies is obtained by dividing the number of RRUs by the maximum number of RRUs that can be connected to a single BBU (fixed and equal to 6).

Figure 4.6 shows the number of cabinets to be activated by an operator. Similarly to the previous figures, the number of active cabinets obtained by RRUP-H is almost the same as for RRUP-ILP. The number of cabinets required by RRUP-ILP and RRUP-H decreases as D increases, and for D equal to 100 $[m]$ it is by one order of magnitude lower than the number obtained by RTB. For LB the number of required cabinets is always equal to 1 (omitted from the graph), since $D=\infty$ allows to place all RRUs in the same location.

Table 4.2 reports the total length of copper cables and optical fibers computed by RRUP-
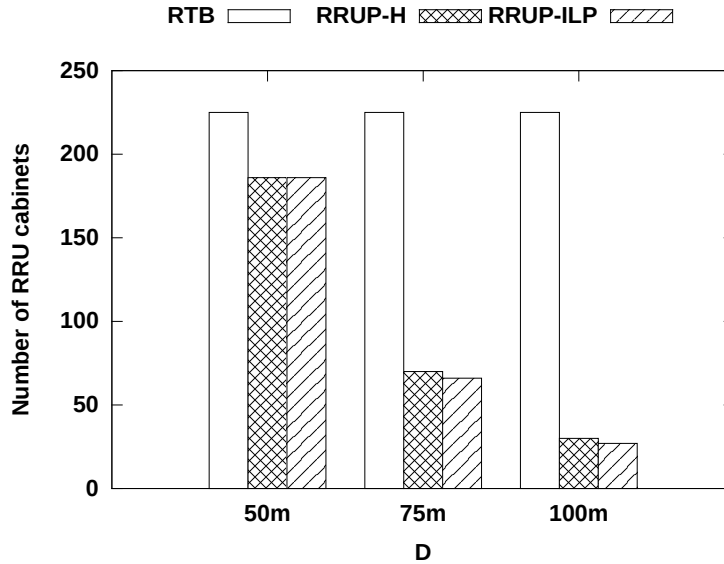
Figure 4.6: Number of RRU cabinets that needs to be activated as a function of D, the maximum distance between antennas and RRU, in residential district scenario.

Table 4.2: Total length of copper and fiber links in the residential district scenario.

Algorithm	Copper cable [km]	Fiber cable [km]
RRUP-ILP 50[m]	45.1	106.4
RRUP-H 50[m]	44.9	110.0
RRUP-ILP 75[m]	82.0	79.9
RRUP-H 75[m]	83.6	82.5
RRUP-ILP 100[m]	102.3	80.3
RRUP-H 100[m]	102.9	80.6
RTB	34.9	132.0

ILP, RRUP-H and RTB. It can be observed that higher values of D allow for greater RRU aggregation and larger distances between RRUs and antennas, thus increasing the length of copper cables and decreasing the length of optical fibers. For RTB, the amount of equipment and active cabinets is constant, so the length of cables does not change with D.

Figure 4.7 shows the capital expenditure values for each approach, calculated as a sum of the normalized cost of each component reported in Table 4.3. The values in the figure refer to the equipment, cables and cabinets to be deployed in each solution, without considering the cost for the pre-installed copper infrastructure inside buildings. As the equipment deployed by RTB does not depend on the values of D, its total cost is also constant. The costs of the RRUP-ILP and RRUP-H solutions decrease for greater values of D, i.e., with a longer reach
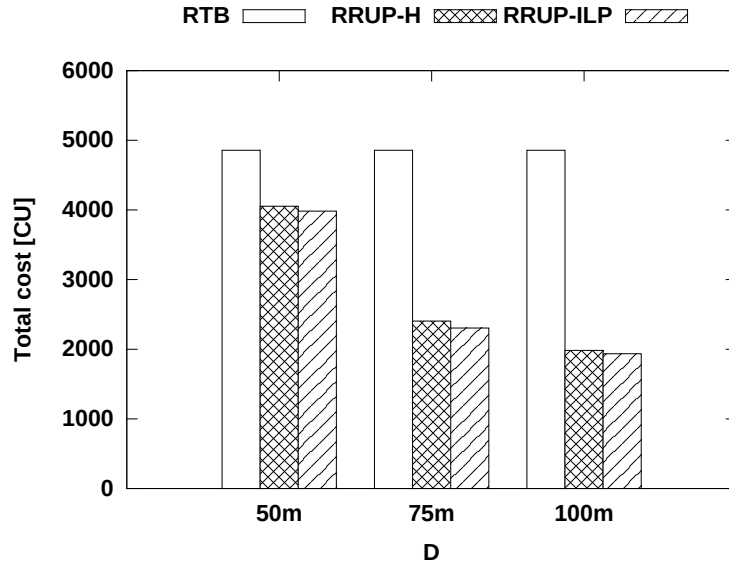
Figure 4.7: Total cost of the network as a function of D, the maximum distance between antennas and RRU, in residential district scenario.

Table 4.3: Normalized cost of the network components [3] [4].

Component	Normalized cost [CU]
SFP+	1
RRU	3.75
BBU	15
RRU Cabinet	10
BBU Cabinet	20
Copper cable (Cat. 6) [km]	1
Multi-modal fiber cable [km]	1

less active cabinets and RRUs are needed. When D equals 100 $[m]$, RRUP-ILP and RRUP-H reduce the cost by 59% with respect to RTB. In addition, they show very similar performance, with RRUP-H yielding only 2% higher costs than RRUP-ILP.

Table 4.4 reports the running times of RRUP-ILP and RRUP-H for different values of D. The ILP can be solved in half an hour for D equal to 100m, which can be acceptable for a network planning problem. The heuristic strategy takes considerably lower running time to find sub-optimal solutions with acceptable quality.

Table 4.4: Average solving time required by RRUP-ILP and RRUP-H for different values of antenna-RRU links (D).

Distance ant-RRU	RRUP-ILP time	RRUP-H time
50 [m]	7.7 [s]	<100 [ms]
75 [m]	19.7 [s]	<100 [ms]
100 [m]	30 [min.]	<100 [ms]

Table 4.5: Number of RRUs, RRU cabinets, and copper cables required by each algorithm for the urban scenario.

Algorithm	RRUs	RRU cabinets	Copper cables [km]
RRUP-H 50 [m]	31387	23175	1317.0
RRUP-H 75 [m]	23585	8619	6269.9
RRUP-H 100 [m]	23343	3525	8778.3
RTB	37605	28224	0
LB	22904	1	N.A.

4.4.2 Urban Scenario

In the Urban Scenario, also based on a Manhattan grid, the map is composed of 3136 blocks organized in a 56×56 matrix for a total of 28224 buildings. The total size of the map is 4745×5320 [m^2], i.e., 25 [km^2], which can be considered as the urban area of a medium-sized European city. The number of buildings per block, the street dimensions and all other parameters match the values used in the Residential District scenario. The simulations are run for values of D equal to 50, 75, and 100 [m].

Table 4.5 reports the amount of the RRUs, RRU cabinets and copper cables required to cover the area with RRUP-H and RTB, as well as the value of LB. Ethernet cables are assumed to be already deployed in the buildings, thus the cost for copper cables in the RTB case, where RRUs can be placed only inside a building, is 0. By comparing the solutions obtained with RRUP-H and RTB, it is possible to observe that the number of RRUs required by RRUP-H is 16%, 37%, and 38% lower than the RTB case for $D = 50$ [m], $D = 75$ [m], and $D = 100$ [m]f, respectively. Moreover, RRUP-H requires 37%, 3%, and 2% more RRUs than LB for the considered values of D. These RRU usage values, which are very close to the ones reported for the Residential District scenario, confirm the effectiveness of the heuristic and demonstrate its capability of
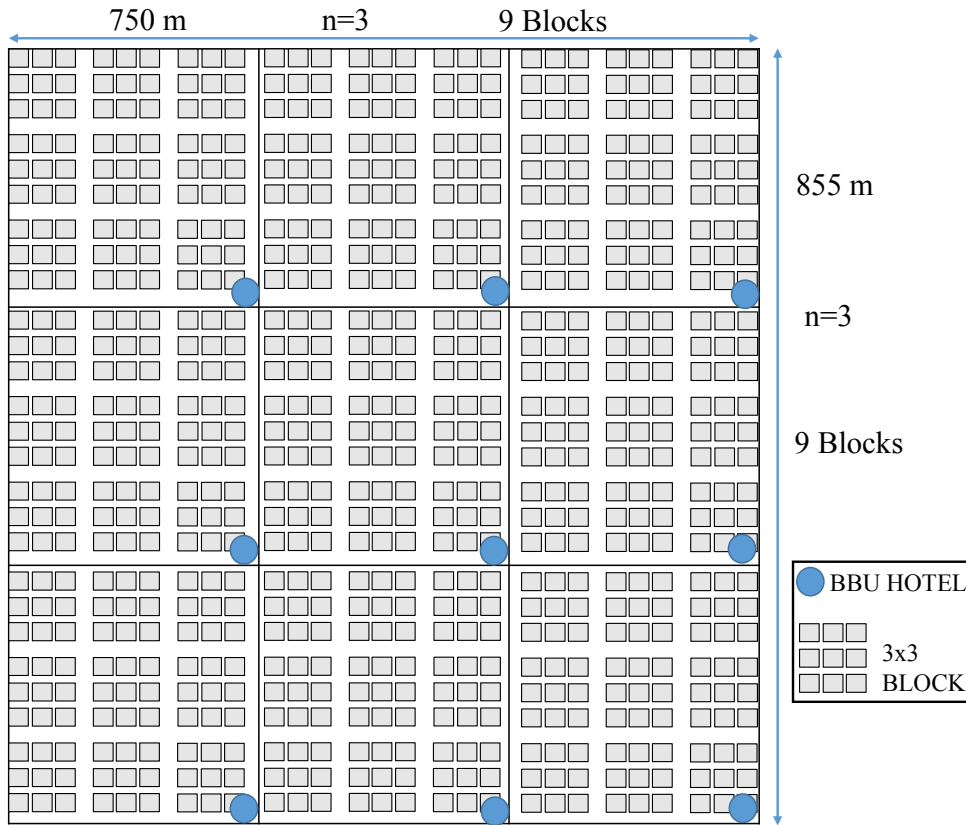
Figure 4.8: Example of a BBU hotel placement for $n = 3$.

reaching superior results also in large scenarios.

To investigate the impact of the number of BBU hotels on the overall solution, the density of their locations is tuned by dividing the area into $n \times n$ sub-areas, each one equipped with a BBU hotel. In the simulations, the set of values assumed by n is a subset of the divisors of 168, $\{1, 2, 3, 6, 7, 12, 42\}$. To clarify this partition, an example with $n = 3$ and 81 blocks is depicted in Fig. 4.8. Each hotel is placed in the bottom right corner of a sub-area (blue circles in Fig. 4.8) and all RRUs in that sub-area connect to it. Each BBU is connected to the CO via an optical grey point-to-point link and two SFP+. The CO performs coordination functions (e.g., CoMP), and is located in the bottom right corner of the map.

Figure 4.9 shows the fiber cost as a function of the number of BBU hotels and different values of D. The reported costs include both the fibers used in the fronthaul link and the fibers that carry the aggregated traffic from the BBUs to the CO. It can be observed from the figure that the RRUP-H approach obtains solutions with lower cost than that of RTB in all test cases. For the most constrained reach of $D = 50$ [m], the RRUP-H obtains 16% lower cost than RTB,

Figure 4.9: Fiber cost for RTB and RRUP-H, for the three values of D, as a function of the number of BBU hotels in the urban scenario.

Table 4.6: Total cost [CU] with 9, 144, and 1764 hotels for each algorithm in the urban scenario.

Algorithm	9 Hotels	144 Hotels	1764 Hotels
RRUP-H 50[m]	575272	544089	557529
RRUP-H 75[m]	349594	326565	341685
RRUP-H 100[m]	298413	275738	291262
RTB	692300	654596	665477

while the savings for $D = 75$ and 100 $[m]$ equal respectively 37% and 38% on average over all considered BBU hotel number values. Moreover, the total fiber cost values drop exponentially with increasing numbers of BBU hotels. This is due to the fact that a higher number of hotels allows for placing BBUs closer to RRUs, thus achieving a consistent reduction of the fronthaul link lengths. However, increasing the number of BBU hotels also increases the number of BBUs, BBU cabinets and SFP+, aggregately referred to as BBU hotels cost. Figure 4.10 reports the BBU hotels cost as a function of the number of BBU hotels. The figure shows that the BBU hotels cost increases linearly with the number of hotels. Again, RRUP-H outperforms RTB, yielding 16%, 37%, and 38% lower costs than RTB for the $D = 50$, 75, and $100[m]$ case,
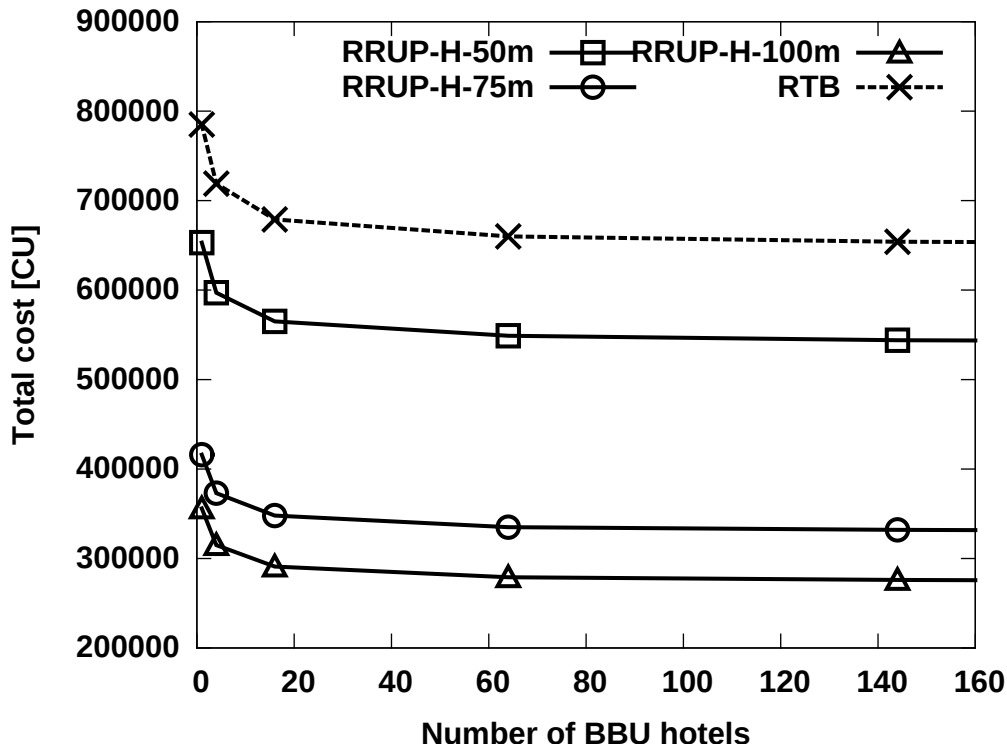
Figure 4.10: Sum of the costs related to BBUs, BBU cabinets, and SFP+ as a function of the number of BBU hotels in the urban scenario.

respectively. These results show that the RRUs minimization introduced by RRUP-H has a direct impact on the cost of the network. In particular, a RRUs reduction of 16%, 37%, and 38% translates into a reduction of 16%, 37%, and 38% of both BBU hotels and fiber cost.

Figure 4.11 shows the total deployment costs, which account for the cost of each CRA component, as a function of the number of BBU hotels and different values of D. It can be observed that, for each value of D, the cost drops significantly when the number of BBU hotels increases. This is because with 144 BBU hotels the costs are dominated by the fiber deployment cost. However, increasing the number of BBU hotels leads to a modest growth (not reported in the graph for the sake of clarity) of the total cost because the cost of the BBU hotels becomes dominant, (i.e., a higher number of BBU hotels implies shorter fronthaul distances). This fact is highlighted in Table 4.6, which reports the exact values of the cost obtained by each algorithm for three different numbers of hotels. The table indicates that the solutions found by RRUP-H for $D = 100[m]$ with 9 and 1764 hotels are 7.6% and 5.3% more expensive than the one with 144 hotels, respectively. Therefore, from an equipment cost perspective, 144 hotels
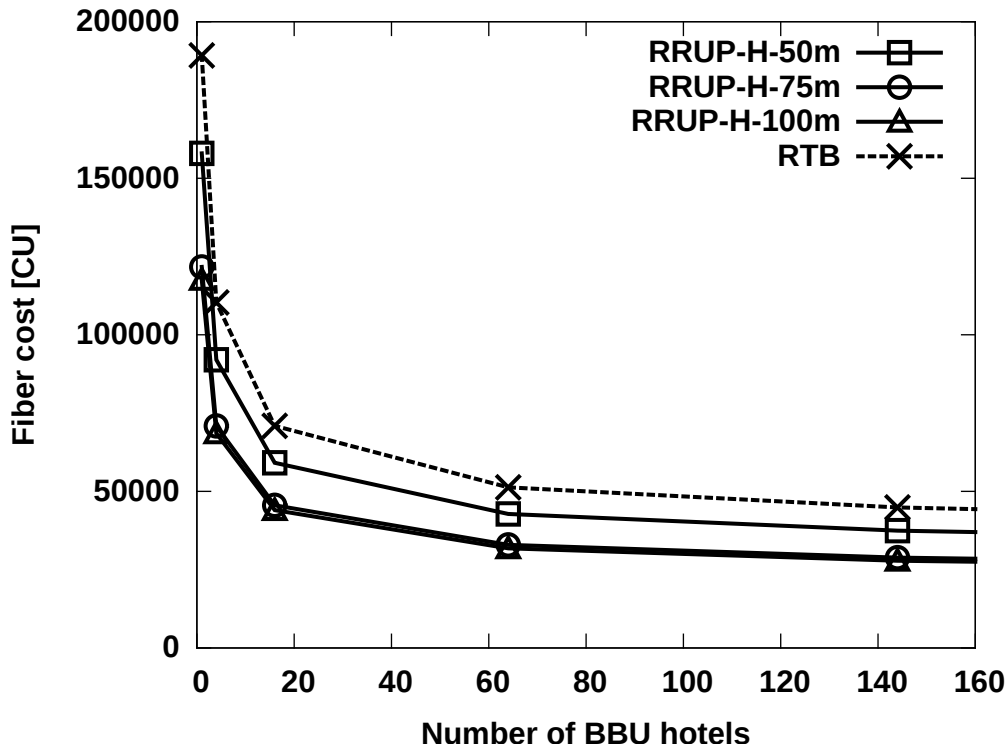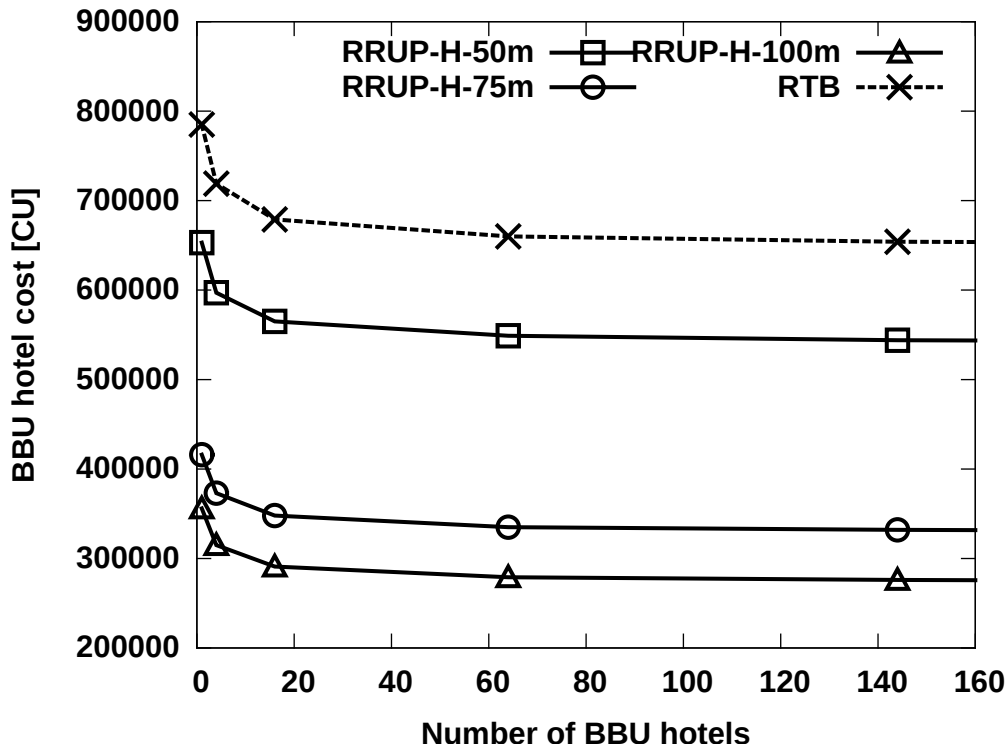
Figure 4.11: Total cost of RTB and RRUP-H, for the three values of D, as a function of the number of BBU hotels in the urban scenario.

can be considered as the best solution. On the one hand, using 144 hotels may lead to excessive operational costs, while on the other hand, reducing the number of hotels by centralizing a large amount of BBUs in the same site may increase the computational resources required for an efficient interference management. This aspect is out of scope and requires additional studies.

Figure 4.12 depicts the contributions of each network component to the total cost of the RRUP-H solutions for each value of D, and for two amounts of BBU hotels, i.e., 1 and 144. The figure shows that increasing the number of hotels to 144 allows for a total cost reduction of 22% for $D = 100$ [m]. Moreover, it can be noticed that the variation of the number of hotels has no effect on the cost contribution from RRUs, RRU cabinets, and copper cables. On the other hand, the cost contributions due to the amount of fiber, BBUs, BBU cabinets, and SFP+ change with different settings.
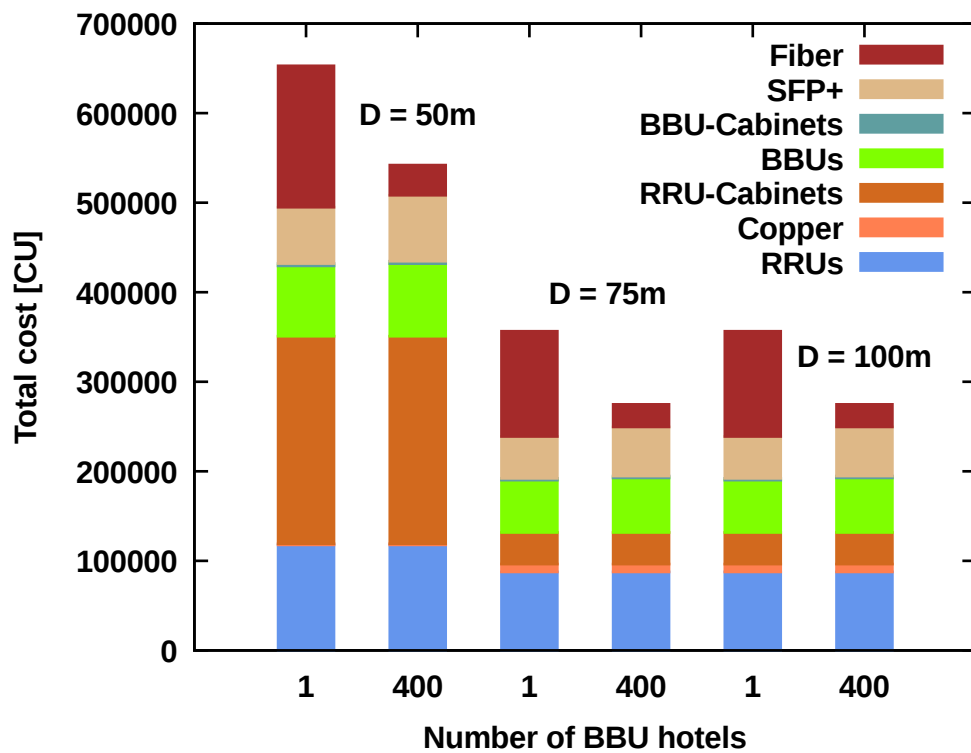
Figure 4.12: Contribution of each network component to the total cost of RRUP-H and RTB as a function of the number of BBU hotels in the urban scenario.

Chapter 5

Fronthaul and Backhaul Traffic Multiplexing Based on Hybrid Switching

In the previous Chapters, dedicated optical resources have been used to provide fronthaul connectivity in the radio access network. Mobile networks are usually composed of a mix of different technologies. Centralized networks will be deployed along with traditional BSs, as depicted in Figure 5.1. Traditional BSs, like LTE eNBs, require backhaul connectivity towards the operator core network. RRHs, instead, require to be connected to BBU hotels, that reach the core network through backhaul links. As a consequence, both fronthaul and backhaul traffic must be transported over the same physical infrastructure. CPRI fronthaul protocol is not designed to be multiplexed, thus researchers and industries have recently started working on new solutions based on encapsulation of CPRI traffic into Ethernet frames (CPRIoE) [78]. The CPRIoE encapsulation allows to multiplex fronthaul traffic streams together or with backhaul streams by means of widely known protocols and existing off-the-shelf equipment. However, strict delay and jitter requirements must be met, thus requiring the introduction of priority mechanisms in Ethernet switches.

The integrated hybrid multiplexing scheme was proposed to implement statistical multiplexing
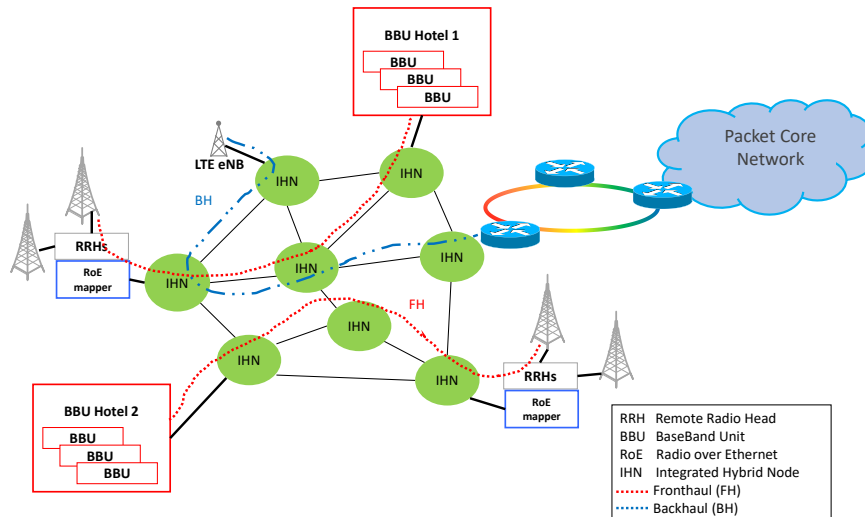
Figure 5.1: Converged fronthaul/backhaul scenario.

of the guaranteed service traffic (GST) and statistical multiplexed (SM) in Ethernet packet-based nodes [79]. The hybrid switching introduces a fixed delay to GST packets, needed to detect the gaps between consecutive GST frames, so that SM packets can be inserted in the GST flow [80][81]. In this scheme, the fronthaul and backhaul traffic can be treated as GST and SM traffic, respectively. However, fronthaul streams are subject to strict latency requirements. A pre-emption of SM traffic can be implemented so that the hybrid switch is transparent to incoming fronthaul traffic, which is immediately sent on the output interface without experiencing any delay (other than the physical time to switch the output).

This Chapter first discusses the CPRIoE encapsulation and then investigates the introduction of integrated hybrid nodes (IHNs) with a pre-emption mechanism to multiplex fronthaul and backhaul traffics. An ad-hoc simulator in C has been developed to resemble the behavior of a hybrid switch with pre-emption. The effectiveness of this solution is shown by means of simulations of a single link of the access network where hybrid switching is applied[a].

---

[a]The outcome of this work is included in [82] [83] [84].

5.1 CPRI over Ethernet

Experimental work exists on CPRIoE encapsulation, such as the ones reported in [85] [86]. A list of parameters used in this study is reported in Table 5.1, while Figure 5.2 depicts what
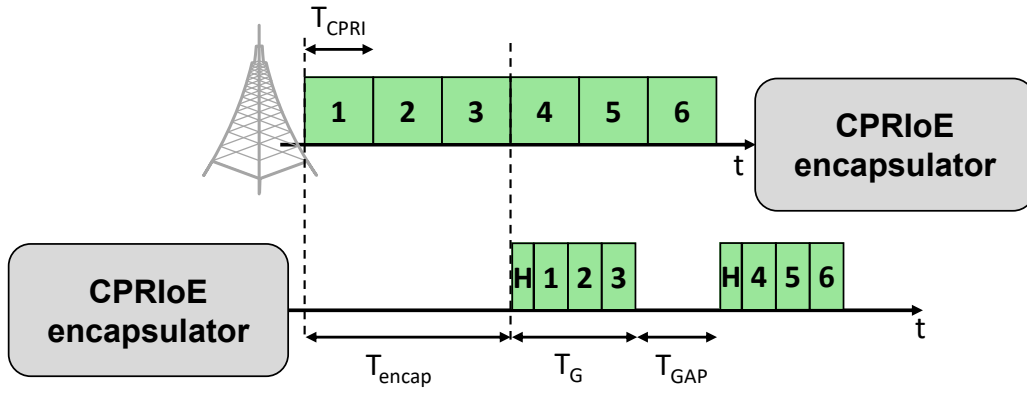
Figure 5.2: Example of CPRIoE encapsulation and gap generation.

Table 5.1: List of parameters used to describe CPRIoE and hybrid nodes.

Parameter	Description
N_F	Number of CPRI basic frames forming a CPRIoE payload.
L_F	Payload length for CPRIoE frame.
R_W	Output channel rate.
T_G	CPRIoE duration.
T_{GAP}	Gap duration.
Δ	Fixed delay to avoid collision.
ρ_B	Offered backhaul load per channel.
L_B	Average length of backhaul frames.
T_{guard}	Guard time.
T_{CPRI}	CPRI basic frame duration.
R_{CPRI}	CPRI flow generation rate.
L_H	Length of CPRIoE header.
m	Number of channels in the switch output interface.

happens when a CPRI flow is encapsulated into Ethernet frames. RRHs generate CPRI flows at different rates (R_{CPRI}) set by the standard [15]. Each flow is composed of CPRI basic frames with fixed duration $T_{CPRI} = 260$ [ns], equal for all CPRI options. A certain number of CPRI basic frames (N_F) are encapsulated in an Ethernet frame forming the CPRIoE payload of length:

$$L_F = N_F * R_{CPRI} * T_{CPRI}. \tag{5.1}$$

From Figure 5.2, it is possible to notice that there is a gap of duration T_{GAP} in the output line after encapsulation, due to higher rate of the output interface. These gaps generated by the CPRIoE encapsulation can be exploited to inject backhaul frames.
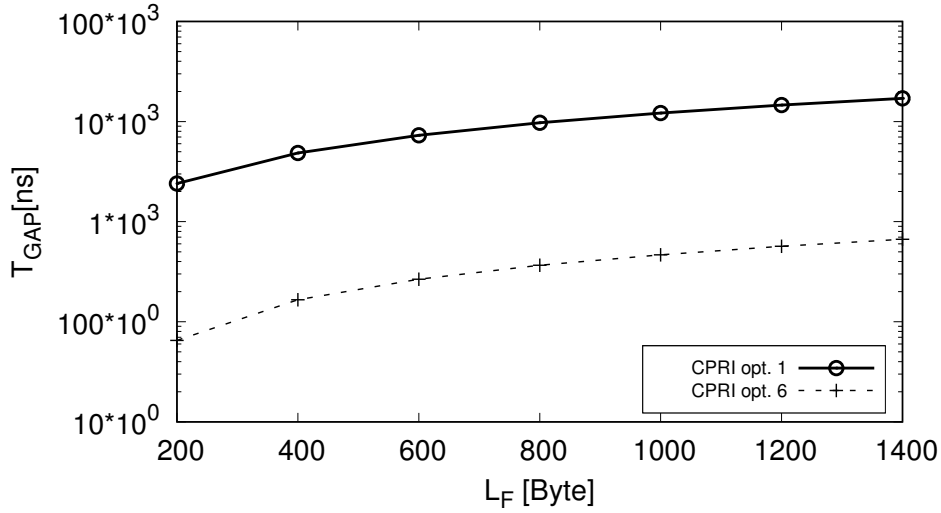
Figure 5.3: T_{GAP} as a function of different values of payload length L_F for CPRI opt. 1 and 6 on a 10 [*Gbps*] line.

5.2 Application of Integrated Hybrid Technology to C-RAN

The integrated hybrid concept with pre-emption is applied here to a network segment of a C-RAN where fronthaul traffic, i.e., CPRIoE flow, is identified as GST, with zero PDV, while backhaul traffic is dealt with pre-emption as SM traffic. An example of IHN multiplexing backhaul and fronthaul traffic together on output lines is provided in Figure 5.4, while the most relevant parameters are shown in Figure 5.5. During the transmission of a fronthaul frame, incoming backhaul frames are stored in a buffer until an output channel is free. A scheduler (represented by the block S in Figure 5.4) senses the input channels to detect fronthaul frames and is in charge of deciding when to start and interrupt the transmission of backhaul packets on the output channels. IHN eliminates PDV of the fronthaul traffic because the fixed delay Δ enables a time-window which gives sufficient time for processing and decision of backhaul packet preemption. This goes beyond, e.g., the IEEE 802.1Qbu pre-emption [87] recommended in the IEEE 802.1CM standard [88] for fronthaul, where fronthaul packets may experience anyway PDV corresponding to the service time of 155 *byte*.

With reference to Figures 5.4 and 5.5, CPRIoE frames are sent by RRHs towards IHNs, where
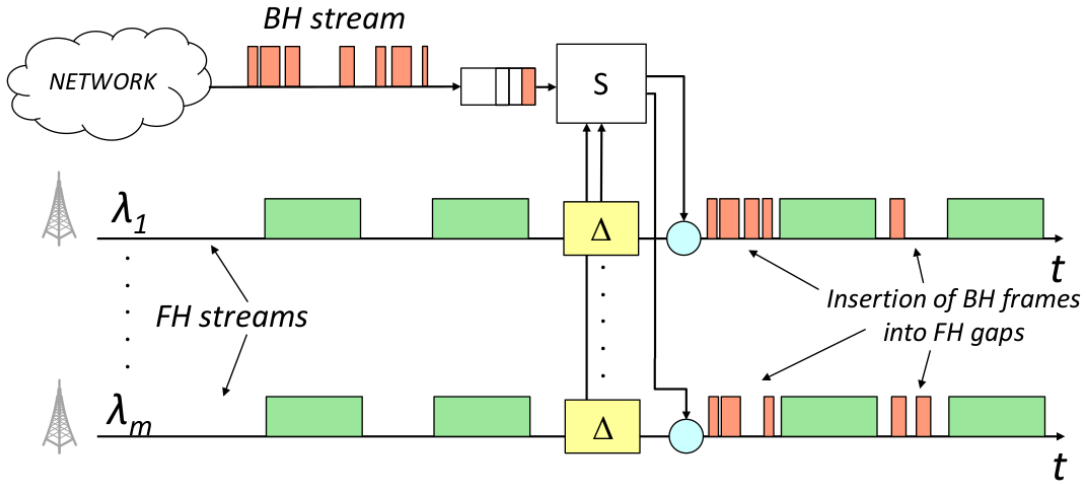
Figure 5.4: IHN multiplexing scheme. BH for backhaul, FH for fronthaul.
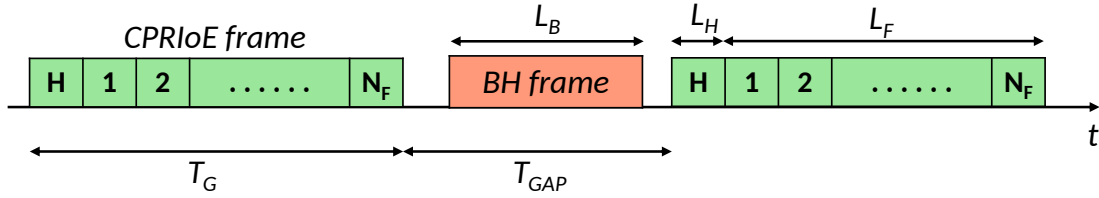
Figure 5.5: Output line of a IHN showing CPRIoE related parameters. BH for backhaul.

they are delayed by a fixed quantity Δ. Also conventional backhaul traffic reaches the switches, loading the output channels with parameter ρ_B. IHN switches have m output channels, each characterized by a rate R_W, and accommodates CPRIoE frames of duration:

$$T_G = \frac{L_H + L_F}{R_W} \tag{5.2}$$

where L_H is the header of CPRIoE frames assumed to be 44 *byte* [86].

Depending on N_F and R_{CPRI}, the gap duration T_{GAP} is selected according to:

$$T_{GAP} = \frac{L_F}{R_{CPRI}} - T_G. \tag{5.3}$$

By looking at (5.3), it is possible to notice that, depending on R_{CPRI}, different values for T_{GAP} can be obtained for the same length of CPRIoE packets L_F, as depicted in Figure 5.3 for CPRI opt. 1 and 6 for a line rate of $R_W = 10 \ [Gbps]$.

This time gap is used in the hybrid multiplexing scheme in order to aggregate backhaul traffic

on the same transport channel. To this end, two different policies are here considered:

- A backhaul packet is transmitted when a gap is available and it is possibly pre-empted upon arrival of a new CPRIoE burst, in case backhaul packet duration is longer than the gap itself. In case of pre-emption the backhaul packet is lost. This policy is indicated as P policy, with insertion of an entire packet into the by-pass CPRIoE flow.

- A backhaul packet waits for a gap and in case the backhaul packet is longer than the gap it is fragmented into as many fragments as needed to fit the gap. This avoid the need of pre-emption but introduces some overhead to manage fragmentation and additional functionalities. This policy is indicated as S policy, where packets are divided into N_S segments of suitable size for their insertion into the CPRIoE flow.

5.3   Simulation Results

To evaluate the benefits introduced by the proposed mechanism, an event-driven simulator in C language has been developed. One RRH generates a CPRI flow according to two different options with rates $R_{CPRI} = 614.4$ [*Mbps*] (option 1) and 6.144 [*Gbps*] (option 6). The IHON fixed delay $\Delta = 99.2$ [*ns*] is assumed, which corresponds to the smallest fragment (124 [*byte*]) that can be preempted [88]. In order to avoid collision between different frames on the output line, a guard time T_{guard} of 10 [*ns*] is applied during which the transmission of any data is not permitted. A single output channel ($m = 1$) with rate $R_W = 10$ [*Gbps*] is considered. The number of CPRI basic frames in a guaranteed burst N_F is varied over the intervals [1, 70] and [1, 7], for CPRI option 1 and 6, respectively [86], so that the payload length L_F varies accordingly. A set of simulations varying the average backhaul packet length L_B is obtained with a load ρ_B such that a backhaul packet is always ready for transmission on the output channel. The length of backhaul frames is considered to be exponentially distributed with parameter L_B. Simulation results are averaged over 10 simulations of 10^8 events each. The obtained confidence interval is always less than 8% with a confidence level of 95%.
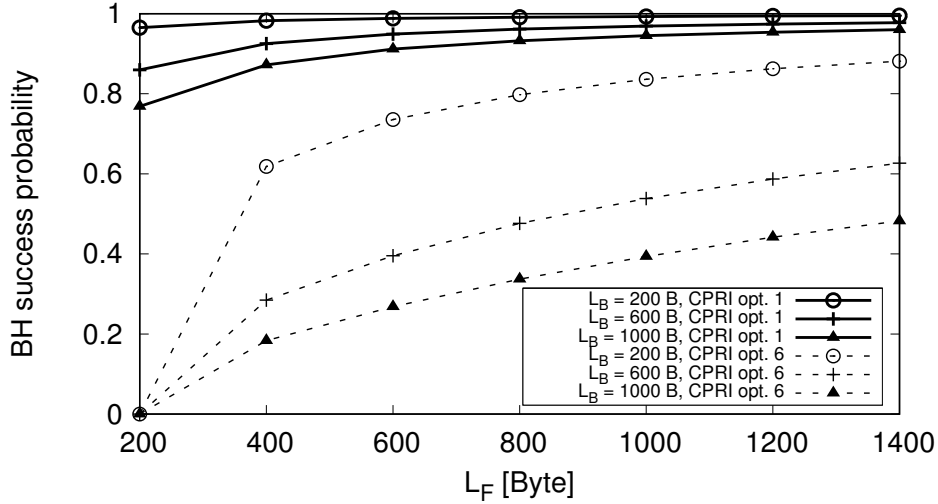
Figure 5.6: Backhaul (BH) success probability as a function of payload length L_F for different backhaul packet length L_B using CPRI opt. 1 and 6.

Figure 5.7: Backhaul (BH) throughput, normalized to the output link capacity, as a function of payload length L_F for different backhaul packet length L_B using CPRI opt. 1. Solid lines for the case with segmentation (S), dashed lines for the no-segmentation case(P).

Figure 5.6 shows the success probability of the backhaul traffic, defined as the ratio between the packets not interrupted and the total packets in service, as a function of L_F, for both CPRI options, varying L_B. In both cases, the success probability increases with L_F, due to the resulting larger T_{gap}. Option 6 shows lower performance than option 1 due to the smaller size of the gap, especially when L_F is low, so suggesting to use larger N_F in this case. However, increasing N_F increases the encapsulation delay, that may impact the maximum reach
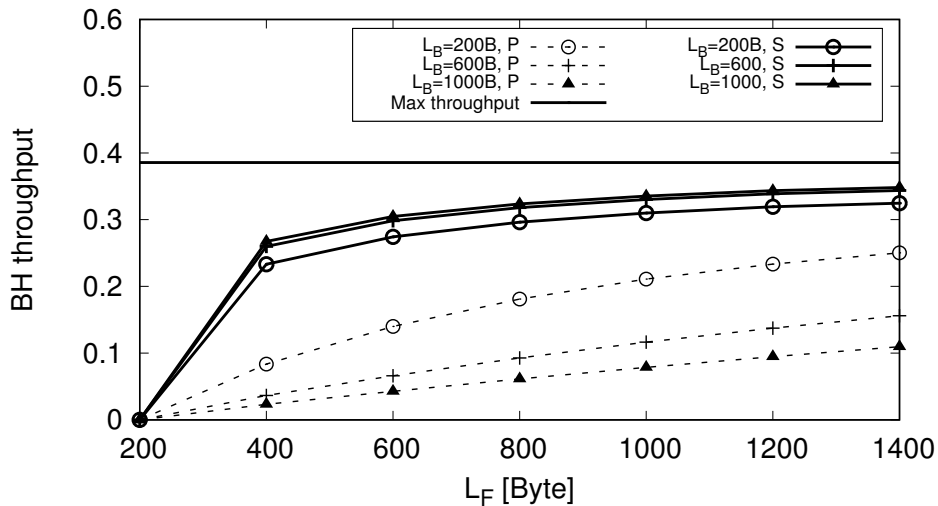
Figure 5.8: Backhaul (BH) throughput, normalized to the output link capacity, as a function of payload length L_F for different backhaul packet length L_B using CPRI opt. 6. Solid lines for the case with segmentation (S), dashed lines for the no-segmentation case (P).

of fronthaul connection.

Figure 5.7 reports the backhaul throughput, normalized to the output line rate (10 [$Gbps$]), as a function of L_F for option 1 varying L_B. The figure also reports the maximum normalized capacity left by fronthaul traffic. The value of throughput in the case of the P policy reaches 8.9 [$Gbps$] only for high values of L_F with quite limited influence of L_B. The S policy, instead, is able to better exploit the available capacity for any value of L_F, except for the influence of the transmission guard times inserted. The same evaluation obtained for option 6 in Figure 5.8 shows a remarkable effect of the shorter gaps in the fronthaul flow, that prevents also the F policy to fully exploit the available capacity for low values of L_F, due to the high numbers of segments needed and related inserted transmission guard time.

Figure 5.9 reports the overhead introduced by the P and S policies calculated as the ratio of the number of bytes for Ethernet headers and the the total number of bytes transmitted as backhaul traffic for option 1. The same evaluation is presented in Figure 5.10 for option 6. The effect of the S policy is more evident with option 6 where, due to the smaller gaps in the fronthaul flow, multiple segments are typically required to transmit each backhaul packet. In any case the additional overhead is quite limited when increasing L_F. It is interesting to analyze the average number of segments to transmit a backhaul packets in option 1 and option

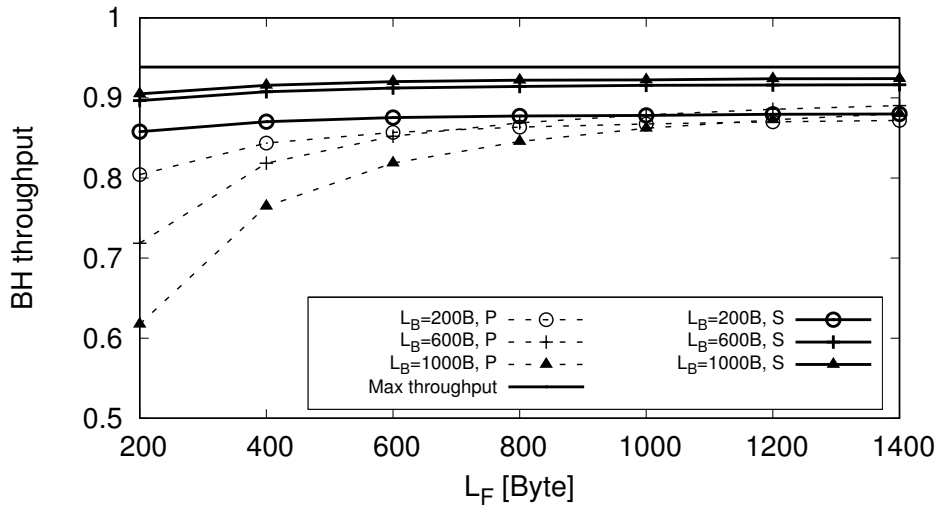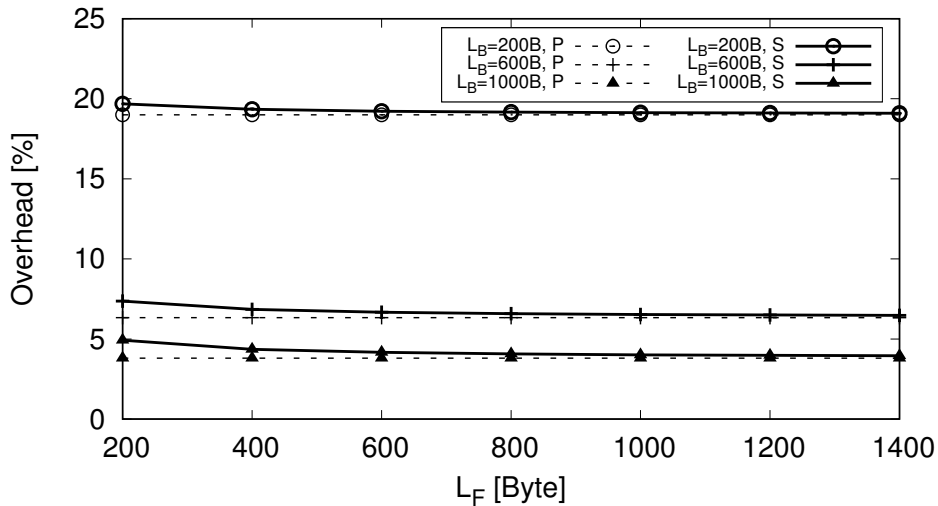Figure 5.9: Overhead for backhaul packets as a function of payload length L_F for different backhaul packet length L_B using CPRI opt. 1. Solid lines for the case with segmentation (S), dashed lines for the no-segmentation case (P).
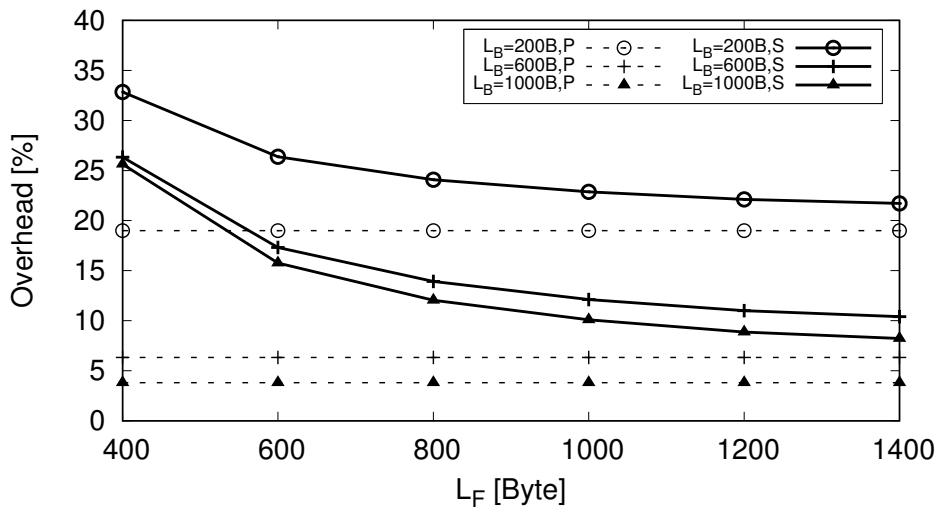
Figure 5.10: Overhead for backhaul packets as a function of payload length L_F for different backhaul packet length L_B using CPRI opt. 6. Solid lines for the case with segmentation (S), dashed lines for the no-segmentation case (P).

6, as shown in Figure 5.11 for the S policy. Option 1 allows transmission of a packet as a single segment in most cases for any L_F. In option 6, instead, reasonable values of L_F seem to be not less than 1000 [$bytes$] which give an average number of segments less than 3 for any L_B, with a resulting overhead around 10%, which is reasonable as well. However, working with high L_F increases the encapsulation delay, which in the worst case is 18.3 [μs] for CPRI option 1 and
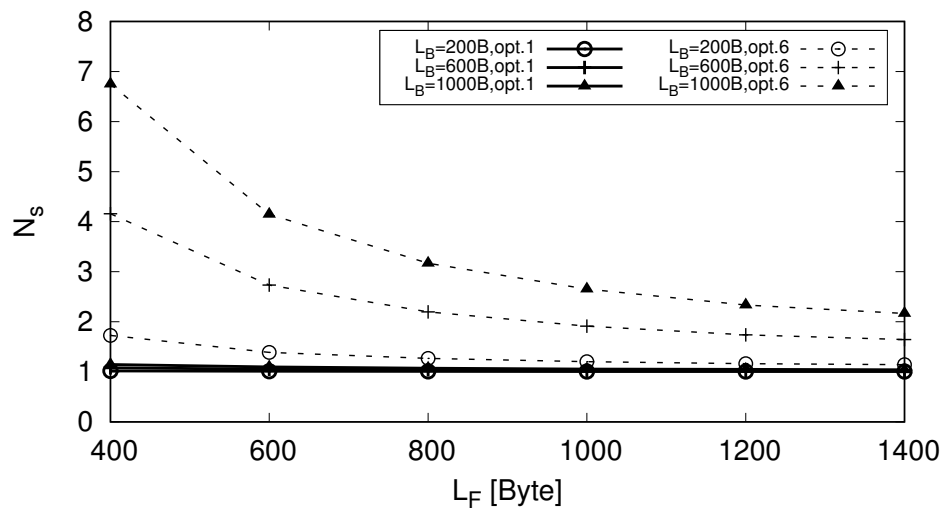
Figure 5.11: Average number of segments (N_S) required to send a backhaul packet as a function of payload length L_F for different backhaul packet length L_B using CPRI opt. 1 and 6.

1.83 $[\mu s]$ for CPRI option 6.

Chapter 6

Centralized Radio Access Newtork Survivability Against Baseband Hotel Failures

In C-RAN, all the baseband processing functions are centralized in one or few hotels and a failure might have a significant impact on the performance of the network, causing service outage for a large number of users. In the literature, cost and energy efficient strategies have been proposed to address cost issues while maximizing resource usage in C-RAN [89, 90, 91, 92]. However, all these works do not account for network reliability, which is also one of the key requirements for 5G [93].

Studies concerning optical network resiliency against attacks can be found in [94] and [95] while survivability against disasters is discussed in [96]. Detection and sensing of anomalies while minimizing also the amount of information for network controllers is studied in [97]. Reliability of optical devices and related failure studies are conducted in [98], while the implications of reliability on the energy efficiency are discussed in [99]. All these studies are equally applicable also to C-RAN even though they were not though for this architecture. However, they do not account for failures in BBU hotels.

In [100], a reliable solution against BBU and link failures in C-RAN has been proposed. The strategy is based on dedicated protection and virtual machine replication, but do not consider latency constraint and limited link capacity. The first work dealing with realiable BBU hotel placement with limited network capacity can be found in [101], where the authors propose to tackle the problem with a heuristic approach.

The work presented in this Chapter proposes an ILP to minimize BBU hotels, wavelengths and backup BBU resources while providing reliability against failures. Given the complexity of the model, it is not always possible to find a solution due to out of memory issues when dealing with large networks. Therefore, a novel heuristic is also proposed, and the ILP is used as a benchmark to test the heuristic strategy. The proposed algorithm is distributed in the transport nodes, that decide the BBU assignment based on local information and communicate the decision to the network controller. This allows to reduce the complexity of the decision-making process and relieve the controller from the decisional process, that can be computationally complex. Moreover, the network reacts faster to changes and new requests[1]. A similar work, also based on an ILP, has been proposed recently in [106]. The results obtained by the authors are in line with the ones obtained here, thus increasing the solidity and validating the work proposed in this chapter. In addition to this, also some problems related to dynamic scenarios are highlighted.

6.1   Optimal and Reliable Deployment of BBU resources in C-RAN

A general example of an access network is depicted in Figure 6.1. In general, an access network is composed of multiple nodes, here referred to as transport nodes, interconnected by means of fiber cables, creating the so-called fronthaul network. Optical links are assumed to have a certain capacity and length and are used to transport fronthaul data to primary and backup BBUs. Transport nodes are assumed to be equipped with computational capacity (e.g., edge data center), where BBU functions can be virtualized and instantiated whenever needed. An

---

[1]The outcome of this work is included in [102],[103],[104],[105].
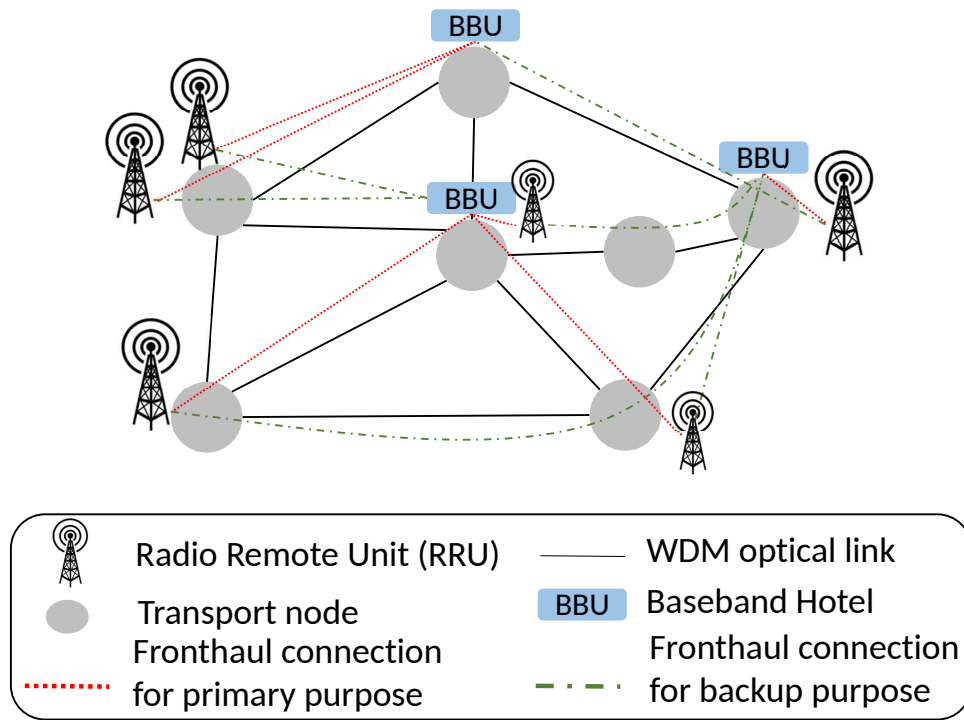
Figure 6.1: Example of a C-RAN architecture.

overarching SDN controller/orchestrator is in charge of instantiating and reserving optical and computational resources and runs the deployment strategy.

6.1.1   Problem Formulation and Cost Contributors

Given a set of transport nodes, each of which provides information regarding:

 (i) total number of connected RRUs;

 (ii) network connectivy among transport nodes;

 (iii) maximum number of wavelengths in each link;

 (iv) maximum allowed distance to connect RRUs with BBUs.

The *survivable BBU hotel placement problem* consists in finding a minimum cost primary BBU hotel placement so that each RRU is assigned to a BBU according to limitations on distance and wavelength availability for fronthaul links, and a backup BBU hotel placement for reliability against single BBU hotel failure.

Table 6.1: List of parameters used in this Chapter.

	Parameters:
S	Set of transport nodes, $|S| = s$.
H	$s \times s$ matrix. h_{ij} is the distance in hops between nodes i and j computed with the shortest path.
α	Weight for the distance in the cost function.
β	Activation cost for a single BBU hotel.
γ	Cost of a single BBU resource.
r_i	Number of RRUs at site $i \in S$.
δ_{ij}^l	1 if shortest path between i and j is using link l, 0 otherwise.
M_W	Maximum number of wavelengths available in each link.
M_H	Maximum allowed distance between RRU and BBU (in hops).
L	Set of links.
$N_i(M_H, M_W)$	Set of eligible nodes within M_H and M_W constraints from node $i \in S$.
w_l	Number of wavelengths in use in the link $l \in L$.
N_i	Set of directly connected nodes to node $i \in S$.
TTL	Time-To-Live in hops.
CS_n	Current Set, used in Alg. 5 containing nodes to be considered at iteration n.
SA_j	Array of cell sites sharing the same primary BBU hotel $j \in S$.
Max	Parameter storing the largest number of cell sites sharing the same primary.
M	A large number.

A list of parameters used in this study is reported in Table 6.1, while the variables are listed in Table 6.2.

To provide reliability against single BBU hotel failure, each RRU is connected simultaneously to two BBU hotels placed in different transport nodes, one for primary and one for backup purposes. Each BBU hotel hosting at least one primary and/or backup BBU must be activated. The activation cost of BBU hotels in transport nodes is calculated as follows:

$$C_B = \beta \cdot \sum_{i \in S} B_i \tag{6.1}$$

where B_i is a boolean variable equal to 1 when the transport node hosts a BBU hotel, 0 otherwise. β is a parameter associated to the activation cost for a BBU hotel in transport nodes and can be set accordingly.

In order to account for the delay introduced in the fronthaul network, a cost can be associated to the distance between BBU hotels and RRUs connecting to them. The distance can be limited by

Table 6.2: List of variables used in this Chapter.

	Variables:
$c_{iji'}$	1 if RRUs at node j are using destination i as primary and i' as backup hotel site; 0 otherwise.
B_i	1 if node $i \in S$ hosts a BBU hotel, 0 otherwise.
p_{ij}	1 if BBU hotel i is assigned as primary for RRUs at node j, $i, j \in S$, 0 otherwise.
b_{ij}	1 if BBU hotel i is assigned as backup for RRUs at node j, $i, j \in S$, 0 otherwise.
x_i	Number of BBU resources required at hotel site i for primary purposes.
y_i	Number of BBU resources required at hotel site i for backup purposes.

imposing a constraint on the maximum allowed distance. Distance between adjacent transport nodes is here assumed to be equal to 1 hop for all links. The overall cost for the distance is expressed as follows:

$$C_H = \alpha \cdot \sum_{i \in S} \sum_{j \in S} p_{ij} h_{ij} + \alpha \cdot \sum_{i \in S} \sum_{j \in S} b_{ij} h_{ij} \tag{6.2}$$

where p_{ij} and b_{ij} are boolean variables that indicate if BBU hotel i is assigned as primary or a backup, respectively, for the group of RRUs at transport node j. h_{ij} represents the distance, in hops, between transport node i and j computed solving the shortest path problem. Both contributions (i.e., the overall distance for primary path and backup path) are multiplied by cost parameter α, which represents the cost for 1 hop link. Finally, the proper number of BBU resources must be allocated in each hotel. The total cost for primary and backup BBU resources is calculated as follows:

$$C_P = \gamma \cdot \sum_{i \in S} x_i + y_i \tag{6.3}$$

C_P is the contribution of the total number of primary (x_i) and backup (y_i) resources in each hotel multiplied by the cost parameter γ associated to a single BBU. Since the protection requires that each RRU is connected to two different BBU hotels, the total number of resources should be twice the number of RRUs, and consequently the value for C_P can be fixed. However, only the number of primary BBU resources is fixed and equal to the number of RRUs. On the contrary, the number of backup resources can be reduced. In fact, RRUs can share the same backup resource if they are assigned to different primary BBU hotels. When a single hotel failure occurs, RRUs assigned to that primary hotel switch to their backup hotel, hence it is

forbidden to share backup resources among RRUs assigned to the same primary. By sharing the backup BBUs, the number of backup resources to be provided in each hotel decreases, decreasing C_P.

6.1.2 Distributed Algorithm

Optimal solutions in telecommunication networks usually require a complete knowledge of the network, which is done by exchanging control messages among nodes and network controller. However, managing a large number of nodes typically involve a large amount of resources, making this approach unpractical. A viable solution to this problem is to use distributed algorithms, similarly to what happens in wireless sensor networks (WSN) [107],[108]. With distributed approaches, decisions on the BBU placement are taken directly by nodes, where the algorithm for the BBU assignment is run based on information exchanged with neighbor nodes. This approach allows to reduce the complexity of the decision-making process and consequently also the time to reach the solution. Since the algorithm runs in each node, the controller is relieved of part of his work, reducing also the time to react to network changes.

The proposed strategy to solve the survivable BBU hotel placement problem is performed in two phases. In the first phase, the algorithm decides where to activate primary and backup hotels. In the second phase, BBU ports are shared, whenever possible, to further minimize the total cost. The distributed procedure proposed for BBU hotel placement in C-RAN is presented as Algorithm 3. The following assumptions are made. At the beginning, each transport node is assumed to have information only regarding the number of directly connected RRUs and transport nodes, and the availability of wavelengths in each directly connected links. In order to provide coverage and resiliency for all RRUs in the network, exchange of information among nodes is required. More specifically, the nodes interact to learn information regarding *i*) wavelengths availability and *ii*) if nodes are already active, i.e., if they are hosting active hotels. After the procedure is performed, the application running in the node asks the network controller to establish the connections with the selected nodes (two, one for primary and one for backup purposes) and to activate/reserve baseband resources in their local DC.

The neighbor nodes set of a transport node i is defined as the set of nodes to which an RRU, attached to i, can be connected, i.e., transport nodes with baseband resources within distance M_H and with sufficient wavelengths along the path. Algorithm 3 is executed in each transport node upon the needs of connecting a new RRU to two BBU functionalities in separate BBU hotels, for primary and backup purposes. Algorithm 3 calls Algorithm 5 to find the neighbors of a node. Since the probability of activating two or more RRUs at the exact same time is rare, only one transport node at a time is assumed to execute Algorithm 3.

The procedure presented by Algorithm 3 is executed in each transport node as long as there is a new request for primary or backup BBU hotel connection. The starting node, namely node i, is chosen randomly. The algorithm starts at line 2. Function NFF is called from node i in line 3 in order to extract set of neighbor nodes $N_i(M_H, M_W)$. This set contains nodes within the maximum number of hops (M_H) from node i that have enough wavelengths to allow the connection of new RRUs. If node i hosts an active BBU hotel (line 5) it is selected to act as a primary BBU hotel for RRUs at node i (line 6). For the backup connection, if exists an active BBU hotel at node j in the set of neighbors for i $N_i(M_H, M_W)$ (line 7), RRUs at node i connects to it for backup purpose (line 8). Lines 9 to 11 reserve the required wavelengths in all the links of the path from i to j, in order to accommodate the traffic from new RRUs. If no node in the set $N_i(M_H, M_W)$ has an active BBU hotel (line 12), then one node will be chosen randomly from the set (line 13) to act as a BBU hotel (line 14) in order to be backup BBU hotel for node i (line 15). The wavelengths in all the links between nodes i and j will be updated accordingly (lines 16-18).

If node i does not have any BBU hotel in its cell site (line 21), three possible situations might happen: the first is the case when two active BBU hotels exist in the set $N_i(M_H, M_W)$ namely nodes j and z (line 23). If there are more active BBU hotels in the set, two are chosen randomly. In this case node i will connect to them one as primary (line 24) and the other as backup BBU hotel (line 25). Consequently all the wavelengths to be used in the links forming the path to primary and backup BBU hotels are be updated accordingly (lines 26 - 28). The second possible situation happens when only one node, namely node j, in the set $N_i(M_H, M_W)$ has an active BBU hotel (line 30). In order to keep the primary BBU hotel as close as possible, node i

activates a BBU hotel in its cell location (line 31) and connects its RRUs to it as primary BBU hotel (line 32). The backup BBU hotel is node j (line 33). In lines 34 to 36 all the wavelengths in the links between nodes i and j are updated accordingly. The last case happens when no active hotel is found in the set $N_i(M_H, M_W)$ (line 38), then with the same line of reasoning of keeping primary BBU hotel as close as possible, in line 39 node i activates its BBU hotel as primary BBU hotel (line 40). One random node, namely node j, from the set $N_i(M_H, M_W)$ is chosen (line 41) and assigned for backup purposes (lines 42 and 43). Like in the other cases, all the wavelengths in the links between nodes i and j are updated accordingly (lines 44 - 46).

Algorithm 3 calls Neighbor Finder Function (NFF), reported here as Algorithm 5, to fill the set of neighbor nodes $N_i(M_H, M_W)$ of an input node i (line 1). In order to keep track of the maximum number of hops, Algorithm 5 sets Time-To-Live (TTL) parameter equal to M_H (line 2) and stops when TTL reaches to zero (line 4). The current set CS_n of nodes to be considered at first iteration ($n = 0$) is initialized with initial node i. While the CS_n is not empty (line 5), a random node (k) contained in this set is considered (line 6). All the neighbor nodes of k are iteratively considered (line 7) and placed in the neighbor set of the initial node i (line 9) if there are enough wavelengths to accommodate the request (line 8). Neighbor node j is then inserted in the set of nodes to be considered in the next iteration (line 10). After all the neighbors of k have been identified, k is removed from the current CS_n (line 13), and these instructions are repeated until CS_n is empty. At this point, TTL is updated (line 15) and the iteration index n is updated (line 16). This procedure is repeated until the limit set by TTL is reached, then the set of neighbors of i is returned (line 18).

BBU port sharing: after finding the BBU hotel placement, RRUs are re-assigned in order to further reduce the amount of ports by sharing backup BBU ports. For this phase, nodes have to interact to exchange the information regarding the primary hotel for RRUs that share the same backup BBU hotel. The rule to perform port sharing is that RRUs assigned to different primary hotels can share the same backup BBU port. Therefore, the minimum number of backup BBU ports equals the maximum number of RRUs that share the same primary hotel. These ports are sufficient to guarantee backup service to all the RRUs connected to the backup hotel and can be used when a single hotel failure occurs. This procedure is reported in Algorithm 4.

Algorithm 4 is executed in every node which has an active BBU hotel. In this pseudo code, the considered active hotel is node i. Algorithm 4 starts at line 2 by introducing SA_j as a set of RRU sites sharing the same primary hotel j, initially set to zero for each node j in the network. Also a parameter Max is initially set to zero, introduced to stores the maximum value of RRUs sharing the same primary. In line 3 BBU hotel located at node i identifies all nodes $j \in S$ that are using BBU hotel at node i as backup. Lines 4 to 7 aims at finding all the other nodes, like node $k \in S$, such that both node j and k have the same primary BBU hotel (line 4). If such hotel exists, namely BBU hotel located at node $z \in S$ (line 5), then the value for SA_j increases by one (6). Since all RRUs at nodes j and k have their primary BBU ports in the same BBU hotel, they must have distinct backup BBU ports in BBU hotel i, so if BBU hotel z fails, there are enough ports at hotel i to accommodate the new RRUs. After checking all the nodes that share the same primary BBU hotel with node j, at line 9 the number of antennas sharing the same primary is compared with Max in order to store the maximum value (line 10). In line 13 the minimum number of backup BBU port (y_i) that node i must have to guarantee protection for all RRUs connected to it is set to be equal to the maximum value (Max).

Algorithm 3 Distributed Location Algorithm

1: **Begin**
2: $i =$ a random node in set S
3: **call** $NFF(i)$
4: //Procedure when node has active hotel:
5:   **if** $B_i = 1$
6:       $p_{ii} = 1$
7:       **if** exists a node $j \in N_i(M_H, M_W)$ s.t. $B_j = 1$
8:           $b_{ji} = 1$
9:           **for** all $l \in L$ between nodes $i, j \in S$
10:               $w_l = w_l + r_i$
11:           **end for**
12:       **else**
13:           $j =$ a random node in set $N_i(M_H, M_W)$
14:           $B_j = 1$
15:           $b_{ji} = 1$
16:           **for** all $l \in L$ between nodes $i, j \in S$
17:               $w_l = w_l + r_i$
18:           **end for**
19:       **end if**
20: //Procedure when node does not have active hotel:
21:   **else**
22: //There are two hotels in the neighbors set:
23:       **if** exist $j, z \in N_i(M_H, M_W)$ s.t. $B_j = B_z = 1$
24:           $p_{ji} = 1$
25:           $b_{zi} = 1$
26:           **for** all $l \in L$ between nodes i and $j, z \in S$
27:               $w_l = w_l + r_i$
28:           **end for**
29: //There is one hotel in the neighbors set:
30:       **else if** exists $j \in N_i(M_H, M_W)$ s.t. $B_j = 1$
31:           $B_i = 1$
32:           $p_{ii} = 1$
33:           $b_{ji} = 1$
34:           **for** all $l \in L$ between nodes $i, j \in S$
35:               $w_l = w_l + r_i$
36:           **end for**
37: //No hotel exists in the neighbors set:
38:       **else**
39:           $B_i = 1$
40:           $p_{ii} = 1$
41:           $j =$ a random node in set $N_i(M_H, M_W)$
42:           $B_j = 1$
43:           $b_{ji} = 1$
44:           **for** all $l \in L$ between nodes $i, j \in S$
45:               $w_l = w_l + r_i$
46:           **end for**
47:       **end if**
48:   **end if**
49: **Stop**

Algorithm 5 Neighbor Finder Function (NFF)
1: **Given:** node $i \in S$
2: **Initialization:** $TTL = M_H, CS_0 \leftarrow i, n = 0$

3: **Begin**
4: **while** $TTL \neq 0$
5:     **while** $CS_n \neq \{\}$
6:         **get** random node k from CS_n
7:         **for** all nodes $j \in N_k$
8:             **if** $w_l + r_i \leq M_W$
9:                 $N_i(M_H, M_W) \leftarrow j$
10:                $CS_{n+1} \leftarrow j$
11:            **end if**
12:        **end for**
13:        **remove** k from CS_n
14:    **end while**
15:    $TTL = TTL - 1$
16:    $n = n + 1$
17: **end while**
18: **Return** $N_i(M_H, M_W)$
19: **Stop**

Algorithm 4 Sharing Backup BBU hotel ports
1: **Begin:**
2: **Initialization:** $SA_j = 0, \forall j \in S, Max = 0$
3: **for** all nodes $j \in S : b_{ij} = 1$
4:     **for** all nodes $k \in S : b_{ik} = 1$
5:         **for** all nodes $z \in S : B_z = 1$ and $p_{zj} = p_{zk} = 1$
6:             $SA_j = SA_j + 1$
7:         **end for**
8:     **end for**
9:     **if** $SA_j \cdot r_j > Max$
10:        $Max = SA_j \cdot r_j$
11:    **end if**
12: **end for**
13: $y_i = Max$
14: **Stop**

6.1.3   Optimization Algorithm

A traditional approach, which requires complete knowledge of the network and can be run on the top of the network controller is here proposed.

Objective function:

$$Minimize \ G = C_B + C_H + C_P \tag{6.4}$$

The multi-objective function (6.4) is composed of three members. The first term takes into account the activation cost of each hotel (C_B). The second term accounts for the cost to connect RRUs to BBU hotels, both primary and backup (C_H) while the third term accounts for the cost of BBU ports required in each hotel (C_P).

The problem is subject to the following constraints:

$$\sum_{i \in S} p_{ij} = 1, \forall j \in S \tag{6.5}$$

$$\sum_{i \in S} b_{ij} = 1, \forall j \in S \tag{6.6}$$

$$p_{ij} + b_{ij} \leq 1, \forall i, j \in S \tag{6.7}$$

$$B_i \cdot M \geq \sum_{j \in S} p_{ij} + b_{ij}, \forall i \in S \tag{6.8}$$

$$(p_{ij} + b_{ij}) \cdot h_{ij} \leq M_H, \forall i, j \in S \tag{6.9}$$

$$\sum_{a \in S} \sum_{b \in S} (p_{ab} + b_{ab}) \cdot \delta_{ab}^l \cdot \delta_{ij}^l \cdot r_b \leq M_W + M \cdot (1 - p_{ij} + b_{ij}), \forall l \in L, i, j \in S \tag{6.10}$$

$$x_i \geq \sum_{j \in S} p_{ij} \cdot r_j, \forall i \in S \tag{6.11}$$

$$c_{iji'} \geq p_{ij} + b_{i'j} - 1, \forall i, j \in S, i' \in S - \{i\} \tag{6.12}$$

$$y_{i'} \geq \sum_{j \in S} c_{iji'} \cdot r_j, \forall i \in S, i' \in S - \{i\} \tag{6.13}$$

Constraints (6.5) and (6.6) ensure that there is one primary and one backup hotel for each RRU, respectively. Constraint (6.7) imposes primary and backup hotels to be disjoint. Constraint (6.8) is related to the activation of BBU hotels. If the hotel is acting as a primary and/or backup for RRUs, it must be activated. Constraint (6.9) ensures that the maximum allowed distance M_H (in hops) is not exceeded, due to limit on the fronthaul delay. Constraint (6.10) limits the number of wavelengths over each link to M_W. This constraint is used in case of limited capacity of optical resources connecting the nodes. If capacity can be added to the link, for example because the problem is also to dimension the capacity of the link, it can be set to infinity (or to a very large number). Constraint (6.11) counts the number of BBU resources to be installed in each primary hotel. Constraint (6.12) tells if a primary hotel is in common to a backup hotel for each source and is used in constraint (6.13) to ensure that there are enough BBU resources in each backup hotel. These two constraints, along with (6.4), allow to minimize the number of BBU resources in each backup hotel. In fact, the number of BBU resources required at each backup hotel equals the largest number of RRUs that shares the same primary hotel.
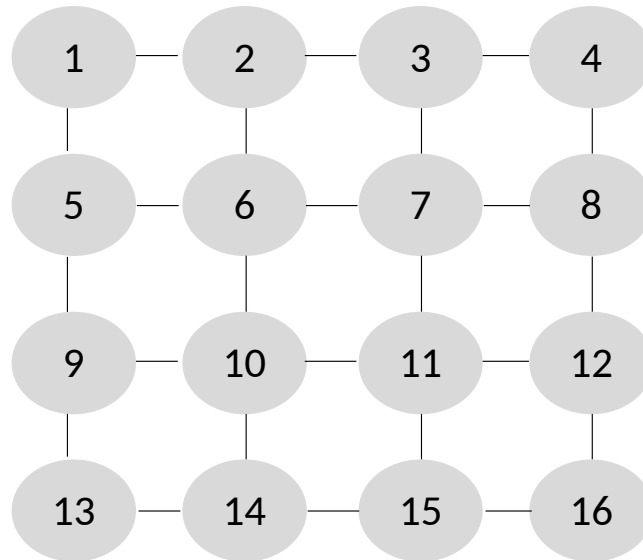
Figure 6.2: Network topology (a) with 16 nodes.
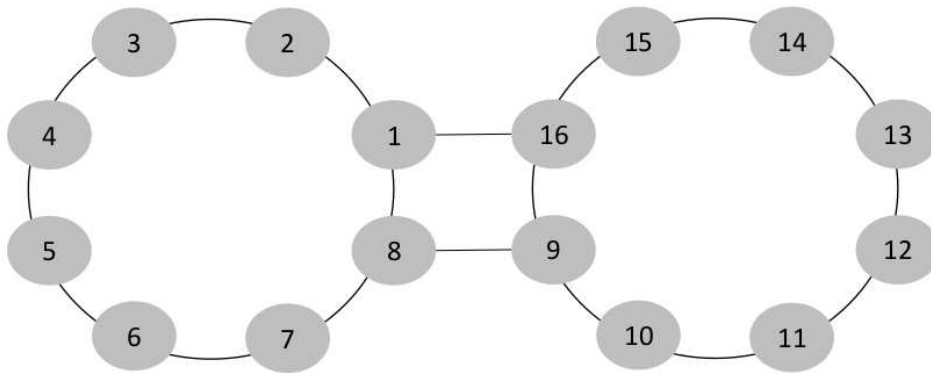
Figure 6.3: Network topology (b) with 16 nodes.

6.1.4   Application to Different Networks

To assess the performance of the proposed strategies, different optical transport network topologies have been used, with a different number of nodes and connectivity. Mesh topologies are considered, similarly to exising works on 5G transport networks [109, 110]. The ILP and heuristic are evaluated firstly in a 16 nodes network (Figure 6.2). In Figure 6.3 a 16 nodes network with different nodal connectivity is presented. Finally, to evaluate a larger scenario, also a 36 nodes network is considered (Figure 6.4).

The results discussed in this section are obtained using a Java-based simulator for the distributed strategy and compared with the optimal solution obtained using CPLEX commercial tool [54]. The ILP results are obtained in the case $\beta >> \alpha >> \gamma$, so to prioritize the minimiza-

Figure 6.4: Network topology (c) with 36 nodes.

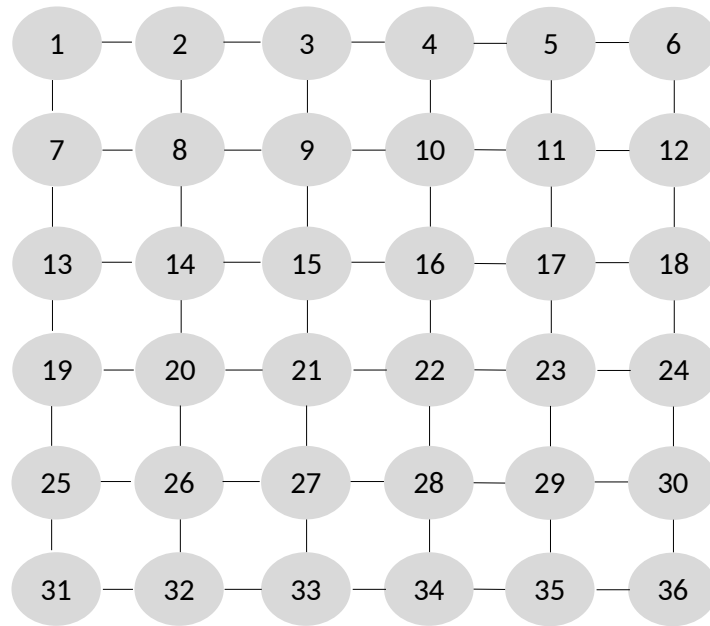tion of BBU hotel activation, then the distance and finally the number of BBU ports. Given the intrinsic randomicity of the distributed strategy, 50 different simulations are performed. The obtained confidence interval is always less than 5% with a confidence level of 95% for the cases up to 4 hop constraints. With 5 and 6 hops constraints instead, the confidence interval slightly increases, but does not exceed 10%.

Figure 6.5 reports the number of BBU hotels required by ILP and heuristic in the best and worst case, i.e., the cases when the active BBU hotels are minimum and maximum, respectively. The ILP provides always the best solution and the number of required BBU hotels decreases when the distance constraint increases. This is due to the fact that, when the allowed distance increases, RRUs can be connected to hotels in farther nodes, requiring less BBU hotels to be activated. In the case of heuristic instead, different behaviors are experienced. In particular, in the best case for the heuristic, i.e., when the choices due to randomness are favorable to reduce the number of active hotels, the proposed strategy follows the trend of the ILP, requiring only one additional hotels, in case of 1 hop constraint, with respect to the optimal solution. In the worst case instead, the number of active BBU hotels is larger, and follows the trend of the ILP only until 3 hops constraint. For larger distance constraints (4 to 6), the amount increases due to the limit on the number of wavelengths. In fact, the distributed strategy tries to connect
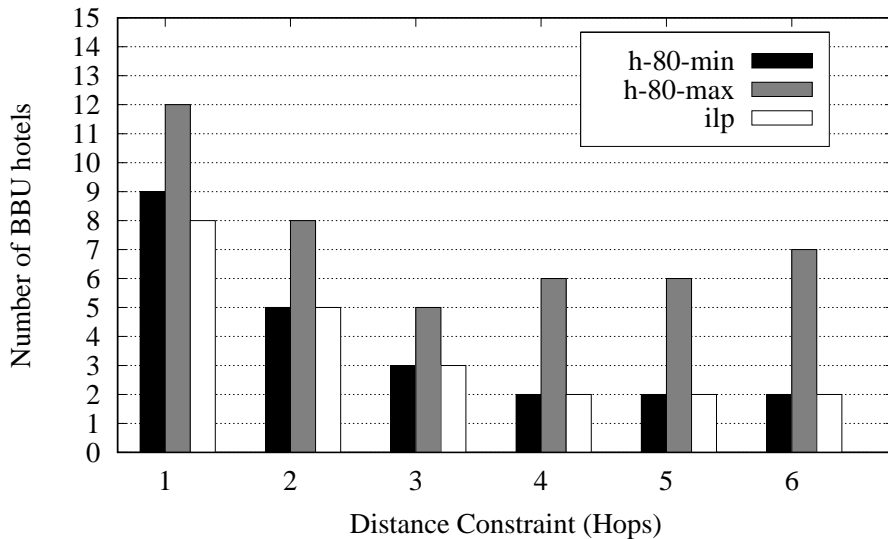
Figure 6.5: Number of active BBU hotels required by ILP and heuristic (h-80-min, h-80-max) in the best and worst case for different distance constraints in the network (a), with wavelength constraint equal to 80.

RRUs to the farthest BBU hotel that can reach, increasing the wavelength need over the links. When the distance constraint is large, some of the links are saturated and therefore closer BBU hotels must be selected, increasing the number of active hotels and decreasing the BBU hotel sharing.

Figure 6.6 depicts the number of BBU hotels required by ILP and heuristic, averaged over all the 50 cases, with and without the hop constraint (h-80-avg and h-inf-avg, respectively). The case without wavelength limitation follows the decreasing trend of the ILP, reaching optimal solutions when the maximum allowed distance is 5 and 6 hops. In the wavelength limited case instead, in these last two cases the number of active BBU hotels increases, following the trend of the maximum case reported in the previous figure.

The wavelengths usage, in the most used link and on average (over links), for ILP and heuristic, with and without hop constraint, in the network (a) is reported in Table 6.3. When the wavelength limit (set to 80) applies, both the ILP and the heuristic require all the wavelengths in the most used link, when the maximum allowed distance is higher than 3 hops. In this case two hotels are enough to ensure protected service for all RRUs (see Figure 6.5), so the links directly attached to the selected hotels becomes fully used. In the case of ILP, the average wavelength usage increases until it reaches the value of 26.7, which is the minimum cost case.
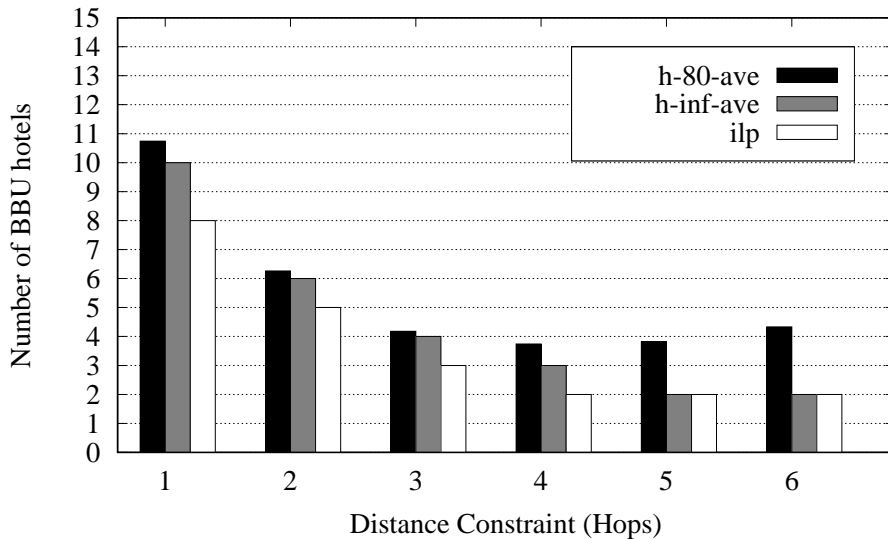
Figure 6.6: Number of active BBU hotels required by ILP and heuristic (h-80-ave, h-inf-ave), with and without wavelength constraint, averaged over 50 cases for different distance constraints in the network (a).

Table 6.3: Number of wavelengths per link (maximum and average cases) required by ILP and heuristic (h-80, h-inf), with and without wavelengths constraint, for different limits over distance in the network (a).

| Maximum distance in [hops] | Number of wavelengths per link | | | | | |
| | ILP | | h-80 | | h-inf | |
	Max	Avg	Max	Avg	Max	Avg
1	20	10	20	8.9	20	8.9
2	40	15.8	50	16.9	50	17
3	50	21.7	70	24	80	23.8
4	80	26.7	80	30.1	90	28.8
5	80	26.7	80	33.8	100	30
6	80	26.7	80	34	130	33.9

The cost for the heuristic, instead, keep increasing, regardless the fact that the active BBU hotels increase when the distance constraint is equal to 5 and 6. This is due to the fact that each node runs the algorithm only once and when the links reaching active BBU hotels are full, BBU hotels in different nodes are selected. However the primary and backup hotels, and the wavelengths already assigned, cannot be changed, even if the new hotels are closer to nodes already assigned, thus increasing the overall link resources usage. The table reports also the case with is no wavelength limitation in the heuristic. In this case both the maximum number of wavelengths allocated in the most used link and the average usage increases over 80, allowing this strategy to reach near-optimal solutions in terms of active BBU hotels.

Table 6.4: Maximum and average number of hops, between RRUs and BBUs for ILP and heuristic (h-80) with different limits over distance in the network (a) with wavelengths constraint equal to 80.

| Maximum distance in [hops] | Distance [hops] | | | |
| | ILP | | h-80 | |
	Max	Avg	Max	Avg
1	1	0.75	1	0.66
2	2	1.19	2	1.25
3	3	1.63	3	1.78
4	4	2	4	2.22
5	4	2	5	2.5
6	4	2	6	2.5

Table 6.4 reports the average distance, in hops, between RRUs and BBUs for ILP and heuristic with different limits over distance in the network (a) and maximum wavelengths limit equal to 80. The hops, both maximum and average, required by ILP increases with the maximum allowed distance, and reaches the maximum value of 4 and an average of 2. In the heuristic instead, the maximum distance increases up to 6, while the average reach a maximum of 2.5. The increasing trend in both cases is due to the fact that, when the maximum allowed distance increases, both strategies try to reach farther BBU hotels to reduce activation of new hotels, therefore reducing the cost.

On the one hand, when the number of wavelengths is limited, a proper choice of the sequence of nodes in which the distributed algorithm is performed can lead to near-optimal solutions. On the other hand, this choice requires a complete knowledge of the network and can be performed only at a higher level (i.e., in the network controller), thus the distributed strategy is not always capable of reaching optimality.

Figure 6.7 reports the number of backup BBU ports as a function of different distance constraints obtained with ILP and heuristic, averaged over the 50 cases, in the network (a). From the figure it is possible to notice that the two strategies are capable of reducing the number of backup ports with respect to the case in which there is no port sharing, that is 160 ports. For low values of distance constraint or, alternatively, when the number of active hotels is large, the number of required BBU ports is low, with the ILP that provides better solutions than
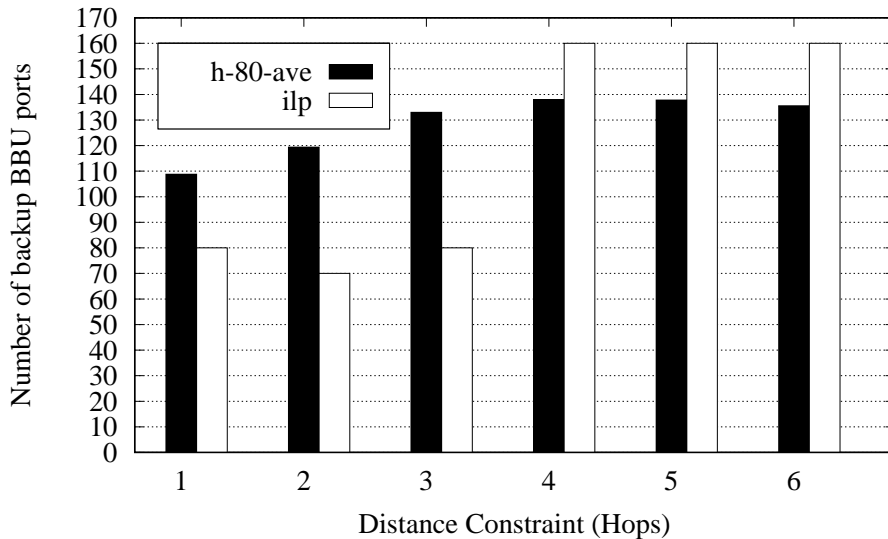
Figure 6.7: Number of backup BBU hotel ports required by ILP and heuristic (h-80-ave), averaged over 50 cases for different distance constraints in the network (a), with wavelength constraint equal to 80.

Table 6.5: Total number of active BBU hotels and wavelengths for ILP and heuristic (h-80) with different limits on distance in the network (b) with wavelengths constraint equal to 80.

Maximum distance in [hops]	BBU hotels		Wavelengths	
	ILP	h-80	ILP	h-80
1	10	11	220	210
2	6	7	380	370
3	5	5	440	580
4	3	4	650	680
5	2	4	800	810
6	2	4	800	960

the distributed strategy. On the other hand, when the distance constraint is large, the number of ports reach 160 in case of ILP. This is due to the fact that with a distance limit of 4, 5 and 6 hops the ILP is capable of finding a solution with only 2 active hotels (see Figure 6.5), and therefore sharing backup BBU port is not allowed and 160 backup ports are needed. On the other hand, the heuristic performs slightly better, having more than 2 active hotels and therefore allowing some port sharing.

Table 6.5 presents the result of both ILP and heuristic in the network (b). The table shows the comparison of the total number of active BBU hotels and wavelengths for ILP and heuristic with the wavelength limitation equal to 80. The result for both approaches shows a decrement
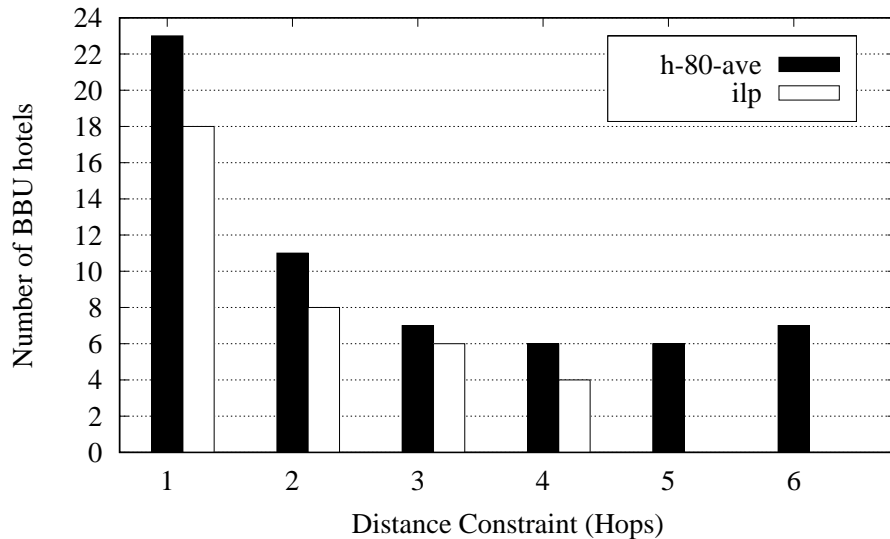
Figure 6.8: Number of active BBU hotels required by ILP and heuristic (h-80-ave), averaged over 50 cases, for different distance constraints in the network (c), with wavelength constraint equal to 80.

in the number of required BBU hotels by relaxing the distance constraint. The ILP can reach the result of having only two active BBU hotels with 5 and 6 hops distance constraint. The heuristic instead, due to the lack of knowledge on network connectivity a priori, can not find any better result than 4 active BBU hotels in 4 to 6 hops distance constraints. By comparing these results with the one obtained in the network (a), it can be seen that ILP obtains the same results due to its knowledge on network connectivity. In the heuristic case instead, the results are slightly different and that is due to the effect of different nodal degree. Table 6.5 also shows a comparison of the total number of wavelengths for both ILP and heuristic under different distance constraints. In this set of results, the limitation on maximum 80 wavelengths per link is also considered. Obviously, by relaxing the distance constraint and decreasing the number of active BBU hotels, the total number of wavelengths increases in both approaches. ILP uses more wavelength when limited to 1 and 2 hops because of less number of active BBU hotels in comparison with the heuristic. From 3 hops, ILP uses less wavelengths with respect to the heuristic due to better choices in routing. With the heuristic instead, the usage of wavelength increases by relaxing the distance constraint, similarly to the outcome obtained for the network (a).

Figure 6.8 shows the active BBU hotels in the network (c) required by ILP and heuristic, on
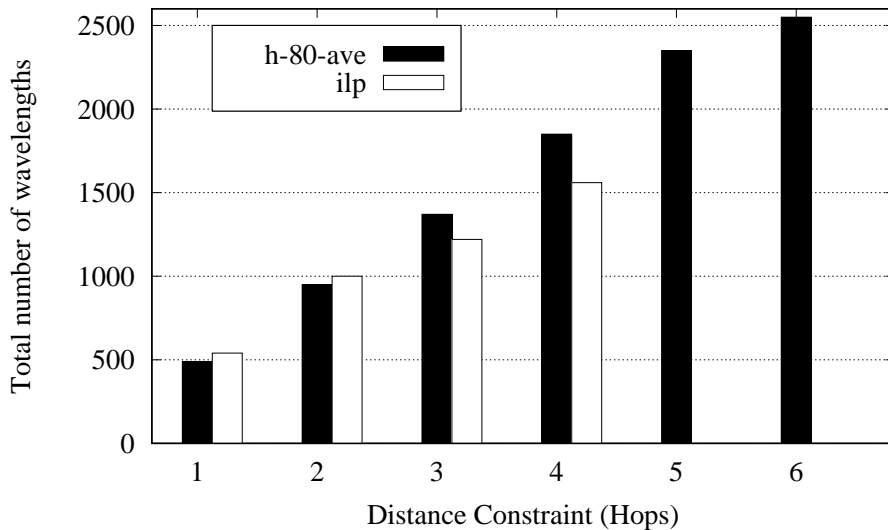
Figure 6.9: Total number of wavelengths required by ILP and heuristic (h-80-ave), averaged over 50 cases for different distance constraints, in the network (c) with wavelength constraint equal to 80.

average. From the figure, it is possible to notice that the ILP requires less active BBU hotels when the distance constraint increases. The hotels required by the heuristic follow the ILP trend, but they increase when the distance constraint is 6. Similarly to the network (a), this is due to the limit on the wavelengths, that forces the algorithm to activate more BBU hotels. The case of 5 and 6 hops are not reported in the ILP case due to the large solution space of the problem that translates into out of memory issues for these cases. In fact, while in the network (a) the time required to solve the model with the ILP is in the order of tens of seconds, in the network (c) this time increases to tens of minutes for a distance constraint less than 4 hops, while for larger values the complexity of the instances makes not possible to find a solution.

Figure 6.9 depicts the total number of wavelengths required by ILP and heuristic, averaged over all the 50 cases. The total amount of wavelengths increases when the distance constraint increases. In fact, when the distance constraint increases, farther BBU hotel can be reached, increasing the overall amount of wavelengths that are needed to connect RRUs and BBUs. The absolute difference between the two strategies also increases with the distance constraint, due to the inability of the heuristic to properly choose locations for BBU hotels.
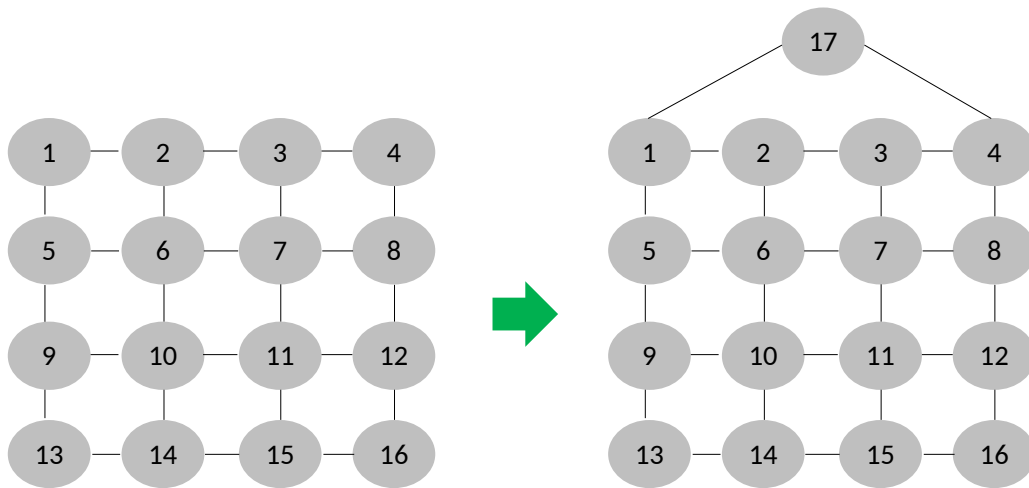
Figure 6.10: Example of a transition from 16 to 17 nodes network.

Figure 6.11: Outcome of developed ILP during a transition from 16 to 17 nodes network limiting the maximum distance to 1 hop.

6.2   Considerations on Dynamic Scenarios

Classical deployment techniques are not suitable for dynamic changes in the network, where more incremental approaches must be developed to minimize the changes in the network during operational time. To better understand the problem, let us suppose that in a network a new node is added. This could be the case of a node in which new computational resources are installed or freed by other services running on that node. An example of a transition from 16 to 17 nodes network is reported in Figure 6.10.

A network controller, which has a complete view of the network, runs the optimal placement algorithm for the 16 nodes network. When it detects a change in the BBU pools, it runs
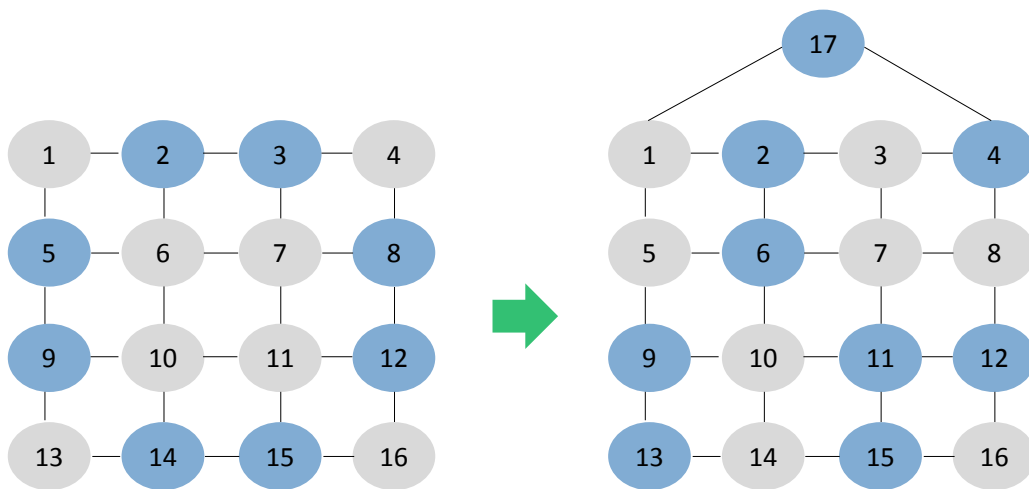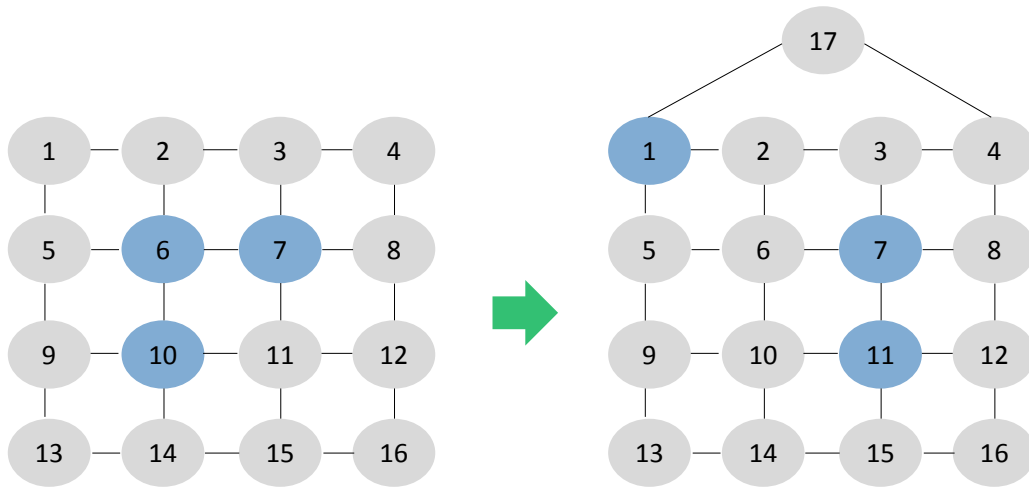
Figure 6.12: Outcome of developed ILP during a transition from 16 to 17 nodes network limiting the maximum distance to 3 hops.

the algorithm again to determine the new optimal solution. The outcome obtained with the optimization algorithm for the networks depicted in Figure 6.10 is reported in Figures 6.11 and 6.12 for the case of 1 hop and 3 hops constraint on the maximum distance, respectively. As it is possible to see, finding a new optimum usually requires to activate different hotels, and consequently migrate BBU resources. In case of 1 hop limit, the transition from 16 to 17 nodes requires an activation of an extra BBU hotel, while in case of 3 hops constraint 3 hotels are sufficient also in the 17 nodes network and no extra BBU hotel is added. A more straightforward solution to the case reported in Figure 6.11 would be to activate directly node 17. However, this requires to use more wavelengths and therefore to reach the optimal solution the whole placement must be changed, due to the objective function (6.4) and the choice of the tuning parameters.

To prove the effectiveness of the distributed approach in dynamic scenarios, Figures 6.13 and 6.14 reports the outcome of the distributed strategy reported in [102] for the case of 1 hop and 3 hops constraint on the maximum distance, respectively. It can be noticed how the resulting deployment, even though it requires more active BBU hotels than the optimal approach, is way more incremental and reaches solutions without requiring migration of BBU resources. On the one hand, a complete knowledge of the network allows to develop optimization algorithms to achieve optimal solutions. On the other hand, distributed strategies cannot reach optimal solutions in most of the cases, but relaxes the controller from heavy exchange of control infor-

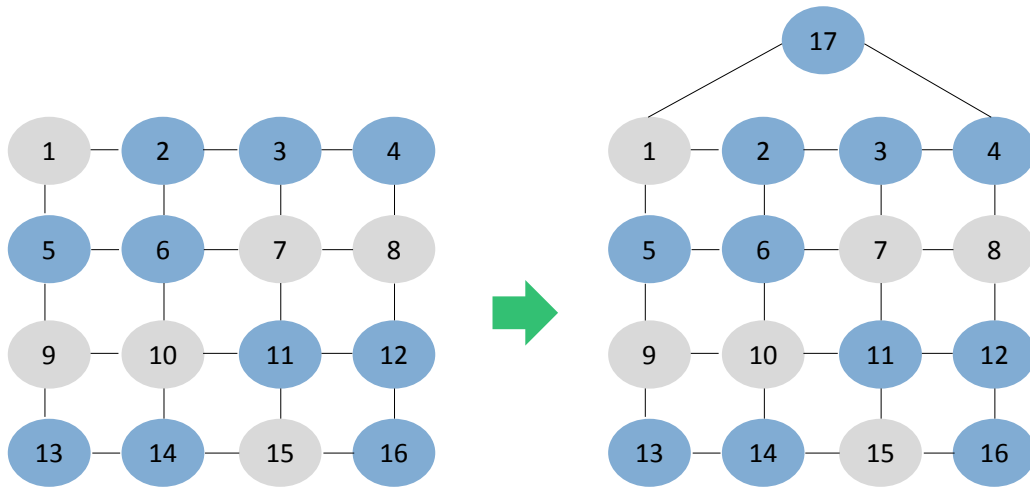Figure 6.13: Outcome of distributed heuristic during a transition from 16 to 17 nodes network limiting the maximum distance to 1 hop.
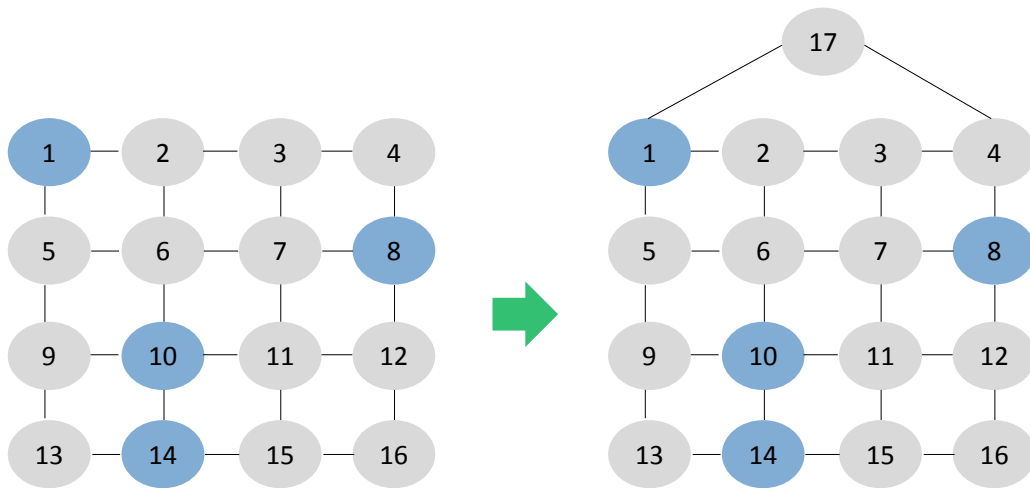

Figure 6.14: Outcome of distributed heuristic during a transition from 16 to 17 nodes network limiting the maximum distance to 3 hops.

mation. This aspect must be considered when decisions are taken with a centralized strategy and requires additional studies.

Chapter 7

Conclusion

This thesis illustrates the main outcomes of the research activities conducted throughout the three years of the Ph.D. program. Novel deployment strategies for a cost-efficient and reliable deployment of C-RAN for 5G transport networks have been proposed.

In Chapter 3, a use case related to capacity provisioning during special events in urban areas is analyzed and a cost-efficient ILP strategy is proposed where mobile network deployment is tackled considering both radio and transport network constraints. The results show a non-negligible impact of the transport network cost, suggesting that including information on the transport network and reusing the existing infrastructure can lower the overall deployment cost. The deployment strategies presented in Chapter 4, based on ILP and heuristic, concern the massive deployment of centralized architectures in indoor scenarios. Evaluations are conducted with reference to a conventional deployment approach and show that by using a more careful deployment strategy, significant cost savings can be achieved. In Chapter 5, the problem of sharing optical transport network resources is addressed. Here, it is proposed to use Ethernet encapsulation of CPRI frames to multiplex backhaul and fronthaul traffic over the same wavelengths, thus enabling high resource utilization. Finally, in Chapter 6 the problem of BBU hotel failures is addressed. Resilient deployment strategies based on ILP and heuristic are used to evaluate the impact of failures in the network resources (i.e., wavelengths and BBU functions). Considerations for dynamic scenarios, where the deployment of BBU functions is

not static, are also provided, showing that conventional design strategies may not be effective in this perspective and requires additional studies.

The work presented in this thesis can be further extended in relation to the emerging baseband functional splits that have been recently proposed. In particular, the adoption of Ethernet switches with more levels of priority can be investigated to multiplex traffic with different requirements over the same physical infrastructure. This would also be effective in dynamic scenarios, where the optimal baseband functional split can be determined based on, for example, traffic conditions, and the network must constantly adapt to these changes.

Bibliography

[1] "ICT COMBO, deliverable 3.4, v1.0." http://www.ict-combo.eu/data/uploads/deliverables/combo_d3.4_wp3_17june2016_v1.0.pdf.

[2] F. Farias, M. Fiorani, S. Tombaz, M. Mahloo, L. Wosinska, J. C. W. A. Costa, and P. Monti, "Cost- and energy-efficient backhaul options for heterogeneous mobile network deployments," *Photonic Network Communications*, vol. 32, pp. 422–437, Dec 2016.

[3] M. Mahloo, P. Monti, J. Chen, and L. Wosinska, "Cost modeling of backhaul for mobile networks," in *2014 IEEE International Conference on Communications Workshops (ICC)*, pp. 397–402, June 2014.

[4] A. A. Widaa, J. Markendahl, and A. Ghanbari, "Toward capacity-efficient, cost-efficient and power-efficient deployment strategy for indoor mobile broadband," tech. rep., International Telecommunications Society (ITS), 2013.

[5] "Third Generation Partnership Project (3GPP) Technical Report 38.801, v.14." https://portal.3gpp.org/desktopmodules/Specifications/SpecificationDetails.aspx?specificationId=3056.

[6] "Ericsson White paper." www.ericsson.com/res/docs/whitepapers/wp5g.pdf, 2015.

[7] "NGMN 5G White Paper." White Paper, 2015.

[8] "UEN 284 233251 rev B." Ericsson White paper, 2017.

[9] Cisco Vision: 5G Thriving Indoors, 2017.

[10] A. Gupta and R. K. Jha, "A survey of 5G network: Architecture and emerging technologies," *IEEE Access*, vol. 3, pp. 1206–1232, 2015.

[11] A. Checko, H. L. Christiansen, Y. Yan, L. Scolari, G. Kardaras, M. S. Berger, and L. Dittmann, "Cloud RAN for mobile networksa technology overview," *IEEE Communications Surveys Tutorials*, vol. 17, pp. 405–426, Firstquarter 2015.

[12] E. J. Oughton and Z. Frias, "The cost, coverage and rollout implications of 5G infrastructure in britain," *Telecommunications Policy*, vol. 42, no. 8, pp. 636 – 652, 2018. The implications of 5G networks: Paving the way for mobile innovation?

[13] "ITU Setting the schene for opportunity and challenges." https://www.itu.int/en/ITU-D/Conferences/GSR/Documents/GSR2018/documents/DiscussionPaper_Setting%20the%20scene%20for%205G_GSR18.pdf.

[14] A. F. Molisch, *Wireless Communications.* John Wiley and Sons, second ed., 2010.

[15] "Common Public Radio Interface (CPRI)." http://www.cpri.info/.

[16] "Open Base Station Architecture Initiative (OBSAI)." http://www.obsai.com/.

[17] M. Xiao, S. Mumtaz, Y. Huang, L. Dai, Y. Li, M. Matthaiou, G. K. Karagiannidis, E. Bjrnson, K. Yang, C. I, and A. Ghosh, "Millimeter wave communications for future mobile networks," *IEEE Journal on Selected Areas in Communications*, vol. 35, pp. 1909–1935, Sept 2017.

[18] M. Fiorani, B. Skubic, J. Mårtensson, L. Valcarenghi, P. Castoldi, L. Wosinska, and P. Monti, "On the design of 5G transport networks," *Photonic Network Communications*, vol. 30, pp. 403–415, Dec 2015.

[19] "ICT COMBO, deliverable 3.3." http://www.ictcombo.eu/data/uploads/deliverables/combo_d3.3_pu.pdf.

[20] China Mobile Research Institute, "C-RAN the road towards green RAN, v. 2.5," *Technical Report*, October 2011.

[21] V. Q. Rodriguez and F. Guillemin, "VNF modeling towards the cloud-RAN implementation," in *2017 International Conference on Networked Systems (NetSys)*, pp. 1–8, March 2017.

[22] M. Fiorani, A. Rostami, L. Wosinska, and P. Monti, "Transport abstraction models for an SDN-controlled centralized RAN," *IEEE Communications Letters*, vol. 19, pp. 1406–1409, Aug 2015.

[23] A. Pizzinat, P. Chanclou, F. Saliou, and T. Diallo, "Things you should know about fronthaul," *Journal of Lightwave Technology*, vol. 33, pp. 1077–1083, March 2015.

[24] X. Wang, L. Wang, S. E. Elayoubi, A. Conte, B. Mukherjee, and C. Cavdar, "Centralize or distribute? A techno-economic study to design a low-cost cloud radio access network," in *2017 IEEE International Conference on Communications (ICC)*, pp. 1–7, May 2017.

[25] A. Alabbasi, X. Wang, and C. Cavdar, "Optimal processing allocation to minimize energy and bandwidth consumption in hybrid CRAN," *IEEE Transactions on Green Communications and Networking*, vol. 2, pp. 545–555, June 2018.

[26] "International Telecommunication Union (ITU) GSTR-TN5G Transport network support of IMT2020/5G." https://www.itu.int/pub/TTUTHOME2018.

[27] M. Fiorani, P. Monti, B. Skubic, J. Mrtensson, L. Valcarenghi, P. Castoldi, and L. Wosinska, "Challenges for 5G transport networks," in *2014 IEEE International Conference on Advanced Networks and Telecommuncations Systems (ANTS)*, pp. 1–6, Dec 2014.

[28] X. Ge, H. Cheng, M. Guizani, and T. Han, "5G wireless backhaul networks: challenges and research advances," *IEEE Network*, vol. 28, pp. 6–11, Nov 2014.

[29] Y. Li, N. Pappas, V. Angelakis, M. Pioro, and D. Yuan, "Optimization of free space optical wireless network for cellular backhauling," *IEEE Journal on Selected Areas in Communications*, vol. 33, pp. 1841–1854, Sept 2015.

[30] H. Dahrouj, A. Douik, F. Rayal, T. Y. Al-Naffouri, and M. Alouini, "Cost-effective hybrid rf/fso backhaul solution for next generation wireless systems," *IEEE Wireless Communications*, vol. 22, pp. 98–104, October 2015.

[31] Z. Ghassemlooy, S. Arnon, M. Uysal, Z. Xu, and J. Cheng, "Emerging optical wireless communications-advances and challenges," *IEEE Journal on Selected Areas in Communications*, vol. 33, pp. 1738–1749, Sept 2015.

[32] F. Demers, H. Yanikomeroglu, and M. St-Hilaire, "A survey of opportunities for free space optics in next generation cellular networks," in *2011 Ninth Annual Communication Networks and Services Research Conference*, pp. 210–216, May 2011.

[33] D. Schulz, V. Jungnickel, C. Alexakis, M. Schlosser, J. Hilt, A. Paraskevopoulos, L. Grobe, P. Farkas, and R. Freund, "Robust optical wireless link for the backhaul and fronthaul of small radio cells," *Journal of Lightwave Technology*, vol. 34, pp. 1523–1532, March 2016.

[34] N. A. Gunathilake and M. Z. Shakir, "Empirical performance evaluation of fso availability under different weather conditions," in *2017 8th International Conference on the Network of the Future (NOF)*, pp. 156–158, Nov 2017.

[35] E. Amaldi, A. Capone, F. Malucelli, and C. Mannino, *Optimization Problems and Models for Planning Cellular Networks*, pp. 917–939. Boston, MA: Springer US, 2006.

[36] A. Taufique, M. Jaber, A. Imran, Z. Dawy, and E. Yacoub, "Planning wireless cellular networks of future: Outlook, challenges and opportunities," *IEEE Access*, vol. 5, pp. 4821–4845, 2017.

[37] L. Suarez, M. A. Bouraoui, M. A. Mertah, M. Morvan, and L. Nuaymi, "Energy efficiency and cost issues in backhaul architectures for high data-rate green mobile heterogeneous networks," in *2015 IEEE 26th Annual International Symposium on Personal, Indoor, and Mobile Radio Communications (PIMRC)*, pp. 1563–1568, Aug 2015.

[38] M. Mahloo, P. Monti, J. Chen, and L. Wosinska, "Cost modeling of backhaul for mobile networks," in *2014 IEEE International Conference on Communications Workshops (ICC)*, pp. 397–402, June 2014.

[39] C. S. Ranaweera, P. P. Iannone, K. N. Oikonomou, K. C. Reichmann, and R. K. Sinha, "Design of cost-optimal passive optical networks for small cell backhaul using installed fibers [invited]," *IEEE/OSA Journal of Optical Communications and Networking*, vol. 5, pp. A230–A239, Oct 2013.

[40] H. Chen, Y. Li, S. K. Bose, W. Shao, L. Xiang, Y. Ma, and G. Shen, "Cost-minimized design for TWDM-PON based 5G mobile backhaul networks," *IEEE/OSA Journal of Optical Communications and Networking*, vol. 8, pp. B1–B11, Nov 2016.

[41] C. Ranaweera, C. Lim, A. Nirmalathas, C. Jayasundara, and E. Wong, "Cost-optimal placement and backhauling of small-cell networks," *Journal of Lightwave Technology*, vol. 33, pp. 3850–3857, Sept 2015.

[42] G. V. Arevalo and R. Gaudino, "Techno-economics for optimal deployment of optical fronthauling for 5G in large urban areas," in *2018 20th International Conference on Transparent Optical Networks (ICTON)*, pp. 1–4, July 2018.

[43] F. Tonini, M. Fiorani, C. Raffaelli, L. Wosinska, and P. Monti, "Benefits of joint planning of small cells and fiber backhaul in 5G dense cellular networks," in *2017 IEEE International Conference on Communications (ICC)*, pp. 1–6, May 2017.

[44] F. Tonini, C. Raffaelli, L. Wosinska, and P. Monti, "Cost-optimal deployment of a C-RAN with hybrid fiber/FSO fronthaul (submitted)," *IEEE/OSA Journal of Optical Communications and Networking*, 2019.

[45] 3rd Generation Partnership Project, "Radio network planning aspects (Rel. 15), TR 43.030." https://portal.3gpp.org/desktopmodules/Specifications/SpecificationDetails.aspx?specificationId=2666, 2018.

[46] Hans-Otto Scheck, "User equipment receiver sensitivity: the forgotten mobile network efficiency factor." https://docbox.etsi.org/workshop/2013/201310_eeworkshop/s04_ee_applicationofmethodologies/NSN_SCHECK.pdf, 2013.

[47] V. S. Abhayawardhana, I. J. Wassell, D. Crosby, M. P. Sellars, and M. G. Brown, "Comparison of empirical propagation path loss models for fixed wireless access systems," in *2005 IEEE 61st Vehicular Technology Conference*, vol. 1, pp. 73–77 Vol. 1, May 2005.

[48] M. F. Catedra, J. Perez, F. S. de Adana, and O. Gutierrez, "Efficient ray-tracing techniques for three-dimensional analyses of propagation in mobile communications: application to picocell and microcell scenarios," *IEEE Antennas and Propagation Magazine*, vol. 40, pp. 15–28, Apr 1998.

[49] A. Medeisis and A. Kajackas, "On the use of the universal okumura-hata propagation prediction model in rural areas," in *VTC2000-Spring. 2000 IEEE 51st Vehicular Technology Conference Proceedings (Cat. No.00CH37026)*, vol. 3, pp. 1815–1818 vol.3, 2000.

[50] S. Seker and F. C. Kunter, "Multi-components mobile propagation model of park environment," *IEEE Transactions on Magnetics*, vol. 47, pp. 1494–1497, May 2011.

[51] "Digital mobile radio towards future generation systems, COST Action 231 final report." http://www.lx.it.pt/cost231/final_report.htm, 2013.

[52] P. Mogensen, W. Na, I. Z. Kovacs, F. Frederiksen, A. Pokhariyal, K. I. Pedersen, T. Kolding, K. Hugl, and M. Kuusela, "LTE capacity compared to the shannon bound," in *2007 IEEE 65th Vehicular Technology Conference - VTC2007-Spring*, pp. 1234–1238, April 2007.

[53] "Metis 2020, deliverable 6.5, v1.0." https://www.metis2020.com/wp-content/uploads/deliverables/METIS_D6.5_v1.pdf.

[54] *IBM ILOG CPLEX Optimization Studio V12.6.3*.

[55] M. Klinkowski, "Planning of 5G C-RAN with optical fronthaul: a scalability analysis of an ILP model," in *2018 20th International Conference on Transparent Optical Networks (ICTON)*, pp. 1–4, July 2018.

[56] L. Ferreira, M. Kuipers, C. Rodrigues, and L. M. Correia, "Characterisation of signal penetration into buildings for gsm and umts," in *2006 3rd International Symposium on Wireless Communication Systems*, pp. 63–67, Sept 2006.

[57] C. E. O. Vargas, L. da Silva Mello, and R. C. Rodriguez, "Measurements of construction materials penetration losses at frequencies from 26.5 ghz to 40 ghz," in *2017 IEEE Pacific Rim Conference on Communications, Computers and Signal Processing (PACRIM)*, pp. 1–4, Aug 2017.

[58] "International Telecommunication Union (ITU), Report ITU-R P.23460, Compilation of measurement data relating to building entry los." https://www.itu.int/dms_pub/itu-r/opb/rep/RREPP.2346-2015PDFE.pdf.

[59] C. Pei, Y. Zhao, G. Chen, R. Tang, Y. Meng, M. Ma, K. Ling, and D. Pei, "Wifi can be the weakest link of round trip network latency in the wild," in *IEEE INFOCOM 2016 - The 35th Annual IEEE International Conference on Computer Communications*, pp. 1–9, April 2016.

[60] P. Li, N. Scalabrino, Y. Fang, E. Gregori, and I. Chlamtac, "Channel interference in ieee 802.11b systems," in *IEEE GLOBECOM 2007 - IEEE Global Telecommunications Conference*, pp. 887–891, Nov 2007.

[61] A. Mahanti, N. Carlsson, C. Williamson, and M. Arlitt, "Ambient interference effects in wi-fi networks," in *Proceedings of the 9th IFIP TC 6 International Conference on Networking*, NETWORKING'10, (Berlin, Heidelberg), pp. 160–173, Springer-Verlag, 2010.

[62] A. Davydov, G. Morozov, I. Bolotin, and A. Papathanassiou, "Evaluation of joint transmission CoMP in C-RAN based LTE-A hetnets with large coordination areas," in *2013 IEEE Globecom Workshops (GC Wkshps)*, pp. 801–806, Dec 2013.

[63] "https://www.slideshare.net/ericsson/ericsson-5g-radio-dot-launch-103121315,"

[64] "Huawei LampSite." http://carrier.huawei.com/en/products/wireless-network/small-cell/lampsite.

[65] F. Tonini, M. Fiorani, M. Furdek, C. Raffaelli, L. Wosinska, and P. Monti, "Radio and transport planning of centralized radio architectures in 5G indoor scenarios," *IEEE Journal on Selected Areas in Communications*, vol. 35, pp. 1837–1848, Aug 2017.

[66] C. Raffaelli, F. Tonini, M. Fiorani, M. Furdek, P. Monti, and L. Wosinska, "Optimization of centralized radio access networks in indoor areas," in *2016 18th International Conference on Transparent Optical Networks (ICTON)*, pp. 1–4, July 2016.

[67] F. Tonini *et al.*, "Minimum cost deployment of radio and transport resources in centralized radio architectures," *Proc. of IEEE International Conference on Computing, Networking and Communications (ICNC) 2016*, Feb. 2016.

[68] J. Gambini and U. Spagnolini, "Wireless over cable for femtocell systems," *IEEE Communications Magazine*, vol. 51, pp. 178–185, May 2013.

[69] "Connecting the dots: small cells shape up for high-performance indoor radio," *Ericsson Review*, Dec 2014.

[70] S. H. R. Naqvi, A. Matera, L. Combi, and U. Spagnolini, "On the transport capability of lan cables in all-analog MIMO-RoC fronthaul," in *2017 IEEE Wireless Communications and Networking Conference (WCNC)*, pp. 1–6, March 2017.

[71] E. Medeiros, Y. Huang, T. Magesacher, S. Hst, P. Eriksson, C. Lu, P. dling, and P. O. Brjesson, "Crosstalk mitigation for LTE-over-copper in downlink direction," *IEEE Communications Letters*, vol. 20, pp. 1425–1428, July 2016.

[72] Y. Huang, E. Medeiros, T. Magesacher, S. Hst, C. Lu, P. Eriksson, P. dling, and P. O. Brjesson, "Time-domain precoding for LTE-over-copper systems," in *2016 IEEE International Conference on Communications (ICC)*, pp. 1–6, May 2016.

[73] R. Acedo-Hernández, M. Toril, S. Luna-Ramírez, C. Úbeda, and M. J. Vera, "Automatic clustering algorithms for indoor site selection in LTE," *EURASIP Journal on Wireless Communications and Networking*, vol. 2016, p. 87, Mar 2016.

[74] K. M. Yang, "Encyclopedia of algorithms," *Springer*, 2008.

[75] V. V. Vazirani, "Approximation algorithms," *Springer Science & Business Media*, 2013.

[76] T. H. Cormen, C. E. Leiserson, and R. L. Rivest, "Introduction to algorithms," *MIT Press and McGraw-Hill*, 2001.

[77] "http://www.ericsson.com/res/investors/docs/2013/ericsson-radio-dot-system-telebriefings-26-sept.pdf,"

[78] "Next Generation Fronthaul Interface (1914) Working Group."

[79] S. Bjornstad, D. R. Hjelme, and N. Stol, "A packet-switched hybrid optical network with service guarantees," *IEEE Journal on Selected Areas in Communications*, vol. 24, p. 107, Aug 2006.

[80] R. Veisllari, S. Bjornstad, J. P. Braute, K. Bozorgebrahimi, and C. Raffaelli, "Field-trial demonstration of cost efficient sub-wavelength service through integrated packet/circuit hybrid network [invited]," *IEEE/OSA Journal of Optical Communications and Networking*, vol. 7, pp. A379–A387, March 2015.

[81] W. Cerroni and C. Raffaelli, "Analytical model of quality of service scheduling for optical aggregation in data centers," *Photonic Netw. Commun.*, vol. 28, pp. 264–275, Dec. 2014.

[82] F. Tonini, C. Raffaelli, B. M. Khorsandi, S. Bjornstad, and R. Veisllari, "Converged fronthaul/backhaul based on integrated hybrid optical networks," in *2018 Asia Communications and Photonics Conference (ACP)*, p. 1/3, Oct 2018.

[83] S. Bjornstad, R. Veisllari, D. Chen, F. Tonini, and C. Raffaelli, "Minimizing delay and packet delay variation in switched 5G mobile access networks," *IEEE/OSA Journal of Optical Communications and Networking, Special issue on Latency in Edge Optical Networks*, 2019.

[84] F. Tonini, B. M. Khorsandi, S. Bjornstad, R. Veisllari, and C. Raffaelli, "C-RAN traffic aggregation on latency-controlled Ethernet links (invited)," *Applied Science*, 2018.

[85] L. Valcarenghi, K. Kondepu, and P. Castoldi, "Analytical and experimental evaluation of cpri over ethernet dynamic rate reconfiguration," in *2016 IEEE International Conference on Communications (ICC)*, pp. 1–6, May 2016.

[86] D. Chitimalla, K. Kondepu, L. Valcarenghi, M. Tornatore, and B. Mukherjee, "5G fronthaul-latency and jitter studies of CPRI over ethernet," *IEEE/OSA Journal of Optical Communications and Networking*, vol. 9, pp. 172–182, Feb 2017.

[87] I. 802.1Qbu, "Frame preemption." http://www.ieee802.org/1/pages/802.1bu.html.

[88] IEEE P802.1CM, "Time Sensitive Networking for fronthaul," 2018.

[89] F. Musumeci, C. Bellanzon, N. Carapellese, M. Tornatore, A. Pattavina, and S. Gosselin, "Optimal BBU placement for 5G C-RAN deployment over WDM aggregation networks," *Journal of Lightwave Technology*, vol. 34, pp. 1963–1970, April 2016.

[90] S. Xu and S. Wang, "Efficient algorithm for baseband unit pool planning in cloud radio access networks," in *2016 IEEE 83rd Vehicular Technology Conference (VTC Spring)*, pp. 1–5, May 2016.

[91] M. Olsson, C. Cavdar, P. Frenger, S. Tombaz, D. Sabella, and R. Jantti, "5GrEEn: Towards green 5G mobile networks," in *2013 IEEE 9th International Conference on Wireless and Mobile Computing, Networking and Communications (WiMob)*, pp. 212–216, Oct 2013.

[92] N. Carapellese, M. Tornatore, and A. Pattavina, "Energy-efficient baseband unit placement in a fixed/mobile converged WDM aggregation network," *IEEE Journal on Selected Areas in Communications*, vol. 32, pp. 1542–1551, Aug 2014.

[93] "The 5G Infrastructure Public Private Partnership: The next generation of communication networks and services." https://5gppp.eu/wpcontent/uploads/2015/02/5GVision-Brochurev1.pdf.

[94] N. Skorin-Kapov, M. Furdek, S. Zsigmond, and L. Wosinska, "Physical-layer security in evolving optical networks," *IEEE Communications Magazine*, vol. 54, pp. 110–117, August 2016.

[95] M. Furdek, N. Skorin-Kapov, and L. Wosinska, "Attack-aware dedicated path protection in optical networks," *Journal of Lightwave Technology*, vol. 34, pp. 1050–1061, Feb 2016.

[96] M. F. Habib, M. Tornatore, F. Dikbiyik, and B. Mukherjee, "Disaster survivability in optical communication networks," *Comput. Commun.*, vol. 36, pp. 630–644, Mar. 2013.

[97] V. W. S. Chan, "Resilient optical networks1," in *2018 20th International Conference on Transparent Optical Networks (ICTON)*, pp. 1–4, July 2018.

[98] P. Wiatr, J. Chen, P. Monti, and L. Wosinska, "Energy efficiency versus reliability performance in optical backbone networks [invited]," *IEEE/OSA Journal of Optical Communications and Networking*, vol. 7, pp. A482–A491, March 2015.

[99] Y. Ye, F. J. Arribas, J. Elmirghani, F. Idzikowski, J. L. Vizcano, P. Monti, F. Musumeci, A. Pattavina, and W. V. Heddeghem, "Energy-efficient resilient optical networks: Challenges and trade-offs," *IEEE Communications Magazine*, vol. 53, pp. 144–150, Feb 2015.

[100] C. Colman-Meixner, G. B. Figueiredo, M. Fiorani, M. Tornatore, and B. Mukherjee, "Resilient cloud network mapping with virtualized BBU placement for cloud-RAN," in *2016 IEEE International Conference on Advanced Networks and Telecommunications Systems (ANTS)*, pp. 1–3, Nov 2016.

[101] B. M. Khorsandi, C. Raffaelli, M. Fiorani, L. Wosinska, and P. Monti, "Survivable BBU hotel placement in a C-RAN with an optical wdm transport," in *DRCN 2017 - Design of Reliable Communication Networks; 13th International Conference*, pp. 1–6, March 2017.

[102] B. M. Khorsandi, F. Tonini, and C. Raffaelli, "Centralized vs. distributed methodologies for resilient 5G access networks (submitted, minor revision required)," *Photonic Network Communication*, 2018.

[103] C. Raffaelli, B. M. Khorsandi, and F. Tonini, "Distributed location algorithms for flexible BBU hotel placement in C-RAN," in *2018 20th International Conference on Transparent Optical Networks (ICTON)*, pp. 1–4, July 2018.

[104] B. M. Khorsandi, F. Tonini, and C. Raffaelli, "Design methodologies and algorithms for survivable C-RAN," in *2018 International Conference on Optical Network Design and Modeling (ONDM)*, pp. 106–111, May 2018.

[105] C. Raffaelli, C. D. Castro, B. M. Khorsandi, and F. Tonini, "Distributed machine learning location algorithm for reliable C-RAN," in *2018 OSA Photonic Networks and Devices*, p. 1/3, Oct 2018.

[106] M. Shehata, O. Ayoub, F. Musumeci, and M. Tornatore, "Survivable BBU placement for C-RAN over optical aggregation networks," in *2018 20th International Conference on Transparent Optical Networks (ICTON)*, pp. 1–4, July 2018.

[107] F. Liu, Y. Wang, M. Lin, K. Liu, and D. Wu, "A distributed routing algorithm for data collection in low-duty-cycle wireless sensor networks," *IEEE Internet of Things Journal*, vol. 4, pp. 1420–1433, Oct 2017.

[108] Y. Chang, H. Tang, B. Li, and X. Yuan, "Distributed joint optimization routing algorithm based on the analytic hierarchy process for wireless sensor networks," *IEEE Communications Letters*, vol. 21, pp. 2718–2721, Dec 2017.

[109] P. Ohlen, B. Skubic, A. Rostami, M. Fiorani, P. Monti, Z. Ghebretensae, J. Martensson, K. Wang, and L. Wosinska, "Data plane and control architectures for 5G transport networks," *Journal of Lightwave Technology*, vol. 34, pp. 1501–1508, March 2016.

[110] S. Zhang, M. Xia, and S. Dahlfort, "Fiber routing, wavelength assignment and multiplexing for DWDM-centric converged metro/aggregation networks," in *39th European Conference and Exhibition on Optical Communication (ECOC 2013)*, pp. 1–3, Sep. 2013.